ASPECTS OF INFLATIONARY MAGNETOGENESIS

A

Thesis submitted

in Fulfillment of the Requirements

for the Degree of

Doctor of Philosophy

by

Sourav Pal

Department of Physics
Indian Institute of Technology Guwahati
Guwahati - 781039, Assam, India

November 2025

Dedicated to my family

Certificate

This is to certify that the thesis entitled "**Aspects of Inflationary Magnetogensis**", submitted by **Sourav Pal** (186121026), a research scholar in the *Department of Physics, Indian Institute of Technology Guwahati*, for the award of the degree of **Doctor of Philosophy**, is a record of an original research work carried out by her under my supervision and guidance. The thesis has fulfilled all requirements as per the regulations of the institute and in my opinion has reached the standard needed for submission. The results embodied in this thesis have not been submitted to any other University or Institute for the award of any degree or diploma.

Prof. Debaprasad Maity
Department of Physics
Indian Institute of Technology Guwahati
Guwahati - 781039, Assam, India

Date: 24.11.2025
Place: IIT Guwahati

Declaration

I, *Sourav Pal*, hereby declare that the work presented in this thesis, entitled **"Aspects of Inflationary Magnetogenesis"**, has been carried out by me under the supervision of *Prof. Debaprasad Maity* in the Department of Physics, Indian Institute of Technology Guwahati, India.

I further affirm that the research embodied in this thesis is entirely original and has not been submitted in whole or in part for the award of any other degree or diploma at this or any other institution. All sources of information and references to the work of others have been duly acknowledged.

Sourav Pal
Roll No. - 186121026
Department of Physics
Indian Institute of Technology Guwahati
Guwahati - 781039, Assam, India

Date: 24.11.2025
Place: IIT Guwahati

Acknowledgement

With profound respect and deep humility, I would like to extend my heartfelt gratitude to my esteemed supervisor, Prof. Debaprasad Maity. His unwavering guidance, constant encouragement, and inspiring insights have been the cornerstone of my research journey. His unparalleled dedication, patience, and attention to every detail of my work have not only enriched this thesis but have also left a lasting impression on my personal and academic growth. I remain deeply indebted to him for his invaluable feedback on every manuscript I prepared and for the generosity with which he shared his time, knowledge, and wisdom.

I owe sincere thanks to the distinguished members of my doctoral committee, Dr. Debasish Borah and Prof. Tarak Nath Dey, for their kind efforts in evaluating my research, offering their time, and providing thoughtful suggestions that greatly enhanced this work. I also express my gratitude to Dr. Bibhas Ranjan Majhi for his insightful comments, constructive remarks, and thought-provoking suggestions during our academic discussions and journal clubs. My collaborative journey has been made richer by Dr. Tanmoy Paul and Dr. Tuan Q. Do, whose support, ideas, and enthusiasm have significantly contributed to the fulfillment of this work.

I am truly grateful to the Head of the Department, Prof. Bosanta R. Boruah, and to all the faculty members whose encouragement and cordial support facilitated the smooth progress of my research. My appreciation also extends to the technical and research staff of the department for their indispensable assistance at various stages of this endeavor.

I take this opportunity to fondly remember the warmth, companionship, and vibrant discussions shared with my dear colleagues, batchmates, seniors, and juniors Dr. Pankaj Saha, Dr. Riajul Haque, Dr. Rajesh Karmakar, Dr. Sovan Sau, Dr. Pradeepkumar Yadav, Gargi, Banashree, Rajesh, Ayan, Subhasish, Jitumani, Sitesh, and Amit, each of whom has in some way contributed to the spirit and joy of this journey. I am especially grateful to Dr. Surojit and Dr. Rajesh, whose guidance and camaraderie as seniors left a meaningful mark. Beyond academics, I am thankful for the lighter moments spent on and off the campus with my camera, which provided much-needed relief and joy amid the pressures of research.

On a more personal note, I am deeply touched by the steadfast moral and emotional support of my dearest friends Kushal, Dhriti, Supriya, Monu, Manish, and Namrata, whose encouragement and companionship carried me through the challenges of my PhD pursuit.

I wholeheartedly acknowledge the generous financial assistance provided by the Ministry of Human Resource Development (MHRD), Government of India, which enabled the successful completion of this research.

Above all, I bow in loving memory before my late grandparents, and especially my grandmother, Lt. Rekha Roy, whose blessings and affection have been a guiding force in my life. My deepest gratitude goes to my beloved parents, Mr. Dilip Kumar Pal and Mrs. Sipra Pal, for their unconditional love, selfless sacrifices, and unflinching encouragement, which formed the bedrock of my aspirations. I also owe a special acknowledgement to my cherished siblings and cousins, Suchismita, Sayanti, Souvik, Anik, and Tanay, for their love, encouragement, and presence in my life journey. To all those who have, in diverse ways, big or small, contributed to my academic and personal growth, I convey my sincerest appreciation and heartfelt thanks.

(Sourav Pal)

Abstract

This thesis explores the generation, evolution, and quantum signatures of primordial large-scale magnetic fields in the context of inflationary cosmology. Magnetic fields are ubiquitous throughout the Universe, observed on scales ranging from planets and stars to galaxies, galaxy clusters, and the intergalactic medium. While astrophysical dynamo mechanisms can explain galactic-scale magnetic fields, the origin of large-scale coherent magnetic fields, particularly in the intergalactic medium with strengths of $\sim 10^{-16}$ to $\sim 10^{-}10$ Gauss and coherence lengths up to Mpc scales, requires primordial generation mechanisms.

The thesis investigates inflationary magnetogenesis as the most viable mechanism for generating such large-scale magnetic fields. In standard cosmology, the electromagnetic field action is conformally invariant under spatially flat Friedmann-Lemaître-Robertson-Walker (FLRW) spacetime, preventing significant magnetic field production during inflation. This work explores three distinct approaches to break conformal invariance and enable primordial magnetogenesis: First, we develop an Effective Field Theory (EFT) framework for inflationary magnetogenesis, where electromagnetic fields couple to scalar and tensor perturbations while preserving spatial diffeomorphism symmetry. This approach naturally breaks conformal invariance and addresses the strong coupling problem inherent in traditional models. We demonstrate that while scale-invariant magnetic spectra suffer from backreaction issues, scale-invariant electric spectra can produce

observationally viable magnetic field strengths when combined with extended reheating phases. The magnetic field evolution during reheating, governed by Faraday induction in low-conductivity plasma, significantly enhances the present-day field strength and provides constraints on the reheating equation of state.

Second, we propose a novel mechanism using anisotropic spacetime backgrounds, specifically Bianchi type I metrics, to break conformal flatness without requiring explicit scalar field couplings. This approach circumvents both strong coupling and backreaction problems while generating magnetic fields with strengths$B_0 \sim 3 \times 10^{-21}$ Gauss for appropriate anisotropic parameters. The anisotropy, treated as a perturbation appearing near the end of inflation, preserves the overall inflationary paradigm while enabling efficient magnetogenesis.

Finally, we develop quantum information theoretic tools to probe the quantum signatures embedded in primordial magnetic fields and gravitational waves. Using squeezed state formalism, we construct quantum Stokes operators and demonstrate how the fuzziness of quantum Poincaré spheres can serve as observational tests for the quantum mechanical origin of these primordial fields. We show that both primordial magnetic fields and gravitational waves exist in highly squeezed quantum states with non-zero squeezing parameters that encode information about their quantum origin during inflation.

Throughout this work, we address the persistent challenges in inflationary magnetogenesis, including the backreaction problem (where electromagnetic energy density threatens to exceed inflationary energy density) and the strong coupling problem (where effective coupling constants become non-perturbatively large). Our proposed mechanisms provide viable pathways to generate observationally consistent magnetic field strengths while maintaining theoretical self-consistency. The thesis contributes to understanding how quantum fluctuations during inflation can seed the large-scale magnetic fields observed today, offering new theoretical frameworks and observational strategies to probe the quantum mechanical nature of the early Universe through electromagnetic and gravitational wave observations.

Contents

List of Figures

List of Tables

Conventions and Abbreviations

- Throughout this thesis we have used the natural unit system that is $\hbar = c = k_B = 1$. Where $\hbar = \frac{h}{2\pi}$ is the reduced Planck constant, c is the speed of light and G is the Newtonian Gravitational constant.
- We have used the $(-,+,+,+)$ signature for the metrics under consideration.
- Throughout the thesis an "overdot" represents a derivative with respect to cosmic time (t) and a "prime" denotes a derivative with respect to the conformal time (η).

CMB	Cosmic Microwave Background
IGM	Inter galactic medium
PMF	Primordial Magnetic fields
EFT	Effective Field Theory
PGW	Primordial Gravitational waves

List of Publications

The thesis comprises of the following publications:

1. D. Maity, **S. Pal** and T. Paul, "Effective Theory of Inflationary Magnetogenesis and Constraints on Reheating," JCAP **05**, 045 (2021).
2. D. Maity and **S. Pal**, "Probing non-classicality of primordial gravitational waves and magnetic field through quantum Poincare sphere," Phys. Lett. B **835**, 137503 (2022).
3. **S. Pal**, D. Maity and T. Q. Do, "Magnetogenesis from an anisotropic universe," Phys. Rev. D **109**, no.8, 083507 (2024).

Other publications

1. M. R. Haque, D. Maity and **S. Pal**, "Probing the reheating phase through primordial magnetic field and CMB," Phys. Rev. D **103**, no.10, 103540 (2021).

1

Introduction

Contents

1.1 Brief introduction to standard Cosmology

Cosmology is the study of the evolution of the Universe. It typically deals with large-scale structures ranging from galaxies (Kpc)[1] and extragalactic medium from ∼Kpc up to several Mpc, which is the typical distance between galaxy clusters and intergalactic medium (IGM). It focuses on the thermal history of the Universe and explains the present-day structures. Einstein put forward the underlying mathematical formalism of the standard cosmology in his famous *Theory of Gravitation* in the early 20^{th} century, which has been confirmed by the recent GW observations [1,2]. With the advancement of cosmological observations and precision cosmology, we could verify the validity of several of the theories proposed to explain the large-scale structure of the Universe. From the *Isotropic CMB radiation* by Penzias and Wilson, it was observed that the Universe has a temperature of ~ 2.725K [3,4]. Furthermore, the Cosmic Background Explorer (COBE) experiment found that the Universe is isotropic at least to 1 part in 10^5 [5,6]. This gave rise to the "Cosmological principle" [7–12] that suggests the Universe is homogenous and anisotropic at scales over 100 Mpc. The generic metric for a homogeneous and isotropic medium can be written as

$$ds^2 = -dt^2 + a^2(t)\left[\frac{dr^2}{1-Kr^2} + r^2\left(d\theta^2 + \sin^2\theta d\phi^2\right)\right]. \tag{1.1}$$

The metric in Eq.(2.3) is known as the Friedman, Lemaître, Robertson, and Walker (FLRW) metric. Here, r, θ, ϕ are three spatial comoving coordinates, and t corresponds to the cosmic time. K corresponds to the spatial curvature of the spacetime. $a(t)$ is the cosmological scale factor. Depending on the curvature of the Universe, it can assume different values[2]. In this context, it is important to mention the discovery and expansion of the Universe. In 1929, Edwin Hubble found that the distant galaxies are receding from an observer on Earth, and the rate is proportional to the distance of the galaxies [13]. This observation suggests the expansion of the Universe and is referred

[1] 1 Kpc $= 3.086 * 10^{19}$ m.

[2] For an open Universe (Negatively curved), $K = -1$, $K = 0$ corresponds to a flat Universe, and $K = +1$ suggests a closed Universe (Positively curved).

to as Hubble's law. In terms of comoving distance, the rate of expansion or the velocity is given by

$$v = \frac{d}{dt}(ax) = \dot{a}x = H_0 d\,. \tag{1.2}$$

Where the 'overdot' represents a derivative with respect to cosmic time t, $a(t)$ is the scale factor of the Universe, x is the comoving distance between two galaxies, and d is the physical distance between them. In the above Eq.(1.2) H_0 is the Hubble constant, which is represented in terms of the dimensionless number $H_0 = 100h$ $\mathrm{kms^{-1}Mpc^{-1}}$. Using the CMB radiation left over from the Big Bang, satellites like Planck estimate H_0 by extrapolating the Universe's expansion from its earliest observable state. These measurements yield a lower expansion rate of $H_0 = 67.66 \pm 0.42$ km/s/Mpc [177]. Whereas, using direct astronomical observations of nearby objects such as Cepheid variable stars and supernovae, and employing the cosmic distance ladder, astronomers measure a higher expansion rate of $H_0 = 73.04 \pm 1.04$ km/s/Mpc [178]. This mismatch in the observed values of H_0, gives rise to *The Hubble Tension* [14, 15].

The standard model of Cosmology assumes the isotropy and homogeneity of the Universe. However, the observation of CMBR shows that all the photons decoupled from the matter-dominated era when the temperature of the Universe reached around $\sim$ 3000K. Therefore, the standard cosmological model stated above cannot successfully explain the uniformity of CMBR temperature in all directions referred to as *The Horizon problem*. Moreover, according to the CMB observations, our Universe is almost spatially flat on large scales at present. The standard model of cosmology fails to explain the phenomenon known as *The Flatness problem*. A detailed description of these problems can be found in [7].

To explain the Horizon and flatness problems of the hot big bang cosmology [7–12, 16], *inflation* was proposed in the 1980s. It successfully explains the large-scale homogeneity of the Universe as we observe today. Furthermore, the quantum fluctuations produced during this period help to explain the observable imprints of seed perturbation in CMBR. In the next subsection, we briefly discuss the problems of standard cosmology and how *inflation* can solve them.

1.2 Problems in standard cosmology and its solution

As discussed in the last section, some of the observations like CMB cannot be explained through the standard cosmology. In order to explain those, inflation is an extremely powerful tool. Inflation is a theoretically proposed era when the Universe expands exponentially. It is a causal theory that successfully explains the large-scale structure of the Universe [43–45]. We will discuss the dynamics of inflation in the next chapter. Here we will discuss how inflation solves the horizon and the flatness problem and its mathematical implications.

The Einstein equation governs the dynamics of the Universe,

$$G_{\mu\nu} \equiv R_{\mu\nu} - \frac{1}{2} g_{\mu\nu} R = -8\pi G T_{\mu\nu}, \tag{1.3}$$

where $T_{\mu\nu}$ is the energy-momentum tensor of all the matter fields,$R_{\mu\nu}$ is the Ricci tensor, $g_{\mu\nu}$ are the metric components, and $R = g^{\mu\nu} R_{\mu\nu}$ is the Ricci scalar, and G is the Newton's gravitational constant. The Eq.(1.3) describes how the Einstein tensor $(G_{\mu\nu})$, i.e., the curvature of the spacetime, evolves due to the presence of matter fields (obtained by computation of $T_{\mu\nu}$). On large scales, these matter fields can be treated as ideal fluid, and therefore, the properties of the matter fields can be represented by the energy density (ρ), pressure (p), and the comoving four-velocity (u^μ) of the fluid. For a matter field in the FLRW metric, the energy-momentum tensor turns out to be diagonal, and to satisfy the isotropy of the spacetime, the spatial components must be equal to each other. The energy-momentum tensor that satisfies all these conditions corresponding to the ideal fluid is given as

$$T_{\mu\nu} = (\rho + p)\, u_\mu u_\nu + p g_{\mu\nu}, \tag{1.4}$$

where $g_{\mu\nu}$ represnts the metric components and $u^\mu = (1, 0, 0, 0)$ is the four-velocity of the comoving observer, with the constraint $u^\mu u_\mu = -1$. Furthermore, to observe the evolution of the scale factor of the Universe, we study the Friedmann equations [18].

$$
\begin{aligned}
H^2 + \frac{K}{a^2} &= \frac{8\pi G}{3}\rho\,, &(1.5)\\
\dot{H} + H^2 &= -\frac{4\pi G}{3}\left(\rho + 3p\right), &(1.6)
\end{aligned}
$$

where the Hubble parameter is defined in terms of the scale factor as $H \equiv \dot{a}/a$. The conservation of energy-momentum tensor gives the continuity equation

$$
\nabla_\mu T^{\mu\nu} = 0\,, \;\; \Rightarrow \;\; \dot{\rho} = -3H(\rho + p), \tag{1.7}
$$

Eq.(1.7) can be coherently written as,

$$
\rho \propto a^{-3(1+\omega)}, \tag{1.8}
$$

where $\omega = p/\rho$ is the equation of state (EoS) of the Universe. The EoS varies during different periods. e.g $\omega = 0$ when the Universe is matter dominated, $\omega = 1/3$ during radiation domination and $\omega = -1$ during the vacuum energy domination.

Flatness problem

To understand the flatness problem, we define a dimensionless density parameter as a ratio of the energy densities $\Omega(t) = \frac{\rho}{\rho_c}$, where $\rho_c = \frac{3H^2(t)}{8\pi G}$ is the critical density. The 1^{st} Friedmann equation (1.5) can be written in terms of this dimensionless parameter as

$$
\Omega_K(t) \equiv \Omega(t) - 1 = \frac{K}{a^2H^2}\,, \tag{1.9}
$$

In the light of recent observations from PLANCK data [19], it is evident that the Universe at present is essentially flat, i.e., $K = 0$. Moreover, $\Omega_K(t_0)$, its value is very close to unity. It turns out that, in order to have $\Omega_K(t_0)$ closer to unity, in the very early Universe $(t = t_{Pl})$ it had to be extremely small so that it could satisfy the ratio

$$
\frac{|\Omega_K|_{t=t_0}}{|\Omega_K|_{t=t_{Pl}}} \approx \mathcal{O}\left(10^{-64}\right)\,. \tag{1.10}
$$

This very small and fine-tuned value of the energy density ratio in the very early Universe cannot be explained through the standard Big Bang cosmology and is known as the *Flatness problem*.

Horizon problem

The horizon problem in cosmology refers to the absence of causal contact between two particles separated by more than the physical horizon distance. We can define three types of horizons in cosmology. Namely,

Particle horizon: The distance that the light can travel within its finite age, i.e., the volume of the Universe, from where we can receive information, is finite. The boundary of this accessible volume of the Universe is called the particle horizon. At any given time t, the particle horizon is defined as

$$d_p(t) = a(t)\int_0^t \frac{dt'}{a(t')} = a(t)\int_0^t d\ln a' \frac{1}{a'H(a')} . \tag{1.11}$$

Here $t_i = 0$ is the beginning of the Universe, and $(aH)^{-1}$ is the comoving Hubble radius.

Event horizon: The complement of the particle horizon is known as the event horizon. The event horizon is the inaccessible part of the Universe, from which any signal emitted at any particular time t would not reach any future observer.

Hubble radius: The expansion rate of the Universe is characterized by the Hubble parameter H, with the corresponding expansion time given by $t_H \equiv H^{-1}$. The Hubble radius denotes the comoving distance that light or any particle would traverse within one expansion time.

The particle and the Hubble horizon can determine the causal connection between two particles. Suppose two particles are separated by a distance larger than the Hubble horizon at any given time t. In that case, it implies that they cannot communicate with each other at that particular time. We have the observational signature of the early Universe from the CMB as the last scattering surface. We can calculate the Hubble radius corresponding to the present value of the Hubble parameter as

$$\lambda(t_{ls}) = d_p(t_0)\left(\frac{a(t_{ls})}{a(t_0)}\right) = d_p(t_0)\left(\frac{T_0}{T_{ls}}\right) , \tag{1.12}$$

where $T_0 = 2.73\text{K}$ is the present temperature of the Universe as observed from CMB radiation. Moreover, $T_{ls} = 3000\ K$ is the temperature of the Universe at the time of last-scattering surface (t_{ls}). During the matter-dominated era, the Hubble parameter

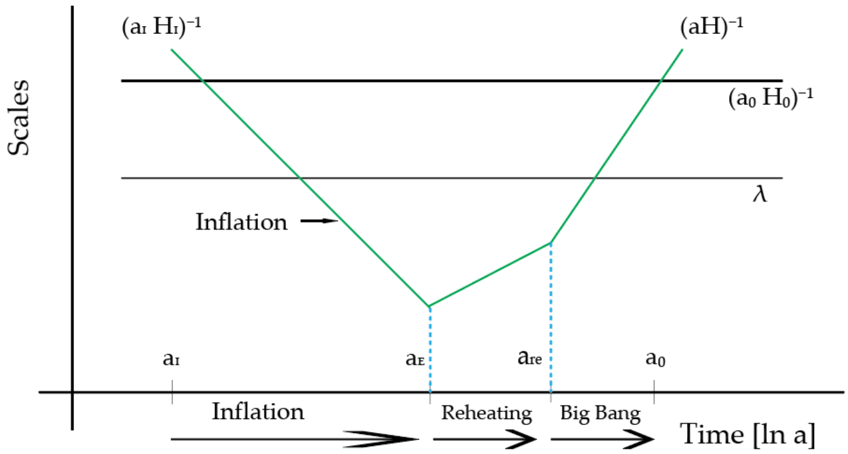

Figure 1.1: Particle horizon vs Hubble horizon.

evolved as $H \propto T^{3/2}$, and with the relation obtained from Eq.(1.12), we can estimate that during the last scattering surface, there were $\approx 10^6$ disconnected regions. Any two photons separated by a distance larger than $d_p(t_{ls})$ are very small. However, we observe almost equal temperatures of the CMB in all directions. This is known as the *horizon problem*, as the uniformity cannot be explained by standard Big Bang cosmology.

Cosmological inflation proposes a mathematical model that provides a causal mechanism to successfully explain the homogeneity and isotropy of the observable Universe. We can see from Eq.(1.9) that in order to have the value of the dimensionless density parameter $(\Omega_0 - 1)$ of the order of unity, its value at the very early Universe should be very close to zero $\mathcal{O}(10^{-64})$. The Hubble parameter (H) remains almost constant during the entirety of the inflation. Following eq.(1.9) and substituting $H \sim$ cosnstant, we get $(\Omega - 1) \propto a^{-2}$. So the value of $\Omega_{end} - 1$ at the end of inflation will be $\sim e^{-2N}$. Where Ω_{end} represents the density parameter at the end of inflation, N is the e-folding number of the inflationary period defined as $N = \ln(a_{end}/a_I)$, a_{end} and a_I corresponds to the scale factors at the end and beginning of inflation respectively.

Furthermore, if the inflation is sustained for an e-folding number of $N = 70$, then at the end of inflation $\Omega_{end} - 1 \sim 10^{-60}$, which is sufficient to observe the present day value of $\Omega_0 - 1 \sim 1$. Thus, by introducing inflation, the flatness problem can be circumvented. Now, focusing on the horizon problem, the Universe goes through exponential expansion during the inflationary era. Thus, the physical length scale λ grows faster than the Hubble radius H^{-1} as it remains almost constant during inflation. In standard Big Bang cosmology, as shown in fig.1.1, we can see that each scale crosses the horizon only once. Therefore, all of the patches cannot be in causal contact. However, during inflation, all the scales start to grow, and then it crosses the horizon and re-enters the horizon of the post-inflationary era. It explains how CMB photons from two causally disconnected regions could have been in contact in the past and have almost the same temperature. To summarize, inflation can solve both the flatness problem and the horizon problem. The main characteristics of the inflationary era, known as the slow-roll conditions, can be listed as follows:

- The Universe goes through an era of exponential expansion. The first slow-roll parameter ϵ must satisfy the condition in terms of the rate of expansion given by the Hubble parameter H,
$$\epsilon \equiv -\frac{\dot{H}}{H^2} < 1. \tag{1.13}$$
- As discussed earlier, to solve the flatness problem, inflation should be sustained at around 70 e-folds. It is achieved by the second slow-roll parameter η satisfying the condition
$$\eta \equiv -\frac{\dot{\epsilon}}{H\epsilon} < 1. \tag{1.14}$$

Apart from solving the horizon and flatness problem of the standard Big Bang cosmology, recent observations of gravitational waves (GW) from LIGO and VIRGO suggest that the secondary GW might have been sourced by primordial gravitational waves (PGW). In the literature, it has been shown that the PGW can be produced during the inflationary era [16, 17]. As we proceed, we will discuss several more scenarios that involve the requirement of an inflationary era.

1.3 Magnetic fields in the Universe

Magnetic fields are omnipresent in the Universe. Its presence has been detected over different length scales. Starting from galaxies, galaxy clusters, and even the intergalactic medium of the vast cosmic web, which contains magnetic fields. Their influence on processes such as star formation, the dynamics of interstellar matter, and the propagation of cosmic rays underscores their astrophysical importance. The existing magnetic fields in the galaxies influence small-scale and large-scale processes. It affects the formation and shape of galaxies and galaxy clusters on a large scale. Small-scale effects of these magnetic fields include star formation processes. Therefore, studying the magnetic fields over different length scales is essential to understanding several astrophysical processes.

Despite extensive theoretical and observational studies, the mechanism underlying the origin of these extensive coherent fields remains a profound question to this day [20, 22, 23, 50]. However, it is widely accepted that the observed field originated from a seed magnetic field and was later amplified by several astrophysical processes. In the case of a strong seed field, the necessary strength of the present-day field can be obtained by flux freezing during the structure formation of the Universe. On the contrary, a weak seed magnetic field needs an efficient dynamo mechanism [97, 107] to enhance it by converting its kinetic energy into electromagnetic field energy. The generation mechanisms can be broadly divided into two groups depending on the coherence length scales of the fields. In one of the cases, it uses astrophysical batteries [24,25] as the origin of the seed magnetic field.

On the other hand, the second mechanism considers primordial fluctuation as the origin of the seed magnetic field. The primordial generation mechanism pertains to electroweak or QCD phase transition [26–29] or during the inflationary era [30–39]. The dynamo mechanism can amplify the magnetic field in collapsing objects, for which astrophysical batteries produce the seed magnetic field. However, the primordial genesis of magnetic fields becomes relevant for intergalactic magnetic fields. In this thesis, we focus mainly on two aspects of magnetic fields. Firstly, we study the quantum signatures embedded in the large-scale magnetic fields that will solidify the proposal for generating large-scale cosmological magnetic fields from quantum fluctuations in the early Universe. Finally, we discuss several generation mechanisms that lead to the observed current magnetic field strength. More precisely, we will study the inflationary magnetogenesis scenario since the large-scale effects are naturally embedded in the magnetic fields generated during the inflationary era; thus, it will infer whether it is generated from the quantum fluctuations as primordial fields. Eventually, we can focus on the different inflationary magnetogenesis scenarios that lead to a sustainable magnetic field. Although the magnetic field generated during the inflationary era can successfully explain the large-scale magnetic fields in the IGM, it is still important to mention that the field generated dies out very rapidly with the expansion of the Universe as the standard electromagnetic (EM) action is conformally invariant and the standard FLRW background is conformally flat. Therefore, it is unsuitable for producing particles in the inflationary era, which would be sufficient to seed the magnetic field to present-day strength. However, if the conformal invariance is broken, we can obtain sufficient strength of magnetic fields as observed today. In all the inflationary magnetogenesis models, the most accepted one is where the inflaton field is coupled to the kinetic term of the EM field to break the conformal invariance. Although inflationary magnetogenesis provides a viable solution to large-scale magnetic fields, it suffers from strong coupling and backreaction problems. In the later chapters, we will discuss them and find a way to circumvent them to generate large-scale magnetic fields without the aforementioned drawbacks.

1.4 Generation mechanisms

In the previous section, we mentioned that the dynamo mechanism amplifies the magnetic field from a seed magnetic field. However, the origin of the seed magnetic field is a tempting question, in both astrophysical and cosmological scenarios. Here, we briefly discuss the astrophysical and primordial generation scenarios.

1.4.1 Astrophysical magnetogenesis mechanisms

All the astrophysical generation mechanisms rely on the charge gradient of the medium. Although the Universe is charge-neutral, it has a non-zero degree of ionization. Any external force acting on the medium can separate the positively and negatively charged particles, leading to a charge gradient in the medium. The charge gradient in the medium generates an electric field. Subsequently, following Faraday's law, the electric field is converted into a magnetic field. The pressure gradient in the medium causes the charge gradient in the medium. Mathematically, it can be represented as

$$E_e = -\frac{\nabla p_e}{e n_e} \,. \tag{1.15}$$

This equation is obtained assuming pressure is applied to a fully ionized gas. In eq.(1.15) $p_e = n_e k_B T$, where n_e is the electron number density, and T is the equilibrium temperature of the electron gas. The non-zero curl of the field generated by the pressure gradient, described in eq.(1.15), will generate a magnetic field, and the collisions between them also lead to some resistance. Incorporating Ohm's law, the magnetic field evolution equation turns out to be

$$\frac{\partial \vec{B}}{\partial t} = \vec{\nabla} \times \left(\vec{v} \times \vec{B} - \frac{1}{\sigma} \vec{\nabla} \times \vec{B} \right) - \frac{1}{e} \frac{\vec{\nabla} n_e}{n_e} \times \vec{\nabla} T \tag{1.16}$$

In the above eq. σ is the conductivity of the medium, t is the time parameter and T is the temperature of the system. The last term on the right suggests that the modified induction equation becomes inhomogeneous if the medium's temperature gradient and density gradient are not aligned. Furthermore, it can lead to a generation of seed magnetic fields from zero magnetic fields. This effect is known as the Biermann battery effect [42], which was initially proposed for stellar magnetic fields and later generalized for cosmic magnetic fields as well [175, 176]. There may be some astrophysical instances when the temperature gradient is not parallel to the number density gradient. During reionization era, the number density gradient is dictated by the local density fluctuations, that later collapse to form the structures. As the density fluctuations are independent of the source of the temperature gradient, the last term of Eq.(1.16) is non-zero and leads to the production of magnetic fields. This helps to generate a seed magnetic field of the coherence length of density fluctuations. To obtain the present-day value of the magnetic field, the seed magnetic field generated through this mechanism needs to be of $B \approx 10^{-21}$ G [97].

1.4.2 Primordial magnetogenesis mechanisms

Several mechanisms can lead to magnetic field generation in the early Universe. However, these mechanisms are most effective in explaining the intergalactic and magnetic fields in the cosmic void. To summarize the possible generation mechanisms, we have

Magnetogenesis during phase transition: Magnetic fields can be generated during different *phase transitions* in the early Universe [26–29]. The magnetic field is generated during a phase transition when the battery effect generates a seed magnetic field, as discussed in the astrophysical magnetogenesis mechanisms. Subsequently, the seed magnetic field gets amplified by small-scale dynamos. The primordial magnetogenesis was proposed by Vachaspati during the electroweak phase transition [26]. The magnetic fields produced through the phase transition are produced via a causal process. Therefore, the coherence length scale is always smaller than the Hubble radius. Although the magnetic fields produced during phase transition are very weak on galactic scales, their strength can be increased through the inverse cascade. However, the magnetic field needs to be helical for this to occur. The small-scale field is converted into large-scale magnetic fields by conserving helicity, strengthening the large-scale field produced through a phase transition.

Inflationary magnetogenesis: Inflationary magnetogenesis provides a viable solution to the origin of large-scale magnetic fields. However, the Universe goes into a radiation-dominated era after the end of inflation, and due to flux freezing, the magnetic field strength decays as $B \propto 1/a^2$, with the scale factor $a(t)$. The free EM action is conformally invariant under the conformally flat spacetime of the standard cosmology. This results in low magnetic field strength, even when seeding the dynamo. Therefore, it is necessary to break the conformal invariance. Production of the magnetic field during the inflationary era by breaking the conformal invariance was first proposed by Turner and Widrow [30]. The modified EM Lagrangian density takes the form $I^2 F_{\mu\nu} F^{\mu\nu}$, where I is a function coupled to the Lagrangian to break the conformal invariance. Further, Ratra [31] proposed that the inflaton field can be coupled to the kinetic term of the EM Lagrangian to break the conformal invariance, and it can produce a sufficient strength of the magnetic field. However, it suffers from strong coupling and backreaction problems. We will discuss these drawbacks in detail in later chapters. In certain models of inflationary magnetogenesis, the Schwinger effect comes into play and produces charged particles, leading to a high conductivity of the medium and a low magnetic field strength.

1.5 Measurement and Constraints on the field strengths

1.5.1 Measurement techniques of galactic and extragalactic magnetic fields

As mentioned earlier, magnetic fields are observed on various length scales and settings, from planets to stars to galaxies and clusters. The Earth hosts a dipolar magnetic field of strength ~ 0.7 G with an angle tilted to the rotational axis, and it shields the

Earth from solar winds and solar flares. Moreover, the Sun also hosts a magnetic cycle. It was first put forward by Hale [46], by observing the Zeeman effect on the Sun's surface. The Zeeman splitting can measure extraterrestrial magnetic fields by line splitting due to an external magnetic field. Mathematically, the splitting of transition lines in a free atom can be represented as

$$\frac{\Delta\nu}{\nu} = 1.4g\left(\frac{B}{\mu G}\right)\left(\frac{Hz}{\nu}\right), \tag{1.17}$$

Where g is the Landé's factor, connecting the orbital angular momentum of an atom to the magnetic field. The splitting in the case of the 21cm line of neutral hydrogen and 18cm OH line are valued as $\Delta\nu/\nu \approx 10^{-9}g(B/\mu G)(Hz/\nu)$. In this context, it is important to mention that magnetic fields using Zeeman splitting are observed in low temperatures and high magnetic fields; otherwise, the Doppler broadening of the lines masks the Zeeman splitting. Therefore, the magnetic fields observed using this method are mostly in star-forming regions.

The magnetic field strength in galaxies, galaxy clusters, and beyond is measured using synchrotron radiation. The radiation emitted by free electrons while performing a spiral motion in a magnetic field is called synchrotron radiation, and the intensity of the radiation is a probe of the normal component of the background magnetic field. Furthermore, the degree of polarization of the emitted radiation describes the uniformity of the magnetic field in the source (galaxies and galaxy clusters).

The Faraday rotation measurement is the most effective method for measuring galaxy clusters' magnetic fields. However, none of the above-mentioned methods are useful in measuring the strength of the intergalactic magnetic fields. Faraday rotation is when a photon's polarization axis rotates due to a magnetic field's presence. As the photon propagates in the medium with a magnetic field, the left circularly polarized and right circularly polarized modes interact differently with the electrons present in the plasma. If a light of wavelength λ passes through a medium of length l_m, then the total phase shift ($\Delta\Phi$) of the polarization mode is calculated as

$$\Delta\Phi = \frac{e^3\lambda^2}{2\pi m_e^2 c^4}\int_0^{l_m} n_e(l)B_{\|}(l)dl\ , \tag{1.18}$$

where $B_{\|}$ is the component along the line of sight of the magnetic field, $n_e(l)$ is the electron density in the medium along the line of sight, $\Delta\Phi$ is the total phase shift of the polarization and m_e is the mass of the electron. Traditionally, the total phase shift is defined as

$$\Delta\Phi = (RM)\lambda^2\ . \tag{1.19}$$

As the polarization angle differs for different wavelengths, measuring them in terms of the rotation (RM) removes the $(\pm\Phi \pm n\pi)$ degeneracy. Where (RM) is defined as

$$RM = \frac{e^3}{2\pi m_e^2 c^4}\int_0^{l_m} n_e(l)B_{\|}(l)dl\ . \tag{1.20}$$

Now, the total rotation measurement of the polarization angle (RM) contains contributions from several sources, like the quasar source itself (S), the effect from the intervening galaxies (IG), the contribution from the intergalactic media (IGM) and finally the rotation caused by the milky way (M) as the observations are made from our solar system. Therefore, it is more advantageous to measure the total rotation of the polarization angle in terms of the rotations contributing from different sources. Therefore,

$$RM = RM_S + RM_{IG} + RM_{IGM} + RM_M\ . \tag{1.21}$$

The Faraday rotation measurement method has been used to measure magnetic fields of strength $\sim \mu G$ in high-redshift galaxies and galaxy clusters.

In this thesis, our area of focus is the large-scale magnetic fields. Therefore, discussing the measurement details and constraints on the fields present in the intergalactic media is also very important. However, the measurement techniques described so far cannot measure this region's very low magnetic fields compared to the galactic fields. Therefore, the magnetic fields in this region are measured with the help of TeV blazars. This measurement is based on the absence of GeV photons in the intergalactic medium. The TeV photons emitted by the blazars interact with the galactic gaseous medium and generate electron (e^-) and positron (e^+) pairs. These pairs further interact with the CMBR and generate GeV photons by inverse Compton scattering. Due to the interaction of the photons with the magnetic field in the intergalactic medium, the photons' trajectories change, suppressing the photons' surface brightness. Moreover, by counting the time delay in these secondary GeV photons, we get a lower bound on the strength of the magnetic field at $\sim 10^{-17}$G for coherence scale $\geqslant 1$ Mpc. However, the field's strength depends on the system's coherence length below 1 Mpc. The strength varies as $l_c^{-1/2}$ with the coherence scale.

1.5.2 Constraints on magnetic field strengths

We discussed different measurement methods for the galactic and intergalactic magnetic fields. However, the constraints are obtained from the CMBR and Big Bang Nucleosynthesis (BBN). As large-scale magnetic fields are produced during the Universe's early stages, the total energy budget is affected by the energy of the EM field. Furthermore, the magnetic fields also affect the evolution of scalar and tensor field perturbations. Therefore, we can get the constraints on the field strength from the signatures in the CMBR and BBN.

Constraints from CMB

CMB plays a crucial role in probing the early Universe. As mentioned earlier, the magnetic field produced during the early Universe also affects the total energy budget and the evolution of scalar perturbations. Therefore, we can constrain the magnetic field strength by analyzing the CMB's temperature anisotropies and polarization properties. The CMB is not fully isotropic. It holds a temperature anisotropy of $\sim 10^{-5}$ called temperature fluctuations. The systematic study of temperature anisotropy constrains the strength of the homogeneous magnetic field in the nano-Gauss range. As the primordial magnetic field alters the energy-momentum tensor of the early Universe, the scalar, vector, and tensor perturbations evolve differently due to the scale-invariant or blue-tilted spectrum of the magnetic field. A detailed study of this evolution can be found in [47–49], and a systematic study of the CMB anisotropies to constrain the magnetic field has been done. From this study, it has been shown that for a nearly scale-invariant spectrum, the strength of the magnetic field on a 1Mpc scale should be $B_0 \leq 0.7$ nG.

Constraints from BBN

Primordial magnetic fields affect the abundance of light nuclei at BBN. Therefore, it works as a probe to constrain the strength of the primordial magnetic fields. The magnetic field consecutively changes the phase space of electrons, resulting in a weak interaction rate. It further contributes to the total energy density, and as a result, it affects the expansion rate of the Universe.

The magnetic field changes the abundance of light nuclei at BBN. The magnetic field alters the phase space of the electrons and their statistics. Increasing the neutron-proton conversion rate. This increment leads to a lesser abundance in ^4He. Furthermore, the magnetic energy density contributes to the total energy-momentum tensor and affects the expansion rate. Leading to an increased freeze-out temperature and higher abundances of ^4He. With the data obtained from the ^4He abundances, Grasso and Rubenstein [50] put a bound on the homogenous magnetic field at $B < 10^{11}$ G at $T \approx 10^9$ K at the time of Big Bang Nucleosynthesis.

1.6 Outline of the thesis

The thesis is organized based on the publications mentioned previously and is as follows:

Chapter 2 discusses the generic evolution of the EM field during the inflationary era. Furthermore, it further shows that it is not possible to generate sufficient strength of magnetic fields like the astrophysical magnetic fields. The reason behind this is the invariance of the EM field action under the spatially flat FLRW background. Further, we discuss some models to break the conformal invariance of the EM action by introducing a coupling of a scalar field and the EM field (in some special cases, the inflaton field is coupled to the EM field). We further find that the spectrum of the magnetic field produced in this mechanism is scale invariant. We conclude this chapter by discussing the challenges in the inflationary magnetogenesis model.

In chapter 3, we propose a magnetogenesis scenario in the Effective Theory framework during the inflationary era. At the beginning of this chapter, we discuss the EFT framework and the setup. In this framework, the EM field is coupled to the scalar and tensor perturbations that satisfy the diffeomorphism symmetry. Further, the conformal invariance of the EM field is broken by coupling the scalar field to the gauge field, and the evolution of the perturbations dictates the background evolution. Furthermore, the background evolution of the fields and the perturbations are also discussed, and the inflationary slow-roll parameters lie within the observed range. For a specific choice of the coupling parameter, the model produces a sufficient magnetic field strength consistent with the present-day observation. However, this specific choice suffers from the backreaction problem. In another scenario, although it does not suffer from the backreaction problem, it fails to produce a sufficient EM field during inflation. Moreover, this problem can be circumvented by introducing an elongated reheating period after the end of inflation.

In Chapter 2 and Chapter 3, we discussed how the conformal invariance of the EM field can be broken under conformally flat FLRW spacetime by explicitly coupling the EM field to a scalar field. As a result of the coupling, these inflationary magnetogenesis models might have a strong coupling problem, depending on the nature and evolution of the coupling factor. In this chapter, we propose a novel mechanism to break the conformal invariance of the EM field by introducing a spacetime with an intrinsic anisotropy, and, thus, it is not conformally flat. We explore the evolution of the EM field in this anisotropic spacetime in the inflationary era. We find that a little anisotropy in the spacetime is sufficient to produce an EM field consistent with the observational constraints and free from the backreaction problem.

In Chapter 5, we first lay down the tools to extract quantum information in a bipartite system. However, few challenges exist in extracting quantum information in the cosmological scenario. We develop the necessary tools to experimentally measure the quantumness of the primordial gravitational waves and primordial magnetic fields. Moreover, we show that the formalism proposed here is consistent with the more traditional methodology of quantum measurements. In Chapter 6, we summarize the main results obtained in the previous chapters and discuss the outlook and future aspects of this thesis.

2

Generation of large-scale magnetic fields

Contents

In the last chapter of the Introduction (Chapter 1), we discussed several possible ways to generate astrophysical and cosmic magnetic fields, in essence, mechanisms to generate seed magnetic fields. As suggested by the Blazar observations, the magnetic fields in the intergalactic medium point toward the primordial generation of the magnetic fields. Inflationary magnetogenesis is the most accepted among the proposed primordial large-scale magnetic field generation models. Therefore, in this chapter, we will discuss the mechanism of inflationary magnetogenesis in detail.

Inflation is an era when the Universe went through an accelerated expansion. The inflationary paradigm also solves the horizon and flatness problem of the standard cosmology. Furthermore, during this inflationary era, small-density perturbations were produced, which led to the large-scale structure of the present observable Universe.

The origin of the Universe is believed to be from the quantum fluctuations of the field generated during the inflationary era. As the horizon problem suggests, all the scales associated with today's cosmological interest should be inside the Hubble horizon to successfully explain causality. The solution to this problem, as discussed in the previous chapter, is that the Universe needs to go through an accelerated expansion phase with an e-folding number $N \approx 60$ if the energy scale associated with the inflationary phase is $\sim 10^{16}$ GeV. To satisfy this high energy scale, the simplest model considers a scalar field called the inflaton, which drives the inflation. Assuming the homogeneity and isotropy of the Universe, the acceleration and the inflaton field $\phi(\eta)$ should only be a function of time. However, small-scale quantum fluctuations in the field can give rise to inhomogeneities. The characteristic length scale (L_c) of these fluctuations between two field points can be expressed in terms of the equal-time two-point correlation function $(\zeta(|\vec{x}-\vec{y}|,\eta))$

$$\zeta(|\vec{x}-\vec{y}|,\eta) = \langle 0|\hat{\phi}(\vec{x},\eta)\hat{\phi}(\vec{y},\eta)|0\rangle = \frac{1}{2\pi^2}\int_0^\infty k^2 dk P(k)\frac{\sin kL_c}{kL_c}\,. \tag{2.1}$$

In the above Eq.(2.1) $L_c = |\vec{x}-\vec{y}|$ is the correlation length, $\hat{\phi}(\vec{x},\eta)$ is the field variable at a particular spacetime point, k corresponds to the momentum mode of the inflaton field, and $P(k)$ is the power spectrum of the fluctuations in momentum space. The amplitude of these fluctuations can be quantified in terms of the power spectra as $\Delta(k) = \frac{1}{4\pi^2} k^3 P(k)$. When the length scale of these fluctuations becomes comparable to the Hubble horizon, the amplitude of these fluctuations freezes with time. Moreover, as the modes exit the Hubble horizon of the Universe, the fluctuations become classical, and the amplitude solely depends on the value of the Hubble parameter at the end of inflation when the modes exit the horizon. A detailed discussion on this can be found in the literature [56]. The detail of the inflationary magnetogenesis is described in the upcoming sections

2.1 Maxwellian field theory in FLRW background

In this section, we discuss the standard evolution of the EM field in the FLRW background and also show why it is impossible to produce sufficient magnetic field strength in a conformally flat spacetime when the action is conformal invariant. The electromagnetic(EM) action and its interaction with charged particles in general spacetime can be written as

$$\mathcal{S}_{EM} = -\int \sqrt{-g} d^4x \left(\frac{1}{4} F_{\mu\nu} F^{\mu\nu} - A_\nu J^\nu \right) , \tag{2.2}$$

where $\sqrt{-g}$ is the determinant of the metric, $F_{\mu\nu} = \partial_\mu A_\nu - \partial_\nu A_\mu$ is the EM field tensor, being A_μ is the 4-electromagnetic potential and J^μ is the 4-current density corresponding to the charged field.

The standard FLRW metric is defined as

$$\begin{aligned} ds^2 &= -dt^2 + a^2(t) \left(dx^2 + dy^2 + dz^2 \right) \\ &= a^2(\eta) \left(-d\eta^2 + dx^2 + dy^2 + dz^2 \right) . \end{aligned} \tag{2.3}$$

where t is the cosmic time, η is the conformal time and $a(\eta)$ is the scale factor of the Universe and (x, y, z) are the comoving spatial coordinates. The cosmic time t and the conformal time η are related by the scale factor as $dt = a d\eta$.

Varying the action (2.2) with respect to A_μ gives us the first set of Maxwell's equations,

$$\partial_\mu \left[\sqrt{-g}F^{\mu\nu}\right] = J^\nu . \tag{2.4}$$

The constraints satisfied by the EM field boil down to the other set of Maxwell's equations, also known as the Bianchi identity.

$$\partial_\mu \left[\sqrt{-g}\frac{1}{2}\varepsilon^{\mu\nu\alpha\beta}F_{\alpha\beta}\right] = 0 \ \Rightarrow \ \partial_\mu \left[\sqrt{-g}\tilde{F}^{\mu\nu}\right] = 0 \tag{2.5}$$

where $\varepsilon^{\mu\nu\alpha\beta}$ is the antisymmetric Levi-Civitta tensor. We will show later that Eq.(2.5) signifies that the EM field is perpendicular to its propagation direction. The Eqs.(2.4) and (2.5) represents the full set of Maxwell's equations collectively.

To this end, we must discuss the conformal invariance of the free EM field under the conformal transformation in a conformally flat background for a source-free case. If we make a conformal transformation of the metric as

$$\tilde{g}_{\mu\nu} = a^2(\eta) g_{\mu\nu}, \tag{2.6}$$

where, $\tilde{g}_{\mu\nu}$ is the transformed metric. Under this transformation $\sqrt{-\tilde{g}} = a^4(\eta)\sqrt{-g}$, and $\tilde{g}^{\mu\nu} = 1/a^2(\eta) g^{\mu\nu}$. As it is only a transformation of the metric, it does not change the field variables. So, if $F^*_{\mu\nu}$ is the EM field tensor in the transformed $\tilde{g}_{\mu\nu}$, and $F_{\mu\nu}$ is the EM field tensor in the original metric, then we have $F^*_{\mu\nu} = F_{\mu\nu}$. The free EM action in the transformed metric transforms as

$$\begin{aligned}
\tilde{\mathcal{S}}_{em} &= -\frac{1}{4}\int d^4x \sqrt{-\tilde{g}}\tilde{g}^{\mu\alpha}\tilde{g}^{\nu\beta}F^*_{\mu\nu}F^*_{\alpha\beta} \\
&= -\frac{1}{4}\int d^4x a^4 \sqrt{-g}\left(1/a^2 g^{\mu\alpha} 1/a^2 g^{\nu\beta}F^*_{\mu\nu}F^*_{\alpha\beta}\right) \\
&= -\frac{1}{4}\int d^4x \sqrt{-g} g^{\mu\alpha} g^{\nu\beta}F_{\mu\nu}F_{\alpha\beta} \\
&= -\frac{1}{4}\int d^4x \sqrt{-g} F_{\mu\nu}F^{\mu\nu} \\
&= \mathcal{S}_{em} \, .
\end{aligned} \tag{2.7}$$

From a field-theoretic point of view, the energy density and pressure are represented in the energy-momentum tensor. Therefore, it is more feasible to represent the electric and magnetic fields in terms of the electromagnetic field tensor $F_{\mu\nu}$. To achieve the prescribed form of the space components of the electric field (E^{μ}) and magnetic field (B^{μ}), we choose an observer with four velocities u^{μ}, who measures the strength of the EM field. The four velocities of the observer are defined as follows, and they satisfy the condition

$$u^{\mu} = \frac{dx^{\mu}}{dt} \;\; ; \;\; u^{\mu}u_{\mu} = -1 \, . \tag{2.8}$$

With respect to the comoving observer, the electric and magnetic fields are defined as,

$$E_{\mu} = F_{\mu\nu}u^{\nu} \;\; ; \;\; B_{\mu} = \frac{1}{2}\varepsilon_{\mu\nu\alpha\beta}u^{\nu}F^{\alpha\beta} \, . \tag{2.9}$$

The definition of E^{μ}, B^{μ} promptly suggests that

$$E_{\nu}u^{\nu} = F_{\mu\nu}u^{\mu}u^{\nu} = 0 \, ; \; B_{\nu}u^{\nu} = \frac{1}{2}\varepsilon_{\mu\nu\alpha\beta}u^{\mu}F^{\alpha\beta}u^{\nu} = 0 \, . \tag{2.10}$$

Eq.(2.10) infers that the spacelike hypersurface formed by the $(E \; and \; B)$ field is orthogonal to the direction of the four velocity vectors of the observer.

To satisfy the constraint on the four-velocity of the observer mentioned in Eq.(2.8), in the case of FLRW background, the comoving four-velocity of the observer turns out as $u^{\nu} = \left(\frac{1}{a}, 0, 0, 0\right)$, using Eq.(2.9) we can define the electric and the magnetic field in terms of the field strength tensor as

$$E_i = \frac{1}{a}F_{i0} \;\; ; \;\; B_i = \frac{1}{2a}\varepsilon_{ijk0}F^{jk} = \frac{1}{2a}\varepsilon_{ijk0}\delta^{l}_{j}\delta^{m}_{k}F_{lm} \, . \tag{2.11}$$

Now, we can get the regular Maxwell's equations by substituting Eq.(2.11) into Eq.(2.4) and (2.5).

2.2 Inflationary dynamics and Generation of magnetic fields during the inflationary era

In this section, we will briefly discuss the dynamics of the scalar field inflation. Furthermore, discuss the mechanism of generating a large-scale magnetic field during an inflationary era.

To observe the accelerated expansion of the Universe, we consider a scalar field $\phi(\vec{x}, t)$ with potential $V(\phi)$. The action corresponding to the field turns out to be,

$$\mathcal{S}_\phi = \int d^4x\sqrt{-g}\left[-\frac{1}{2}\partial_\mu\phi\partial^\mu\phi - V(\phi)\right]. \tag{2.12}$$

The energy-momentum tensor of the field $\phi(\vec{x}, t)$ is given by

$$T_{\mu\nu} = \partial_\mu\phi\partial_\nu\phi - g_{\mu\nu}\left(\frac{1}{2}g^{\alpha\beta}\partial_\alpha\phi\partial_\beta\phi - V(\phi)\right). \tag{2.13}$$

Inherently, the Universe is assumed to be homogeneous and isotropic. Therefore, the scalar field ϕ should be only a function of time. Calculating the energy density ($\rho_\phi = -T^0_0$) and the pressure density ($p_\phi\delta^i_j = -T^i_j$) for the field turns out as

$$\rho_\phi = \frac{1}{2}\dot{\phi}^2 + V(\phi), \tag{2.14}$$

$$p_\phi = \frac{1}{2}\dot{\phi}^2 - V(\phi). \tag{2.15}$$

Extremizing Eq.(2.12), we get the evolution equation of the field as,

$$\ddot{\phi} + 3H\dot{\phi} + \frac{dV}{d\phi} = 0. \tag{2.16}$$

Now, substituting Eq.(2.14) into Eq.(1.5), we get the conditions satisfied by the scale factor

$$\left(\frac{\dot{a}}{a}\right)^2 + \frac{K}{a^2} = \frac{8\pi G}{3}\left(\frac{1}{2}\dot{\phi}^2 + V(\phi)\right), \tag{2.17}$$

$$\frac{\ddot{a}}{a} = -\frac{8\pi G}{3}\left(\dot{\phi}^2 - V(\phi)\right). \tag{2.18}$$

For accelerated expansion of the Universe, the scale factor has to satisfy $\ddot{a} > 0$. Now, from the above equation, it is evident that to satisfy this condition, we need to have $V(\phi) > \dot{\phi}^2$, i.e., the potential energy of the field must be greater than the kinetic energy. The slow roll parameters introduced in Eq.(1.13) and (1.14) can also be represented in terms of the potential of the scalar field as

$$\epsilon \equiv \frac{M_{pl}^2}{2}\left(\frac{V_{,\phi}}{V}\right)^2 < 1 \;\; ; \;\; \eta \equiv M_{pl}^2\left|\frac{V_{,\phi\phi}}{V}\right| < 1. \tag{2.19}$$

Where $V_{,\phi} = dV/d\phi$ and $V_{,\phi\phi} = d^2V/d^2\phi$. As the parameters satisfy the slow roll condition, this gives us slow-roll inflation. This higher potential energy ensures that the Universe goes through an accelerated expansion, and the Hubble parameter stays almost constant during this period. Considering a de-Sitter Universe, the scale factor during inflation varies as

$$a = e^{H_f t} = -\frac{1}{H_f \eta}, \tag{2.20}$$

a is the scale factor, t is the cosmic time, η is the conformal time, and H_f is the Hubble parameter during inflation, which remains constant throughout this period. For the FLRW metric, Maxwell's first Eq.(2.4) transforms into

$$\eta^{\mu\alpha}\eta^{\nu\beta}\frac{\partial}{\partial x^\mu}F^{\alpha\beta} = a^4 J^\nu. \tag{2.21}$$

In the literature, specific gauge choices are taken to remove the degeneracy, and the Coulomb gauge is the most convenient one. The Coulomb gauge follows $A_0 = 0$ and $\partial_i A^i = 0$. During the inflationary era, there was no ionization, so we can safely assume that the current density was zero. Furthermore, the density will be negligible even if there is some residual charge due to the accelerated expansion. So from Eq.(2.21) for the spatial components of the electromagnetic vector potential, we get the time evolution of the field components as

$$A_i'' - a^2\partial_j\partial^j A_i = 0. \tag{2.22}$$

Where the prime denotes a derivative with respect to the conformal time (η) and the contravariant derivative is defined as $\partial^i \equiv g^{ij}\partial_j = a^{-2}\delta^{ij}\partial_j$. It is also necessary to evaluate the modes affected during the inflation, that is, the modes inside the Hubble horizon during the inflationary era. Therefore, we can write the EM vector potential in terms of its Fourier modes as

$$A_i(\vec{x},\eta) = \int \frac{d^3k}{(2\pi)^3} u_i(\vec{k},\eta) e^{i\vec{k}\cdot\vec{x}}. \tag{2.23}$$

In terms of the momentum mode function $u_i(\vec{k},\eta)$ the Eq.(2.22) boils down to

$$u_i'' + k^2 u_i = 0. \tag{2.24}$$

In Eq.(2.24) k is the comoving wave number, defined as $k^2 = \delta^{ij}k_ik_j$. As all the different momentum modes satisfy the same equation, we can choose a set of bases for each momentum mode, known as the polarization basis, and it is represented as

$$u_i(\vec{k},\eta) = \sum_p u_k^p(\eta) g_{ij} \mathbf{e}_p^j. \tag{2.25}$$

Here, e_p^j forms an orthonormal set of four basis vectors.

$$\mathbf{e}_0^\alpha = \left(\frac{1}{a}, \vec{0}\right) \; ; \; \mathbf{e}_p^\alpha = \left(0, \frac{e_p^i}{a}\right) \; ; \; \mathbf{e}_3^\alpha = \left(0, \frac{\hat{k}}{a}\right). \tag{2.26}$$

The basis vectors follow the relation that e_p^α are orthogonal to each other and also orthogonal to the direction of propagation $\hat{k}$. The polarization vectors follow the Coulomb gauge condition in momentum space and satisfy the relation

$$\sum_{p=1,2} e_p^i(\vec{k}) e_{jp}(\vec{k}) = \delta_j^i - \frac{\delta_{jm}k^ik^m}{k^2}. \tag{2.27}$$

The relation mentioned in Eq.(2.27) is also known as the projection relation, as it can be used to calculate the projection of any vector along a particular polarization direction. Substituting Eq.(2.27) into Eq.(2.24), we get the evolution for each polarization mode

$$\bar{u}_k^{p''} + k^2 \bar{u}_k^p = 0, \tag{2.28}$$

where $\bar{u}_k^p \equiv a u_k^p$. The Eq.(2.28) is essentially a harmonic oscillator equation. By the linearity property of the equation, the full solution of this equation consists of the linear combination of the real (u_k^p) and complex conjugate (u_k^{p*}) of the equation. Therefore, the full solution to Eq.(2.28) is

$$\bar{u}^p_k(\eta) = c^p_k \bar{u}^p_k + d^p_k \bar{u}^{p*}_k , \tag{2.29}$$

where c^p_k and d^p_k are integration constants.

Therefore, the full solution to the EM vector potential of Eq.(2.23) requires the field to be real

$$A_i(\vec{x},\eta) = \int \frac{d^3k}{(2\pi)^3} \sum_{p=1,2} e^p_i \left(c^p_k u^p_k e^{i\vec{k}\cdot\vec{x}} + c^{p\dagger}_k u^{p*}_k e^{-i\vec{k}\cdot\vec{x}} \right) . \tag{2.30}$$

To evaluate the quantum fluctuation produced as an EM field, we need to quantize the field. So, we promote the field variable A_i to an operator $\hat{A}_i$. The free EM Lagrangian in terms of A_i boils down to,

$$\begin{aligned} \mathcal{L}_{em} &= -\frac{1}{4} F_{\mu\nu} F^{\mu\nu} \\ &= \frac{1}{2} a^2 g^{ij} A'_i A'_j - \frac{1}{4} g^{ij} g^{mn} F_{im} F_{jn} . \end{aligned} \tag{2.31}$$

The conjugate momentum corresponding to the field operator $\hat{A}_i$ is defined as

$$\Pi^i = \frac{\delta \mathcal{L}_{em}}{\delta A'_i} = a^2 g^{ij} A'_j \ ; \ \Pi_i = a^2 A'_i . \tag{2.32}$$

The quantization of the field is done as

$$\left[\hat{A}^i(\vec{x},\eta), \hat{\Pi}_j(\vec{y},\eta) \right] = i \int \frac{d^3k}{(2\pi)^3} e^{i\vec{k}\cdot(\vec{x}-\vec{y})} \left(\delta^i_j - \frac{k^i k_j}{k^2} \right) . \tag{2.33}$$

As we promote the field variable A_i to the operator, the constants c^p_k also become an operator. They are called $\hat{c}^p_k$, $\hat{c}^{p\dagger}_k$ creation and annihilation operators respectively. They follow the commutation relation

$$\left[\hat{c}^p_k, \hat{c}^{p'}_{k'} \right] = 0 \ ; \ \left[\hat{c}^{p\dagger}_k, \hat{c}^{p'\dagger}_{k'} \right] = 0 \ ; \ \left[\hat{c}^p_k, \hat{c}^{p'\dagger}_{k'} \right] = (2\pi)^3 \delta^3(\vec{k} - \vec{k}') \delta_{pp'} . \tag{2.34}$$

Therefore, using the commutation relation between the field operator and its conjugate momentum, it turns out that by employing the commutation relation between the creation and annihilation operators, we get that the momentum mode u^p_k satisfies the normalization condition

$$i\left(u_k^{p'}u_k^{p*}-u_k^{p}u_k^{p*'}\right)=\frac{1}{a^2}\,. \tag{2.35}$$

The energy density of the produced EM field needs to be calculated using a proper vacuum. The vacuum is defined as

$$\hat{c}_k^p|0\rangle=0\,. \tag{2.36}$$

The proper choice of vacuum is fixed by the Bunch-Davies vacuum condition, which means there are only outgoing waves at the past infinity of the Universe. From the normalization condition obtained in Eq.(2.35), we finally get the solution of the field mode

$$\bar{u}_k^p=\frac{1}{\sqrt{2k}}e^{-ik\eta}\,. \tag{2.37}$$

Now, with the formalism in hand, we can calculate the energy density and, correspondingly, the strength of the generated EM field during inflation. The energy-momentum tensor of the produced EM field can be obtained by

$$T\mu\nu=-\frac{2}{\sqrt{-g}}\frac{\delta\left[\sqrt{-g}\mathcal{L}_{EM}\right]}{\delta g^{\mu\nu}}=g^{\alpha\beta}F_{\mu\alpha}F_{\nu\beta}-\frac{1}{4}g_{\mu\nu}F^{\alpha\beta}F_{\alpha\beta}. \tag{2.38}$$

The total energy density consists of the electric and magnetic fields. In terms of the comoving observers, it is defined as,

$$\begin{aligned}\rho_{em}=T_{\mu\nu}u^\mu u^\nu &= -\frac{1}{2a^2}g^{ij}A'_iA'_j-\frac{1}{4}g^{ij}g^{kl}\left(\frac{\partial A_k}{\partial x^i}-\frac{\partial A_i}{\partial x^k}\right)\left(\frac{\partial A_l}{\partial x^j}-\frac{\partial A_j}{\partial x^l}\right)\\ &= T^E_{\mu\nu}u^\mu u^\nu+T^B_{\mu\nu}u^\mu u^\nu\,. \end{aligned} \tag{2.39}$$

In Eq.(2.39), the total energy density has been represented as a sum of the electric and magnetic fields. From the definition of the electric and magnetic field shown in Eq.(2.9), ρ_E and ρ_B can be written in terms of the field as,

$$\rho_E=T^E_{\mu\nu}u^\mu u^\nu = \frac{1}{2a^2}g^{ij}A'_iA'_j=\frac{1}{2}E_iE^i \tag{2.40}$$

$$\rho_B=T^B_{\mu\nu}u^\mu u^\nu = \frac{1}{4a^2}g^{ij}g^{kl}\left(\frac{\partial A_k}{\partial x^i}-\frac{\partial A_i}{\partial x^k}\right)\left(\frac{\partial A_l}{\partial x^j}-\frac{\partial A_j}{\partial x^l}\right)=\frac{1}{2}B_iB^i\,. \tag{2.41}$$

The energy densities are calculated with respect to the vacuum expectation values of the EM field tensor. Therefore, using the field as the operator (Eq.(2.30)), we get ρ_B

$$\rho_B = \langle 0|T_{\mu\nu}u^\mu u^\nu|0\rangle = \frac{1}{2\pi^2 a^4}\int \frac{dk}{k} k^5 |\bar{u}_k(\eta)|^2 \,. \tag{2.42}$$

It is more convenient to represent the energy density in terms of spectral density. Thus, in terms of spectral density, we have

$$\rho_E = \int d\ln k \frac{d\rho_E}{d\ln k}\; ; \; \rho_B = \int d\ln k \frac{d\rho_B(\eta,k)}{d\ln k} \,. \tag{2.43}$$

In terms of the mode functions, the electric and magnetic field power spectra are represented as

$$\frac{d\rho_E}{d\ln k} = \frac{1}{2\pi^2 a^4} k^3 |\bar{u}_k'|^2 \; ; \; \frac{d\rho_B}{d\ln k} = \frac{1}{2\pi^2 a^4} k^5 |\bar{u}_k|^2 \,. \tag{2.44}$$

It is important to mention that in Eq.(2.44), the quantities are represented in SI units. As the power spectra are a function of time, we can estimate the energy density and, correspondingly, the strength of the EM field at the end of inflation when the production seizes. Substituting Eq.(2.37) in Eq.(2.44), we get the power spectra at the end of inflation

$$\left.\frac{d\rho_E}{d\ln k}\right|_{\eta=\eta_f} = \frac{1}{2\pi^2}\left(\frac{k^4}{a^4 H_f^4}\right) H_f^4 \; ; \; \left.\frac{d\rho_B}{d\ln k}\right|_{\eta=\eta_f} = \frac{1}{2\pi^2}\left(\frac{k^4}{a^4 H_f^4}\right) H_f^4 \,. \tag{2.45}$$

Where η_f represents the conformal time corresponding to the end of inflation, a_f is the scale factor at the end of inflation, and H_f is the Hubble parameter during inflation. We have already shown in Eq.(2.40) that the EM energy is proportional to $\rho_{E/B} \propto (E/B)^2$. Following that argument, the amplitude of the fluctuation of the magnetic field over a length scale L_c can be estimated as [57]

$$B(L_c,\eta) \approx \sqrt{8\pi}\left.\left(\frac{d\rho_B}{d\ln k}\right)^{1/2}\right|_{k\sim 1/L_c} \,. \tag{2.46}$$

Furthermore, to compare the strength of the magnetic field with the present observational constraints, we need to evolve the produced EM field in the post-inflationary era. In the next section, we discuss different evolution scenarios depending on the evolution of the Universe.

2.3 Post-inflationary evolution of the electromagnetic field

The strength of the magnetic field at the present day depends on the post-inflationary evolution of the Universe. The Universe undergoes a short reheating period, where the inflaton field decays into several standard model particles and charged particles. That gives rise to a finite conductivity of the Universe. Generally, for simplicity, the Universe is assumed to undergo an instantaneous reheating scenario, where it is assumed that the Universe instantly goes into plasma after the end of inflation. Although an extended period of reheating enhances the strength of the magnetic field, we will show that in this scenario, when the conformal invariance of the EM field action is not broken, the strength of the magnetic field is way below the observed value. Therefore, in this section, we will specifically discuss the evolution of the EM field in the instantaneous reheating case.

Due to the decay of the inflaton field into charged particles, the conductivity of the Universe rises, and it plays a crucial role in the evolution of the EM field produced during the inflationary era. If the conductivity of the relativistic plasmonic medium is σ and the charge density in the medium is ρ_e, then the four-current density J^μ of the medium for an observer moving with four-velocity u^μ turns out as

$$J^\mu = \rho_e u^\mu + \sigma E^\mu \,. \tag{2.47}$$

Now substituting the expression of J^μ from Eq.(2.4) and E^μ from the definition in terms of the field variable $A_i(\vec{x}, \eta)$ in Eq.(2.22) we get the evolution of the EM vector potential in a relativistic medium with conductivity σ as

$$\ddot{A}_i + (H + 4\pi\sigma)\,\dot{A}_i - \partial_j\partial^j A_i = 0 \,. \tag{2.48}$$

Here, the conductivity of the medium (σ) is considered constant in time, and the dot represents the derivative with respect to cosmic time. In the post-inflationary evolution, all the modes of interest are outside the Hubble horizon. Therefore, for large-scale limits, the spatial derivative of the field can be neglected in comparison to the time derivative. Furthermore, in the instantaneous reheating scenario, the Universe turns into plasma almost instantly; therefore, the conductivity is very high. So, we can assume $\sigma >> H$, and under this assumption the solution to Eq.(2.48) becomes

$$A_i(\vec{x},t) = \frac{C_1(\vec{x})}{\sigma}\exp(-4\pi\sigma t) + C_2(\vec{x})\,. \tag{2.49}$$

The first term of the solution in Eq.(2.49) reveals that it decays very rapidly with a characteristic time scale $\sigma^{-1} << 1/H$. Effectively, the solution of the field variable in the plasma is $A_i(\vec{x},t) \approx C_2(\vec{x})$. As shown in the power spectrum of the EM field in Eq.(2.44), we can see that the electric field power spectrum depends on the time derivative of the mode function. Therefore, the electric field essentially goes to zero after inflation when the Universe has finite conductivity ($E_i \sim 0$) and the magnetic field gets frozen in and decays as $B_i \propto 1/a$. During the radiation-dominated era, the energy density of the magnetic field decays similarly to the energy density of the Universe $\rho_B \propto a^{-4}$.

The present strength of the magnetic field is evaluated considering the decay rate of the magnetic field energy density. It is related to the spectral energy density of the field at the end of inflation

$$\left.\frac{d\rho_B}{d\ln k}\right|_0 = \left(\frac{a_f}{a_0}\right)^4 \left.\frac{d\rho_B}{d\ln k}\right|_f, \tag{2.50}$$

where a_f is the scale factor at the end of inflation, and a_0 is the current scale factor. We have already established the spectral density at the end of inflation in Eq.(2.45). We can evaluate the strength at present by calculating the ratio (a_f/a_0). We assume the Universe instantly goes to radiation domination after the end of inflation and evolves adiabatically; then, the ratio turns out to be

$$\frac{a_f}{a_0} = \frac{g_0^{1/3}}{g_f^{1/12}} \frac{T_0}{(H_f M_{pl})^{1/2}} \left(\frac{8\pi^3}{90}\right)^{1/4} . \tag{2.51}$$

In the above equation, g_f and g_0 are relativistic degrees of freedom at the end of inflation and present, respectively. T_0 is the current CMB temperature, H_f is the Hubble parameter at the end of inflation and M_{pl} is the Planck mass. Considering the standard model (SM) particles contribute to the radiation degrees of freedom, we get $g_f = 106.75$. Therefore, the ratio becomes

$$\frac{a_f}{a_0} \sim 10^{-29} \left(\frac{H_f}{10^{-5} M_{pl}}\right)^{-1/2} . \tag{2.52}$$

The largest modes under consideration leave the Hubble horizon at the end of inflation $(k_f = a_f H_f)$. The value of $H_f = 10^{-5} M_{pl}$ comes from the CMBR constraints on the amplitude of scalar fluctuations during inflation. Hence, we obtain the present-day strength of the magnetic field for $k \sim 1 Mpc^{-1}$ as

$$B_0|_{k=1Mpc^{-1}} \approx 2 \times 10^{-57}\, G \, . \tag{2.53}$$

This strength of the magnetic field is too low to work as a seed magnetic field to be amplified by the Dynamo mechanism.

Therefore, from the above discussion, it is evident that due to the conformal invariance of the EM field under conformally flat spacetime, it is impossible to generate sufficient magnetic field strength from quantum fluctuations of the inflaton field during inflation without breaking the conformal symmetry.

2.4 Inflationary magnetogenesis by breaking the conformal symmetry

In the last section, we saw the evolution of the EM field when the conformal symmetry of the field was not broken. Moreover, we inferred that with the symmetry preserved, the strength of the produced field is very low, not even enough to work as a seed magnetic field. Therefore, breaking the conformal invariance of the EM field is important to produce sufficient magnetic field strength consistent with the observation.

Several mechanisms have been proposed in the literature to break the conformal invariance of the EM field. Conformal symmetry can be broken by coupling the EM field to any time-dependent scalar field during inflation [30,31]. However, the easiest possibility is to couple the EM field to the inflaton field, as it evolves during inflation [30–39]. In this section, we discuss the mechanism of breaking conformal symmetry by coupling the EM field to the inflaton field and study the evolution of both the inflaton and the gauge field during inflation. The total action of the system after breaking the conformal symmetry with a function of the inflaton field $I(\phi)$ is given by,

$$\mathcal{S} = -\int d^4x\sqrt{-g}\left[\frac{1}{4}I^2(\phi)F_{\mu\nu}F^{\mu\nu} + J^{\nu}A_{\nu}\right] - \int d^4x\sqrt{-g}\left[\frac{1}{2}\partial_{\nu}\phi\partial^{\nu}\phi + V(\phi)\right] . \tag{2.54}$$

The evolution of the inflaton and EM field satisfies, respectively:

$$\frac{1}{\sqrt{-g}}\frac{\partial}{\partial x^{\nu}}\left[\sqrt{-g}I^2(\phi)g^{\mu\alpha}g^{\nu\beta}F_{\alpha\beta}\right] = 0 , \tag{2.55}$$

$$\frac{1}{\sqrt{-g}}\frac{\partial}{\partial x^{\nu}}\left[\sqrt{-g}g^{\nu\alpha}\partial_{\alpha}\phi\right] - \frac{dV}{d\phi} = \frac{I}{2}\frac{dI}{d\phi}F_{\mu\nu}F^{\mu\nu} . \tag{2.56}$$

It is evident that if the coupling factor goes to unity, this action reduces to the Maxwellian action. Also, the gauge field does not affect the geometry of the background spacetime; it is solely dictated by the inflaton field ϕ. As the background spacetime is isotropic and homogeneous, assuming that the inflaton field is only a function of time is appropriate; the EM vector potential (A_i) of this modified action evolves as

$$A_i'' + 2\frac{I'}{I}A_i' - a^2\partial_j\partial^j A_i = 0 . \tag{2.57}$$

In momentum space, the evolution equation turns out to be

$$\bar{u}_k'' + 2\frac{I'}{I}\bar{u}_k' + k^2\bar{u}_k = 0 . \tag{2.58}$$

Where $\bar{u}_k = au_k$ is the scaled momentum mode of the EM vector potential corresponding to comoving wavenumber k. For further simplification, we transform the mode function as $\tilde{u}_k = Iau_k$, and it transforms into an equation of a harmonic oscillator with time-dependent frequency

$$\tilde{u}_k'' + \left(k^2 - \frac{I''}{I}\right)\tilde{u}_k = 0\,. \tag{2.59}$$

The coupling function I in Eq.(2.59) shows that if the quantity $I'' > 0$, then there is a possible growth in the EM field, i.e., the choice of the coupling function enhances EM field production. The spectral energy densities in terms of the mode function $\tilde{u}_k$ can be calculated as

$$\frac{d\rho_B}{d\ln k} = \frac{1}{2\pi^2}\frac{k^5}{a^4}|\tilde{u}_k|^2\,, \tag{2.60}$$

$$\frac{d\rho_E}{d\ln k} = \frac{I^2}{2\pi^2}\frac{k^3}{a^4}\left|\left(\frac{\tilde{u}_k}{I}\right)'\right|^2, \tag{2.61}$$

To study the mode function's evolution and calculate the EM field's spectral energy densities, we must solve Eq.(2.59) and the functional form of the coupling function I. As mentioned earlier, the EM field can grow depending on the coupling function. Therefore, considering the coupling function I to be only a function of time, it can be modeled as

$$I(\eta) \propto a^m\,, \tag{2.62}$$

where, m is a free index, and a is the scale factor during inflation. This model of the coupling function has been realized in the literature for different inflationary models [33]. The coupling term contributing to the mode evolution boils down to

$$\frac{I''}{I} = \frac{m(m+1)}{\eta^2}\,. \tag{2.63}$$

In the above equation, the scale factor is $a = -\frac{1}{H_f\eta}$, as the spacetime is de-Sitter and the Universe expands exponentially during inflation. Substituting the term in Eq.(2.59) becomes

$$\tilde{u}_k'' + \left(k^2 - \frac{m(m+1)}{\eta^2}\right)\tilde{u}_k = 0\,. \tag{2.64}$$

The solution of the evolution equation turns out to be a combination of the Bessel functions

$$\tilde{u}_k = (-k\eta)^2\left[c_1(k)J_{-m-1/2}(-k\eta) + c_2(k)J_{m+1/2}(-k\eta)\right]\,, \tag{2.65}$$

where $c_1(k)$ and $c_2(k)$ are the integration constants fixed by the initial conditions at the beginning of inflation. $J_{\pm m\pm 1/2}(-k\eta)$ are Bessel functions of first kind. Here, we can numerically show the growth of the mode function due to the introduction of the coupling function $I(\eta) \propto a^m$ (see 2.1). The modes under consideration during inflation

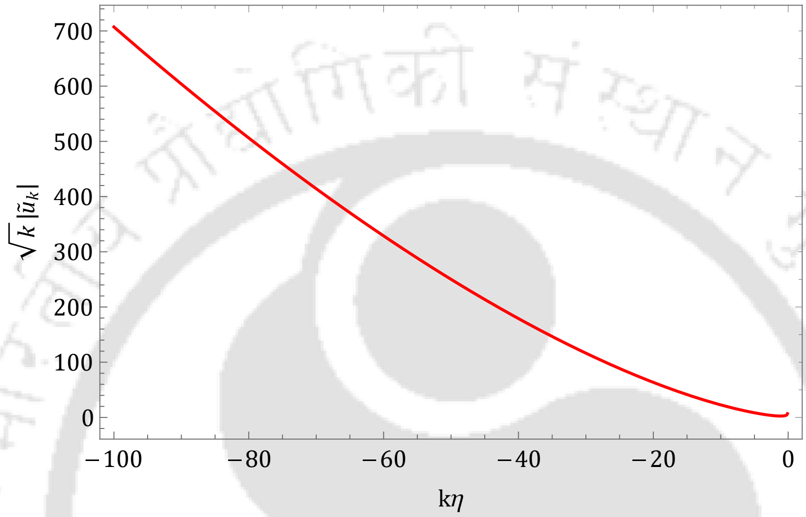

Figure 2.1: Evolution of the mode function $\tilde{u}_k$ with time for the coupling parameter $m = 2$.

are within the Hubble horizon, i.e., $(k/aH_f) >> 1$. We have already established that the scale factor during the inflationary era behaves as $a = -1/H\eta$; therefore, for all the modes towards the beginning of inflation, which satisfy $-k\eta >> 1$, in this limit, the evolution equation of the mode function (2.64) can be approximated as

$$\tilde{u}_k'' + k^2 \tilde{u}_k = 0 \,. \tag{2.66}$$

With the condition of the mode function having to be finite, we get the solution of the mode function at infinite past, or the Bunch-Davies vacuum solution, as

$$\tilde{u}_k(\eta) = \frac{1}{\sqrt{2k}} e^{-ik\eta} \,. \tag{2.67}$$

Now comparing the initial condition of the solution to Eq.(2.65) and expanding the Bessel function in the limit $|k\eta| >> 1$ we get the constants as,

$$c_1(k) = \sqrt{\frac{\pi}{4k}} \frac{\exp(\frac{i\pi m}{2})}{\cos(\pi m)} \;\; ; \;\; c_2(k) = \sqrt{\frac{\pi}{4k}} \frac{\exp\left(\frac{i\pi(-m+1)}{2}\right)}{\cos(\pi m)} \,. \tag{2.68}$$

As we have seen earlier, the present strength of the magnetic field is established in terms of the spectral energy density of the magnetic field at the end of inflation. In the superhorizon limit, i.e., towards the end of inflation ($k\eta \to 0$), all the modes of interest are outside the Hubble horizon. In the superhorizon limit, the solution of the mode function can be expressed as

$$\tilde{u}_k(\eta) = d_1(k)(-k\eta)^{-m} + d_2(k)(-k\eta)^{1+m} \,, \tag{2.69}$$

where,

$$d_1(k) = \frac{\sqrt{\frac{\pi}{2k}}}{2^{-m}} \frac{\exp(\frac{i\pi m}{2})}{\Gamma(-m+1/2)\cos(\pi m)} \;\; ; \;\; d_2(k) = \frac{\sqrt{\frac{\pi}{2k}}}{2^{m+1}} \frac{\exp\left(\frac{i\pi(1-m)}{2}\right)}{\Gamma(m+3/2)\cos(\pi m)} \,. \tag{2.70}$$

The first term in Eq.(2.69) dominates when $m > -1/2$, and the second term dominates when $m < -1/2$; with the substitution of the solution, we get the spectral energy density of the magnetic field

$$\frac{d\rho_B}{d\ln k} \approx \frac{\mathcal{F}(n)}{2\pi^2} H_f^4 (-k\eta)^{4+2n} \,, \tag{2.71}$$

where,

$$\mathcal{F}(n) = \frac{\pi}{2^{2n+1}(\Gamma(n+1/2))^2 \cos^2(\pi n)} \,. \tag{2.72}$$

Here the argument has been represented by n, where $n = -m$ when $m \geq -1/2$ and $n = 1+m$ when $m \leq -1/2$. From the spectral energy density expression, we can see that the spectrum is scale variant when $4+2n = 0$, which gives us the choice of $m = 2$ or $m = -3$. With those specific choices of the coupling parameter, the magnetic field becomes scale invariant and time independent.

Similarly, the spectral density of the electric field can be written as

$$\frac{d\rho_E}{d\ln k} \approx \frac{\mathcal{G}(l)}{2\pi^2} H_f^4 (-k\eta)^{4+2l} \,. \tag{2.73}$$

In the above expression

$$\mathcal{G}(l) = \frac{\pi}{2^{2l+3}(\Gamma(l+3/2))^2 \cos^2(\pi l)} \,. \tag{2.74}$$

Here $l = 1 - m$ for $m \geq 1/2$ and $l = m$ for $m \leq 1/2$. The choice of parameters, in order to have a scale-invariant electric field spectrum, does not coincide with the choice for a scale-invariant magnetic field. Therefore, obtaining a scale-invariant magnetic field and a scale-invariant electric field simultaneously is impossible.

2.5 Post-inflationary evolution and present strength of the magnetic field

After the end of inflation, the inflaton decays into radiation. In the literature, two different evolution pictures have been proposed: when the inflaton instantly decays, and the Universe turns into plasma. Therefore, in that scenario, the radiation-dominated era starts just after the end of inflation. However, in a more realistic scenario, all the inflatons take some time to turn into radiation, and this elongated period is known as the reheating period. Therefore, during this period, the conductivity of the Universe is finite, and the evolution of the EM field is different. Hence, the present strength of the magnetic field is different in these two cases.

2.5.1 Evolution for instant reheating scenario

After the end of inflation, the inflaton instantly decays into radiation. Moreover, as a result, the Universe turns into plasma, and the conductivity of the Universe is very high. The electric field dies instantly, and the magnetic field freezes in the medium. Consequently, the magnetic field decays according to the energy decay law of the Universe. The strength of the magnetic field in the present day is related to the spectral energy density at the end of inflation. The magnetic field spectral density for scale-invariant magnetic field $m = -3$, at the end of inflation turns out to be,

$$\left.\frac{d\rho_B}{d\ln k}\right|_f \approx \frac{9}{4\pi^2} H_f^2 \,. \tag{2.75}$$

During the radiation domination, the energy density decays as $\rho_B \propto a^{-4}$; with this, the present strength of the magnetic field in the case of instantaneous reheating. And following the relations (2.50) and (2.51) we can estimate the strength as,

$$B_0 \approx 10^{-10}\, G \left(\frac{H_f}{10^{-5} M_{pl}}\right) . \tag{2.76}$$

The above analysis shows that if we can break the conformal invariance of the EM field during inflation by introducing a coupling of $I \propto a^2$ or a^{-3}, we can produce sufficient EM field during inflation, such that the present strength of the magnetic field is $\sim 10^{-10}$ G. Which is enough to seed several amplification processes, even when we consider that the Universe goes through an instant reheating scenario.

2.5.2 Evolution for an elongated reheating period

After the end of inflation, until the radiation domination occurs, the corresponding period is considered a reheating period, when the inflaton decays into radiation. As the conductivity of the Universe is finite during this period, the electric field does not go to zero instantly. Moreover, due to the Faraday effect, it converts into a magnetic field and vice versa [70,92].

In the last section, we have already established that it is impossible to obtain a scale-invariant electric field and a scale-invariant magnetic field simultaneously. Therefore, the strength of the electric field is much higher when dealing with a scale-invariant magnetic field. Hence, by converting into a magnetic field, the electric field further enhances the present strength of the magnetic field.

In Eq.(5.2), we have considered the coupling function proportional to the power law of the scale factor. In a general scenario, the coupling function is taken as

$$I(\eta) = \left(\frac{a}{a_f}\right)^m , \tag{2.77}$$

where a_f is the scale factor at the end of inflation. This form of coupling is chosen to restore the conformal invariance of the EM field after inflation ends. And the evolution of the EM follows the Maxwellian evolution.

At the end of inflation, the coupling factor goes to unity. The evolution of the mode function is dictated by

$$\tilde{u}_k''^{(re)} + k^2 \tilde{u}_k^{(re)} = 0 \,, \tag{2.78}$$

where $\tilde{u}_k^{(re)}$ is the momentum space mode function during the reheating era. The solution of the mode function during reheating turns out to be

$$\tilde{u}_k^{(re)}(\eta) = \frac{1}{\sqrt{2k}} \left[\alpha_k e^{-ik(\eta-\eta_f)} + \beta_k e^{ik(\eta-\eta_f)}\right] \,. \tag{2.79}$$

The integration constants α_k and β_k are known as the Bogoliubov coefficients. They are evaluated by the continuity of the mode function in the reheating era and at the end of inflation, where η_f corresponds to the end of inflation. The constants turn out to be

$$\alpha_k = \sqrt{\frac{k}{2}} \tilde{u}_k(\eta_f) + \frac{i}{\sqrt{2k}} \tilde{u}_k'(\eta_f) \,, \tag{2.80}$$

$$\beta_k = \sqrt{\frac{k}{2}} \tilde{u}_k(\eta_f) - \frac{i}{\sqrt{2k}} \tilde{u}_k'(\eta_f) \,. \tag{2.81}$$

The power spectra of the EM field during the reheating period turn out to be

$$\frac{d\rho_E}{d\ln k} = \frac{1}{4\pi^2} \frac{k^2}{a^4} |\tilde{u}_k'^{(re)}(\eta)|^2 \,, \tag{2.82}$$

$$\frac{d\rho_B}{d\ln k} = \frac{1}{4\pi^2} \frac{k^5}{a^4} |\tilde{u}_k^{(re)}(\eta)|^2 \,. \tag{2.83}$$

The spectra can also be represented in terms of Bogoliubov coefficients, by substituting Eq.(4.39) into Eq. (2.82) it boils down to

$$\frac{d\rho_E}{d\ln k} \simeq \frac{2}{\pi^2} \frac{k^4}{a_{re}^4} |\beta_k^{re}|^2 \,, \tag{2.84}$$

$$\frac{d\rho_B}{d\ln k} \simeq \frac{1}{2\pi^2} \frac{k^4}{a^4} |\beta_k^{re}|^2 \left(\theta_k^{re}\right)^2 \,. \tag{2.85}$$

Where the phase factor is $\theta_k \equiv arg(\alpha_k \beta_k^*) - \pi$. In the reheating era, the phase factor is calculated

$$\theta_k^{re} = \{Arg\left[\alpha_k(k\eta_f)\beta_k^*(k\eta_f)\right] - \pi\} - 2k \int_{a_f}^{a_{re}} \frac{da}{a^2 H} \,. \tag{2.86}$$

Depending on the evolution of the Universe, the last term takes a simpler form [70]

$$2k\int_{a_f}^{a_{re}}\frac{da}{a^2H}\rightarrow\frac{4k}{3\omega+1}\left(\frac{1}{a_{re}H_{re}}-\frac{1}{a_fH_f}\right). \tag{2.87}$$

After the end of reheating, the Universe goes into radiation domination. The energy density decays as $\rho\propto a^{-4}$, and the present strength of the magnetic field is calculated from the conservation of total energy

$$\left.\frac{d\rho_B}{d\ln k}\right|_0=\left(\frac{a_{re}}{a_0}\right)^4\left.\frac{d\rho_B}{d\ln k}\right|_{re}. \tag{2.88}$$

The ratio of the scale factors $a_0/a_{re}, a_{re}/a_f$ and the evolution of the Hubble parameter are dependent on the reheating parameters (T_{re},N_{re}) and the effective equation of state (ω_{eff}) of the Universe. The relations among the reheating parameters are obtained by the conservation of entropy in the inflationary and the reheating era. It can be listed as,

$$H_{re} = H_f\left(\frac{a_{re}}{a_f}\right)^{-\frac{3}{2}(1+\omega_{eff})}, \tag{2.89}$$

$$T_{re} = \left(\frac{43}{11g_{s,re}}\right)^{1/3}\frac{a_0T_0}{k'}H_ke^{-N_k}e^{-N_{re}}, \tag{2.90}$$

$$\frac{a_0}{a_{re}} = \left(\frac{11}{43g_{s,re}}\right)^{1/3}\frac{T_{re}}{T_0}. \tag{2.91}$$

Where $g_{s,re}$ is the total degrees of freedom of the SM particles during reheating, a_{re} is the scale factor at the end of reheating, T_{re} is the reheating temperature, N_{re} is the duration of the reheating period, H_k is the Hubble parameter during the horizon crossing, N_k is the e-folding number during the horizon crossing, T_0 is the present temperature of the Universe, and a_0 is the present scale factor.

The present strength of the magnetic field depends on the background evolution. If the Universe goes through an elongated reheating period, the strength of the magnetic field enhances. Furthermore, the reheating parameters play a crucial role in determining the strength of the field. Moreover, from the CMB constraints on the present-day magnetic field strength, we can also constrain the effective equation of state of the Universe during the reheating era. Essentially, the primordial magnetic field works as a probe to the dynamics of the Universe during reheating.

2.6 Challenges in inflationary magnetogenesis

We observed that it is possible to generate sufficient magnetic field strength via the power law coupling ($I \propto a^m$) during inflation, which breaks the conformal invariance of the EM field. In the scale-invariant magnetic field, we established that power must be $m = 2, -3$. However, obtaining a scale-invariant electric field is impossible when the spectral energy density of the magnetic field is already scale-invariant. Therefore, it causes some challenges in the inflationary magnetogenesis scenario. The challenges are discussed below.

2.6.1 Backreaction problem

In the first case, when $m = -3$, we have scale-invariant magnetic energy density spectra. However, from Eq.(2.73), we have $4 + 2l = -2$, which implies that the energy density of the electric field in the superhorizon limit varies as $\rho_E \propto (-k\eta)^{-2}$. Towards the end of inflation ($-k\eta \to 0$) the electric field energy density increases rapidly ($\rho_E \to \infty$). Therefore, the total energy density of the produced EM field might exceed the inflation energy density even before sufficient inflation has occurred. This problem is called the backreaction problem of inflationary magnetogenesis. Therefore, the production of scale-invariant magnetic fields is very much constrained. It also gives rise to the finite conductivity of the medium, and the Schwinger effect [36] further suppresses the production.

2.6.2 Strong coupling problem

In the case of $m = 2$, the electric field energy density spectra vary as $\rho_E \propto (-k\eta)^2$ and the magnetic field remains scale-invariant. Therefore, towards the end of inflation, $\rho_E \to 0$, when ($-k\eta \to 0$). As the electric field energy density decreases towards the end of inflation, the backreaction problem is avoided in this scenario. However, the coupling factor increases as $I \propto a^2$ and saturates at I_f at the end of inflation. Maxwell's equation with the source term becomes

$$\frac{1}{\sqrt{-g}} \frac{\partial}{\partial x^\nu} \left[\sqrt{-g} F^{\mu\nu}\right] = \frac{J^\mu}{I^2} \, . \tag{2.92}$$

The above equation suggests that the coupling parameter normalizes the effective charge of the electron as $e_N = \frac{e}{I^2}$. In the earlier section, it was discussed that the EM field's Maxwellian evolution must be restored after inflation as the coupling between the inflaton field and the EM field goes to unity. Therefore, the coupling factor at the end of inflation (I_f) must satisfy $I_f = 1$. Since it increases as a^2, the initial value of the coupling function has to be very low towards the beginning of inflation. The large value of the effective charge of the electron (e_N) suggests the EM theory cannot be treated as a free theory, and it has to be treated in a non-perturbative way, and this formalism breaks down in that regime. It is known as the strong coupling problem of inflationary magnetogenesis.

2.7 Conclusions

In this chapter, we discussed the framework of the generation and evolution of the EM field during the inflationary era. Today's large-scale structure of the Universe originated from the quantum fluctuations during inflation. They result from the perturbations provided by the inflaton field or any other scalar field present during the inflation. We explored the possibility of generating a seed magnetic field from quantum fluctuations during inflation. However, we concluded that the strength produced without breaking the conformal symmetry of the EM field in the conformally flat spacetime is very low, even to play the role of a seed magnetic field. Moreover, to produce sufficient magnetic field strength, the conformal invariance can be broken by introducing a coupling between the EM and inflaton fields in the form of $I^2 F_{\mu\nu} F^{\mu\nu}$. Although it overcomes the problem of producing a very low magnetic field to meet the constraints of the observations, it suffers from the backreaction and strong coupling problem in certain regimes.

3

Inflationary Magnetogenesis in the EFT framework

Contents

Based on *"Effective Theory of Inflationary Magnetogenesis and Constraints on Reheating"* by D. Maity, Sourav Pal and T. Paul, **JCAP 05 (2021) 045, [arXiv:2103.02411]**

In Chapter 2, we discussed the inflationary magnetogenesis model, where the conformal invariance of the EM field action under a conformally flat background was broken by coupling the inflaton field to the EM field in the form $I^2 F_{\mu\nu} F^{\mu\nu}$. We also observed that scale-invariant magnetic field spectra were obtained for the coupling parameter values $m = 2$ or $m = -3$. However, a scale-invariant magnetic field poses the problem of backreaction or strong-coupling, depending on the choice of coupling parameter. Specifically, for $m = -3$, the energy density of the produced EM field surpasses the inflaton energy density before sufficient inflation has been achieved, as discussed in 3.82. On the other hand, $m = 2$ does not pose any backreaction problem, and therefore it is more favourable in inflationary magnetogenesis. However, it might suffer from the strong coupling problem discussed in 2.6.2. This chapter proposes an inflationary magnetogenesis model in the Effective Field Theory (EFT) framework. EFT of cosmology is a very powerful tool and has been widely used to study inflation [59,60], bounce cosmology [61,62], and dark energy [63–65]. Here, the EM field is coupled to the inflationary fluctuations. The time-dependent inflaton field breaks the background time diffeomorphism symmetry, and the spatial diffeomorphism symmetry remains intact. Apart from the coupling with the spacetime perturbation, the EM field also has self-interactions that behave as a scalar under spatial diffeomorphism symmetry transformation. However, the self-interactions and the coupling to the spacetime perturbations break the conformal symmetry of the EM field, leading to the production of gauge fields from the primordial vacuum. Within this framework, we have explored the evolution of the EM field and the scalar and tensor perturbations throughout the cosmological evolution beginning from the inflationary era.

Furthermore, we discuss the two cases of electric field or magnetic field power spectra becoming scale-invariant, depending on the choice of the coupling parameter of the EM field and the inflaton field on the superhorizon limit. As discussed earlier, in the post-inflationary Universe, depending on the evolution of the Universe, we study the evolution of the EM field for two cases: (i) Firstly, an instantaneous reheating era where the Universe directly jumps into radiation domination after the end of the inflationary epoch, (ii) In the second scenario, we consider that the Universe goes through a reheating period with non-zero e-folding number. Specifically, we consider the regular reheating mechanism where the reheating period is parameterized by a constant equation of state (ω_{eff}) proposed by Kamionkowski et al. [66, 67]. Where the inflaton field instantly converts into a radiation field. (iii) Finally, we consider perturbative reheating, where the inflaton field continuously transforms into a radiation field perturbatively and the effective EoS becomes time-dependent [68]. Depending on the decay process of the inflaton field, the presence of a reheating period with a non-zero e-folding number enhances the magnetic field strength.

3.1 Evolution of EM field and perturbations during inflation

The total effective action of the system can be written as

$$\mathcal{S} = \mathcal{S}_{bg} + \mathcal{S}_{em} + \mathcal{S}_{sp} + \mathcal{S}_{int}, \tag{3.1}$$

with S_{bg} denotes the background action, S_{em} is the electromagnetic field action, S_{sp} symbolizes the action of the metric perturbation and S_{int} represents the interaction between the electromagnetic field and the metric perturbation variable. Following the idea of effective field theory (EFT) inflation [59, 60], the background action can be expressed as,

$$\mathcal{S}_{bg} = \int d^4x\sqrt{-g}\left[\frac{1}{2}M_{\rm Pl}^2 R - \Lambda(\eta) - c(\eta)g^{00}\right] \tag{3.2}$$

where $M_{\rm Pl}$ is the Planck mass and R is the Ricci scalar. Moreover, $f(\eta)$, $\Lambda(\eta)$ and $c(\eta)$ are the background EFT parameters and can be fixed by the background equations. The metric component g^{00} is one of the scalars under spacial diffeomophism symmetry $x^i = x^i + \xi^i(x,t)$, where ξ^i is arbitray spatial vector. We work in a spatially flat FLRW background metric in the present scenario.

$$ds^2 = -dt^2 + a^2(t)\delta_{ij}dx^i dx^j = a^2(\eta)(-d\eta^2 + \delta_{ij}dx^i dx^j) \ . \tag{3.3}$$

with η being the conformal time and related to the cosmic time (t) as $\eta = \int dt/a(t)$. The above FRW metric, along with the action (3.2), boils down to the background Friedmann equations as,

$$\begin{aligned} 3M_{\rm Pl}^2\mathcal{H}^2 &= a^2(\eta)\Big(c(\eta) + \Lambda(\eta)\Big) \\ -M_{\rm Pl}^2\Big(2\mathcal{H}' + \mathcal{H}^2\Big) &= a^2(\eta)\Big(c(\eta) - \Lambda(\eta)\Big), \end{aligned} \tag{3.4}$$

where $\mathcal{H} = a'/a$ is the conformal Hubble parameter, related to the cosmic Hubble parameter ($H = \dot{a}/a$) as: $\mathcal{H} = aH$. Comparing the Friedmann equations (3.4) with that of a specific gravity model, one can get certain forms of the functions $c(\eta)$ and $\Lambda(\eta)$ that correspond to the respective model. For example, scalar-Einstein-Gauss-Bonnet gravity theory, which can be consistent with Planck results for suitable choices of the Gauss-Bonnet coupling function and the scalar field potential [71–82], is described by the following time dependent effective theory parameters,

$$\begin{aligned} c(\eta(t)) &= \frac{1}{2}\dot{\phi}^2 - 4H^2\ddot{h} - 8H\dot{H}\dot{h} + 4H^3\dot{h} \\ \Lambda(\eta(t)) &= V(\phi) + 4H^2\ddot{h} + 8H\dot{H}\dot{h} + 20H^3\dot{h} \end{aligned} \tag{3.5}$$

where ϕ is the scalar field under consideration (generally the inflaton field), $V(\phi)$ and $h(\phi)$ denote the scalar field potential and the Gauss-Bonnet coupling function (with the scalar field), respectively.

Thereby, the scalar-Einstein-Gauss-Bonnet model is mapped into the EFT action (3.2) with the above expression for $c(\eta)$ and $\Lambda(\eta)$. Similarly the $F(R)$ gravity theory [83–85] can be embedded within the EFT action (3.2) for the following forms of $c(\eta)$

and $\Lambda(\eta)$ as,

$$\begin{aligned} c(\eta(t)) &= \dot{H}f'(R) + 3\big(\dddot{H} + 4\dot{H}^2 + 3H\ddot{H} - 4H^2\dot{H}\big)f''(R) + 18\big(4H\dot{H} + \ddot{H}\big)^2 f'''(R) \\ \Lambda(\eta(t)) &= -\frac{f(R)}{2} + \big(2\dot{H} + 3H^2\big)f'(R) - 3\big(\dddot{H} + 4\dot{H}^2 + 9H\ddot{H} + 20H^2\dot{H}\big)f''(R) \\ &- 18\big(4H\dot{H} + \ddot{H}\big)^2 f'''(R) \end{aligned} \tag{3.6}$$

respectively, with $f(R)$ being the correction of $F(R)$ over Einstein gravity, i.e $f(R) = F(R) - R$. Moreover, in the context of holographic inflation [86, 87], $c(\eta)$ and $\Lambda(\eta)$ in turn determine the corresponding holographic cut-off.

The electromagnetic field action, $\mathcal{S}_{em}$ is taken as,

$$\mathcal{S}_{em} = \int d^4x\sqrt{-g}\Big[-\frac{1}{4}f_1(\eta)F_{\mu\nu}F^{\mu\nu} + f_2(\eta)F_i^0F^{0i} + f_3(\eta)\epsilon^{ijk}F_i^0F_{jk} + f_4(\eta)\epsilon^{\mu\nu\alpha\beta}F_{\mu\nu}F_{\alpha\beta}\Big] \tag{3.7}$$

where $F_{\mu\nu} = \partial_\mu A_\nu - \partial_\nu A_\mu$ is the field strength tensor of the electromagnetic field A_μ. Following the same argument mentioned for the g^{00} metric component, the A^0 component of the A_μ will be invariant under the special diffeomorphism transformation. $f_i(\eta)$ $(i = 1, 2, 3, 4)$ are arbitrary analytic functions of η and denote the non-minimal coupling of the electromagnetic field. Such time-dependent coupling functions break the conformal invariance in the electromagnetic sector and lead to the gauge field production from the primordial quantum vacuum. It may be observed that $\mathcal{S}_{em}$ consists of all possible electromagnetic terms (up to second order) which behave as a scalar quantity under the spatial diffeomorphism. Moreover, at a later stage, we will consider The functions $f_i(\eta)$ are such that in the early Universe, the couplings introduce a non-trivial correction to the electromagnetic field evolution, while at late times, specifically at the end of inflation, $f_i(\eta)$ will turn out to be $f_1(\eta) = 1$, $f_2(\eta) = f_3(\eta) = f_4(\eta) = 0$ leading to standard Maxwellian evolution. The spacetime perturbation action $\mathcal{S}_{sp}$, following the line of EFT, is given by,

$$\mathcal{S}_{sp} = \int d^4x\sqrt{-g} \quad \Bigg[\quad \frac{M_2^4(\eta)}{2}\left(\delta g^{00}\right)^2 - \frac{m_3^3(\eta)}{2}\delta K\delta g^{00} - m_4^2(\eta)\left(\delta K^2 - \delta K_{\mu\nu}\delta K^{\mu\nu}\right)$$
$$+ \quad \frac{\tilde{m}_4^2(\eta)}{2}R^{(3)}\delta g^{00} - \bar{m}_4^2(\eta)\delta K^2 - \frac{m_5(\eta)}{2}R^{(3)}\delta K - \frac{\lambda_1(\eta)}{2}\left(R^{(3)}\right)^2$$
$$- \quad \frac{\lambda_2(\eta)}{2}\nabla_i R^{(3)}\nabla^i R^{(3)}\Bigg] \tag{3.8}$$

where all the coefficients are allowed to vary with η. All EFT parameters are so chosen that dimensions $[m_i] = 1$ and $[\lambda_i] = 0$. In the above expression, $\delta K_{\mu\nu} = K_{\mu\nu} - H\sigma_{\mu\nu}$, $\delta K = K - 3H$ where $K_{\mu\nu}$ and $\sigma_{\mu\nu}$ are the extrinsic curvature and induced metric on a constant time hypersurface, respectively. Moreover, δg^{00} is connected to the curvature perturbation variable $\Psi(\vec{x},\eta)$ in a non-trivial way, which we will introduce later. The quadratic action of $\Psi(\vec{x},\eta)$ from Eq.(3.8) contains terms like $\left(\partial\Psi(\vec{x},\eta)\right)^2$, $\left(\partial^2\Psi(\vec{x},\eta)\right)^2$ and $\left(\partial^3\Psi(\vec{x},\eta)\right)^2$; which, upon Fourier transformation, behave as, $\left(\partial\Psi\right)^2 \sim k^2\Psi_k^2$, $\left(\partial^2\Psi\right)^2 \sim k^4\Psi_k^2$ and $\left(\partial^3\Psi\right)^2 \sim k^6\Psi_k^2$ respectively. Where $\Psi_k(\eta)$ is the Fourier mode with momentum k. Even though they are quadratic in fluctuation, higher derivative terms will be generically suppressed by the inflationary energy scale H. We, therefore, will consider the curvature perturbation action up to the quadratic order in k. Hence, we choose the following condition for our subsequent discussions, [61,62],

$$\bar{m}_4 = m_5 = \lambda_1 = \lambda_2 = 0 \tag{3.9}$$

Correspondingly, δg^{00} is related to the metric curvature perturbation in the following way [61],

$$\delta g^{00} = \frac{4\left(\frac{1}{\kappa^2} + 2m_4^2\right)}{a(\eta)\left(\frac{2H}{\kappa^2} + 4Hm_4^2 - m_3^3\right)}\frac{\partial\Psi}{\partial\eta} \tag{3.10}$$

where $1/\kappa^2 = M_{\rm Pl}^2$ and as mentioned earlier, H is the Hubble parameter in cosmic time. For computational simplicity, we consider the inflationary phase to be nearly de-Sitter with scale factor $a(\eta) = -1/H\eta$. Now using Eqs.(3.9) and (3.10), the quadratic action

$\mathcal{S}_{sp}$ for the fluctuation becomes,

$$\mathcal{S}[v] = \int d^4x \left[(v')^2 + \frac{z''}{z} v^2 - c_s^2 g^{ij} \partial_i v \partial_j v \right], \tag{3.11}$$

where, $v(\vec{x}, \eta)$ is the Mukhanov-Sasaki variable defined as $v(\vec{x}, \eta) = z(\eta)\Psi(\vec{x}, \eta) = a(\eta)\sqrt{c_1}\ \Psi(\vec{x}, \eta)$. The quantity c_s^2 symbolizes the sound speed for the scalar perturbation and has the following expression,

$$c_s^2 = \frac{1}{c_1}\left(\frac{c_3'(\eta)}{a^2} - \frac{1}{\kappa^2} \right) \tag{3.12}$$

with c_1 and c_3 are expressed in terms of EFT parameters (i.e M_2, m_3, m_4 and $\tilde{m}_4$) as follows:

$$\begin{aligned} c_1(\eta) &= \frac{\left(\frac{1}{\kappa^2} + 2m_4^2 \right)\left(3m_3^6 + 8M_2^4\left[\frac{1}{\kappa^2} + 2m_4^2 \right] \right)}{\left(\frac{2H}{\kappa^2} + 4Hm_4^2 - m_3^3 \right)^2} \\ c_3(\eta) &= \frac{2a(\eta)\left(\frac{1}{\kappa^2} + 2m_4^2 \right)\left(\frac{1}{\kappa^2} + 2\tilde{m}_4^2 \right)}{\left(\frac{2H}{\kappa^2} + 4Hm_4^2 - m_3^3 \right)}. \end{aligned} \tag{3.13}$$

Moreover, the quadratic action for the tensor perturbation comes as,

$$\mathcal{S}[v_T] = \int d^4x \left[(v_T')^2 + \frac{z_T''}{z_T} v_T^2 - c_T^2 \left(\partial v_T \right)^2 \right] \tag{3.14}$$

with $z_T^2 = a^2(\eta)\left(1 + 2\kappa^2 m_4^2\right)$ and the speed of the gravitational wave (c_T^2) in terms of the EFT parameters is given by $c_T^2 = \left(1 + 2\kappa^2 m_4^2\right)^{-1}$.

Finally $\mathcal{S}_{int}$ refers to the quadratic interaction between the electromagnetic field and δg^{00}, which, in the context The form of EFT has the following form,

$$\mathcal{S}_{int} = \int d^4x \sqrt{-g} \left[h(\eta) \left(\partial_i \delta g^{00} \right) F^{0i} \right] \tag{3.15}$$

with $h(\eta)$ being the interaction coupling strength. Such interaction of electromagnetic field (A_μ), the curvature perturbation appears naturally in the EFT language due to the underlying spatial diffeomorphism symmetry. However, the possible interaction of A_μ with the tensor perturbation appears in higher-order action, and thus we do not consider those terms for our present study. Along with the quadratic terms with time dependent coupling functions $f_i(\eta)$ in Eq.(3.7), the term $h(\eta)\partial_i\delta g^{00}\ F^{0i}$ (present in S_{int}) also contributes to breaking the conformal invariance of the electromagnetic field action. In terms of the Mukhanov-Sasaki variable, Eq.(3.15) can be written as,

$$\mathcal{S}_{int} = -2\int d^4x\frac{h(\eta)B(\eta)}{a(\eta)\ z(\eta)}\ \partial_i\big[v' - \frac{z'}{z}v\big]\ F_{0i}\ , \ \text{ with }\ B(\eta) = \frac{4\left(\frac{1}{\kappa^2}+2m_4^2\right)}{\left(\frac{2H}{\kappa^2}+4Hm_4^2-m_3^3\right)} \tag{3.16}$$

Thus as a whole, $\mathcal{S}_{bg}$, $\mathcal{S}_{em}$, $\mathcal{S}_{sp}$ and $\mathcal{S}_{int}$ are given in Eqs.(3.2), (3.7), (3.8) and (3.16) respectively. In such a scenario, we aim to study inflationary magnetogenesis. In this regard, let us point out some salient features of the model

(i) The present magnetogenesis scenario will consider the coupled evolution of electromagnetic field and the spacetime perturbation, where, in particular, the electromagnetic field gets coupled with the curvature perturbation. However, the tensor perturbation evolves freely as it does not interact with the electromagnetic field or the scalar perturbation up to the quadratic order.

(ii) The time-dependent self-coupling of electromagnetic field denoted by the coupling strengths $f_i(\eta)$ and the interaction term with δg^{00} spoil the conformal invariance of the electromagnetic field action. The coupling strengths will be chosen so that after the inflationary epoch, the conformal invariance of A_μ will be restored and consequently the standard Maxwell's equations will be recovered.

(iii) Moreover, as we will show later, the well-known backreaction and strong coupling problem will be resolved in the present scenario for suitable parameter spaces.

In order to determine the equations of motion, let us recall that there are three independent fields in the model- the electromagnetic field A_μ, the scalar and tensor Mukhanov-Sasaki variables $v(\vec{x},\eta)$ and $v_T(\vec{x},\eta)$ respectively. The variation of action (3.1) with respect to the gauge field leads to the following equation of motion for A_μ,

$$
\begin{aligned}
&-\partial_a\left[a^4(\eta)f_1(\eta)g^{\mu a}g^{\nu b}F_{\mu\nu}\right]+2\partial_0\left[f_2(\eta)g^{ib}\,\partial_0 A_i\right]-2\delta_0^b\,\partial_j\left[f_2(\eta)g^{ij}\,\partial_0 A_i\right]\\
+&\;\;2\partial_0\left[a^2(\eta)f_3(\eta)\epsilon^{0bjk}\,\partial_j A_k\right]+2\partial_j\left[a^2(\eta)f_3(\eta)\epsilon^{0ijb}\,\partial_0 A_j\right]-2\delta_0^b\,\partial_i\left[a^2(\eta)f_3(\eta)\epsilon^{0ijk}\,\partial_j A_k\right]\\
+&\;\;8\partial_a\left[a^4(\eta)f_4(\eta)\epsilon^{\mu\nu\alpha\beta}\,\partial_\mu A_\nu\right]+\partial_0\left[a^2(\eta)h(\eta)g^{ib}\,\partial_i\delta g^{00}\right]=0
\end{aligned}
\tag{3.17}
$$

where we consider the spatially flat FRW metric ansatz as shown in Eq.(3.3). In the Coulomb gauge ($A_0=0$ and $\partial^i A_i=0$) condition, the relevant equation of motions for A_i's are,

$$
\begin{aligned}
&f_1(\eta)\left[A_i''+\frac{f_1'}{f_1}A_i'-\partial_l\partial_l A_i\right]+\frac{2}{a^2(\eta)}f_2(\eta)\left[A_i''+\frac{f_2'}{f_2}A_i'-\frac{2a'}{a}A_i'\right]+\frac{2}{a^2}f_3(\eta)\epsilon_{ijk}\left[\frac{f_3'}{f_3}-\frac{2a'}{a}\right]\partial_j A_k\\
&-8f_4'(\eta)\epsilon_{ijk}\,\partial_j A_k-h(\eta)\,\partial_0\partial_i\left(\delta g^{00}\right)-h'(\eta)\,\partial_i\left(\delta g^{00}\right)=0
\end{aligned}
\tag{3.18}
$$

with a prime denoting $\frac{d}{d\eta}$.

The equation of motion for the scalar and tensor perturbations will take the following form,

$$
\begin{aligned}
v''(\vec{x},\eta)-\frac{z''}{z}v-c_s^2\,\partial_i\partial^i v=0\\
v_T''(\vec{x},\eta)-\frac{z_T''}{z_T}v_T-c_T^2\,\partial_i\partial^i v_T=0\quad.
\end{aligned}
\tag{3.19}
$$

where the Coulomb gauge condition is used in the above derivation. with recall, $z(\eta)=a(\eta)\sqrt{c_1(\eta)}$ and c_s^2 is given in Eq.(3.12). It may be observed that the scalar perturbation evolves freely, but the electromagnetic field evolution depends on the scalar perturbation evolution through $h(\eta)$ as evident from Eq.(3.18). This is due to the Coulomb gauge condition. The solution of these equations requires a certain ansatz of the background spacetime scale factor $a(\eta)$ and the coupling functions $f_i(\eta)$, $h(\eta)$. For the background spacetime, we consider a de-Sitter inflationary spacetime, $a(\eta)=-1/H\eta$. H is a slowly varying function representing the Hubble parameter in cosmic time. The assoicated Hubble parameter in conformal time assumes, $\mathcal{H}=\frac{1}{a}\frac{da}{d\eta}=-1/\eta$. Furthermore, we introduce the inflationary e-folding number as $N(\eta)=\ln\left(a(\eta)\right)$, which is counted from the beginning of inflation where $N = 0$, and we consider the beginning of inflation to be the instant when the CMB scale mode crosses the horizon.

In particular, here we assume the EFT parameters are non-zero (i.e all the electromagnetic terms present in the EFT action (3.7) have been taken into account) and have the power law forms of the scale factor

$$f_1(\eta) = \begin{cases} \left(\frac{a(\eta)}{a_f(\eta_f)}\right)^2 & \eta \leq \eta_f \\ 1 & \eta \geq \eta_f \end{cases} \tag{3.20}$$

and

$$f_2(\eta) = \left(\frac{a_i(\eta_i)}{a(\eta)}\right)^m ; \; f_3(\eta) = \left(\frac{a_i(\eta_i)}{a(\eta)}\right)^r ; \; f_4(\eta) = \left(\frac{a_i(\eta_i)}{a(\eta)}\right)^s ; \; h(\eta) = h_0\left(\frac{a_i(\eta_i)}{a(\eta)}\right)^2 \tag{3.21}$$

where a_i and a_f are the scale factors at the beginning η_i and at the end of inflation η_f respectively. Moreover, h_0 is a constant having mass dimension unity. The exponents m, r, and s are positive numbers and can act as model parameters in the present context. Later, we will show that $m = r = s = 2$ leads to a scale-invariant magnetic power spectrum in the superhorizon limit. It is evident from the above expressions that $f_1(\eta)$ starts from e^{-2N_f} and monotonically increases till $\eta = \eta_f$, while the other coupling functions monotonically decrease with time during the inflationary stage. However in the post-inflationary phase, $f_1(\eta)$ becomes unity and $f_2(\eta) \approx f_3(\eta) \approx f_4(\eta) \approx h(\eta) \approx 0$, which in turn recovers the standard Maxwell's equations at a later time. Before embarking on our study with the aforementioned forms of the EFT parameters, let us contextualise our discussions by giving a few explicit model examples with elaborate discussions given in Appendix A **Generalized Ratra Model**: In this model, the conformal invariance is broken by a generic scalar function as a gauge kinetic function as

$$\mathcal{S}_{m1} = \int d^4x\sqrt{-g}\left[f^2(\phi, R, \mathcal{G})F_{\mu\nu}F^{\mu\nu}\right], \tag{3.22}$$

where $(\phi, R, \mathcal{G})$ are scalar field, Ricci scalar, and Einstein tensor, respectively. $f(\phi, R, \mathcal{G}) = f(\phi)$ is the well-known Ratra model, which has been studied extensively in the present context [31]. Comparing this to our formalism, the associated EFT parameters can be mapped as:

$$f_1(\eta) = f(\phi, R, \mathcal{G}) \quad , \quad f_2(\eta) = f_3(\eta) = f_4(\eta) = 0.. \tag{3.23}$$

If we further generalize by adding a parity-violating term in the above Lagrangian,

$$\mathcal{L}_{pv} = \frac{\alpha}{M^2}\epsilon^{\mu\nu\alpha\beta}RF_{\mu\nu}F_{\alpha\beta} + \frac{\beta}{M^2}\epsilon^{\mu\alpha\beta\delta}R_{\mu\nu}F^{\nu}_{\alpha}F_{\beta\delta} + \frac{\gamma}{M^2}\epsilon^{\mu\nu\alpha\beta}R_{\mu\nu}^{\ \ \rho\sigma}F_{\rho\sigma}F_{\alpha\beta}, \tag{3.24}$$

The parity non-conserving EFT will become

$$\begin{aligned} f_3(\eta) &= \frac{1}{M^2}\left\{2\beta\left(aa'' + a'^2\right) - 3\beta\left(\frac{a''}{a} - \frac{a'^2}{a^2}\right) - \gamma\left(\frac{a''}{a} + \frac{a'^2}{a^2}\right)\right\} \\ f_4(\eta) &= 6\frac{\alpha}{M^2}\left(\frac{a''}{a^3}\right) \end{aligned} \tag{3.25}$$

The more general models can be constructed by introducing multiple fields coupled with the electromagnetic Lagrangian, which we will study in the future. Our following discussions will be based on the EFT parameters chosen in Eqs. (3.20),(3.21).

3.2 Energy density and power spectra for electromagnetic and metric perturbation fields

In the present section, we will calculate the power spectra for the electromagnetic and metric perturbation fields. Regarding the electromagnetic field, it may be mentioned that the electric and the magnetic fields are frame-dependent. In the present context, the electric and magnetic fields are referred with respect to the comoving observer, in which case the proper time becomes identical with the cosmic time or equivalently the four velocity components of a comoving observer are given by $u^\mu = (1/a(\eta), 0, 0, 0)$. For the computation of the power spectrum, first, we need to know the energy density for the respective fields and, secondly, the vacuum state associated with the field in the background inflationary evolution. Thereby, from the action (3.1), we first determine the energy-momentum tensor associated with the electromagnetic field,

$$\begin{aligned}
T_{ab} &= -\frac{1}{4}f_1(\eta)\,\big[g_{ab}F^2 - 4g^{\mu\alpha}F_{\mu a}F_{\alpha b}\big] + f_2(\eta)\,\big[\frac{1}{a^4}g_{ab}g^{ij}F_{0i}F_{0j} - \frac{2}{a^4}F_{0a}F_{0b} - \frac{4}{a^2}\,\delta^0_a g^{ij}F_{0i}F_{bj}\big] \\
&+ \frac{2}{a^4}\,f_3(\eta)\epsilon_{ijk}\,\delta^0_a\,F_{bi}F_{jk} + h(\eta)\,\big[g_{ab}g^{0\mu}g^{i\nu}F_{\mu\nu}\,\partial_i\big(\delta g^{00}\big) - 2\delta^0_a g^{i\nu}F_{b\nu}\,\partial_i\big(\delta g^{00}\big) \\
&- 2g^{0\mu}F_{\mu b}\,\partial_a\big(\delta g^{00}\big)\big]
\end{aligned} \tag{3.26}$$

The energy density of the EM field in the background FRW spacetime is given by $T^0_0 = -\frac{1}{a^2}T_{00}$ and thus the above expression of $T_{\alpha\beta}$ immediately leads to the following form of T^0_0:

$$\begin{aligned}
T^0_0 &= f_1(\eta)\,\big[-\frac{1}{2a^4}(A'_i)^2 - \frac{1}{4a^4}F_{ij}F_{ij}\big] + f_2(\eta)\,\big[-\frac{3}{a^6}(A'_i)^2\big] \qquad (3.27)\\
&+ f_3(\eta)\,\big[-\frac{4}{a^6}\epsilon_{ijk}A'_i\,\partial_j A_k\big] + h(\eta)\,\big[\frac{1}{a^4}A'_i\,\partial_i\big(\delta g^{00}\big)\big]
\end{aligned}$$

where we use the Coulomb gauge condition. Having determined T^0_0, we express the total electromagnetic energy density in terms of electric, magnetic and interaction energy density as,

$$\rho^{em}_{total} = \rho(\vec{E}) + \rho(\vec{B}) + \rho_{int}(\vec{E},\vec{B}) + \rho_{int}(\vec{E},\delta g^{00}) \tag{3.28}$$

$$\begin{aligned}
\rho(\vec{E}) &= \langle 0\big|f_1(\eta)\,\big[-\frac{1}{2a^4}(A'_i)^2\big] + f_2(\eta)\,\big[-\frac{3}{a^6}(A'_i)^2\big]\big|0\rangle \\
\rho(\vec{B}) &= \langle 0\big|f_1(\eta)\,\big[-\frac{1}{4a^4}F_{ij}F_{ij}\big]\big|0\rangle \\
\rho_{int}(\vec{E},\vec{B}) &= \langle 0\big|f_3(\eta)\,\big[-\frac{4}{a^6}\epsilon_{ijk}A'_i\,\partial_j A_k\big]\big|0\rangle \\
\rho_{int}(\vec{E},\delta g^{00}) &= \langle 0\big|h(\eta)\big[\frac{1}{a^4}A'_i\,\partial_i\big(\delta g^{00}\big)\big]\big|0\rangle
\end{aligned} \tag{3.29}$$

Here $|0\rangle$ is the quantum vaccum defined at the distant past which is Bunch-Davies state. For quantization we promote $A_i(\eta,\vec{x})$ and $v(\vec{x},\eta)$ to hermitian operators $\hat{A}_i(\vec{x},\eta)$ and $\hat{v}(\vec{x},\eta)$ and expanding them in a Fourier basis as follows,

$$\hat{A}_i(\vec{x},\eta) = \int \frac{d^3k}{(2\pi)^3}\sum_{p=+,-}\epsilon^{(p)}_i\left[\hat{b}_p(\vec{k})A_p(k,\eta)e^{i\vec{k}.\vec{x}} + \hat{b}^\dagger_p(\vec{k})A^*_p(k,\eta)e^{-i\vec{k}.\vec{x}}\right] \tag{3.30}$$

$$\hat{v}(\vec{x},\eta) = \int \frac{d^3k}{(2\pi)^3}\left[\hat{c}(\vec{k})\tilde{v}(k,\eta)e^{i\vec{k}.\vec{x}} + \hat{c}^\dagger(\vec{k})\tilde{v}^*(k,\eta)e^{-i\vec{k}.\vec{x}}\right]. \tag{3.31}$$

Here, $\epsilon_i^{(p)}$ is the polarization vector with p being polarization index $p = \pm$. Here we consider the polarization vectors in helicity basis, in which case $\epsilon_i^+ = 1/\sqrt{2}(1, i, 0)$ and $\epsilon_i^- = 1/\sqrt{2}(1, -i, 0)$. The Coulomb gauge indicates that the propagating direction or the momentum of the electromagnetic wave is perpendicular to its polarization vector $\epsilon_i^\pm$, i.e, $k^i \epsilon_i^\pm = 0$. Consequently, the polarization vectors further satisfy the following relation, $\epsilon_{ijk} k_j\ \epsilon_k^\pm = \mp i k \epsilon_i^\pm$. Moreover, $\hat{b}_p(\vec{k})$, $\hat{b}_p^\dagger(\vec{k})$ and $\hat{c}(\vec{k})$, $\hat{c}^\dagger(\vec{k})$ are the annihilation, creation operators for the respective fields defined in the distant past to the Bunch-Davies vacuum state $|0\rangle$, i.e $\hat{b}_r(\vec{k})|0\rangle = 0$ and $\hat{c}(\vec{k})|0\rangle = 0,\ \forall\ \vec{k}$. Such creation and annihilation operators follow the quantization rule, as

$$\left[\hat{b}_p(\vec{k}), \hat{b}_q^\dagger(\vec{k}')\right] = \delta_{pq}\ \delta(\vec{k} - \vec{k}')\ \ ,\ \ \left[\hat{c}(\vec{k}), \hat{c}^\dagger(\vec{k}')\right] = \delta(\vec{k} - \vec{k}') \tag{3.32}$$

Moreover, all the other commutators are zero. With these mode decomposition of $A_i(\vec{x}, \eta)$ and $v(\vec{x}, \eta)$, the individual component of the electromagnetic energy densities in the Bunch-Device vacuum state turn out to be,

$$\begin{aligned}
\rho(\vec{E}) &= \left\{\frac{f_1(\eta)}{a^4} + \frac{6 f_2(\eta)}{a^6}\right\} \sum_{p=+,-} \int \frac{k^2}{2\pi^2} \left|A_p'(k,\eta)\right|^2 dk \\
\rho(\vec{B}) &= \frac{f_1(\eta)}{a^4} \sum_{p=+,-} \int \frac{k^4}{2\pi^2} \left|A_p(k,\eta)\right|^2 dk \\
\rho_{int}(\vec{E}, \vec{B}) &= \frac{4 f_3(\eta)}{a^6} \sum_{p=+,-} \int \frac{k^3}{2\pi^2} \left|A_p(k,\eta) A_p'(k,\eta)\right| dk \\
\rho_{int}(\vec{E}, \delta g^{00}) &= 0
\end{aligned} \tag{3.33}$$

The vacuum expectation for the interaction energy between electric field and the scalar perturbation is zero because the creation/annihilation operators of the scalar perturbation i.e $\hat{c}^\dagger(\vec{k}), \hat{c}(\vec{k})$ commute with that of the electromagnetic field. As can be observed that the energy $\rho_{int}(\vec{E}, \vec{B})$ dilutes much faster than the other energy component. Hence, we will ignore this term in our subsequent discussion. The power spectra, defined as the energy density associated with a logarithmic interval of k, of the electric and magnetic fields follow

$$
\begin{aligned}
P^{(E)}(k,\eta) &= \left\{\frac{f_1(\eta)}{a^4}+\frac{6f_2(\eta)}{a^6}\right\}\sum_{p=+,-}\frac{k^3}{2\pi^2}\left|A'_p(k,\eta)\right|^2 \\
P^{(B)}(k,\eta) &= \frac{f_1(\eta)}{a^4}\sum_{p=+,-}\frac{k^5}{2\pi^2}\left|A_p(k,\eta)\right|^2 \quad .
\end{aligned}
\tag{3.34}
$$

Furthermore, the scalar and tensor power spectra are given by,

$$
P_s(k,\eta)=\frac{k^3}{2\pi^2}\left|\frac{\tilde{v}(k,\eta)}{z(\eta)}\right|^2 \quad , \quad P_T(k,\eta)=\frac{k^3}{2\pi^2}\left|\frac{\tilde{v}_T(k,\eta)}{z_T(\eta)}\right|^2 \quad . \tag{3.35}
$$

As the effective theory Lagrangian has parity-violating operators, the gauge field components in helicity basis (A_+, A_-) evolve differently. Hence, the quantity which measures this is related to helicity density, which is defined as $\rho_h(\eta,k)=\langle 0|A_iB^i|0\rangle$ in the Bunch-Davies vacuum. The expression takes the following well-known form,

$$
\rho_h(k,\eta)=\frac{1}{2\pi^2}\int\frac{dk}{k}\left(\frac{k^4}{a^3}\right)\left(\left|A_+(\eta,k)\right|^2-\left|A_-(\eta,k)\right|^2\right) \quad . \tag{3.36}
$$

Following the definition of electric and magnetic power spectrum, we can find out the helicity spectrum as

$$
P^{(h)}=\frac{\partial\rho_h}{\partial\ln k}=\left(\frac{k^4}{2\pi^2a^3}\right)\left\{\left|A_+(k,\eta)\right|^2-\left|A_-(k,\eta)\right|^2\right\} \quad . \tag{3.37}
$$

We have all the necessary expressions of the electromagnetic spectrum, which indeed depend on the evolution of the electromagnetic mode function. Thereby, the explicit k and η dependence of the power spectra demands the solution of the mode function. It will be discussed in the next section.

3.3 Solving for the electromagnetic mode function and metric perturbation variables

The evolution of the vector potential in terms of the conformal time is given in Eq.(3.18), which, in Fourier space, can be recast as,

$$f_1(\eta)\ \left[A''_\pm + \frac{f_1'}{f_1}A'_\pm + k^2 A_\pm\right] + \frac{2}{a^2}f_2(\eta)\ \left[A''_\pm - A'_\pm\big(\frac{2a'}{a} - \frac{f_2'}{f_2}\big)\right] \mp \frac{2}{a^2}f_3(\eta)kA_\pm \left[\frac{2a'}{a} - \frac{f_3'}{f_3}\right]$$
$$\mp \quad 8f_4'(\eta)kA_\pm \mp \frac{\sqrt{2}B(\eta)}{az}h'(\eta)k\left[\tilde{v}' - \frac{z'}{z}\tilde{v}\right] \mp \frac{\sqrt{2}B(\eta)}{az}h(\eta)k\left[\big(\tilde{v}'' - \frac{z''}{z}\tilde{v}\big) + \left(\tilde{v}' - \frac{z'}{z}\tilde{v}\right)\right.$$
$$\left.\left(\frac{B'}{B} - \frac{a'}{a} - \frac{2z'}{z}\right)\right] = 0 \tag{3.38}$$

where $B(\eta)$ is shown in Eq.(3.16) and $k = \left|\vec{k}_{(em)}\right| = \left|\vec{k}_{(sp)}\right|$ in the above expression, with $\left|\vec{k}_{(em)}\right|$ and $\left|\vec{k}_{(sp)}\right|$ being the momentum modulus of the electromagnetic and the scalar perturbation field, respectively. It is evident from Eq.(3.38) that the dynamical equation of $A_+(k,\eta)$ and $A_-(k,\eta)$ differ from each other due to the presence of the couplings $f_3(\eta)$, $f_4(\eta)$ and $h(\eta)$ in the electromagnetic action. Similarly the The scalar and tensor Mukhanov-Sasaki equations in Fourier space can be obtained from (3.20) as given by,

$$\tilde{v}''(k,\eta) + \left(c_s^2(\eta)k^2 - \frac{z''}{z}\right)\tilde{v}(k,\eta) = 0 \tag{3.39}$$

$$\tilde{v}_T''(k,\eta) + \left(c_T^2(\eta)k^2 - \frac{z_T''}{z_T}\right)\tilde{v}_T(k,\eta) = 0 \tag{3.40}$$

respectively. Recall, $c_s^2 = \frac{1}{c_1}\big(\frac{c_3'}{a^2} - \frac{1}{\kappa^2}\big)$, $c_T^2 = \frac{1}{1+2\kappa^2 m_4^2}$, $z^2(\eta) = a^2 c_1(\eta)$ and $z_T^2(\eta) = a^2(1 + 2\kappa^2 m_4^2)$, where c_1 and c_3 are formed by the EFT coefficients (i.e M_2, m_3, m_4 and $\tilde{m}_4$) as shown earlier in Eq.(3.13).

With the above equations of motion, we first solve the scalar and tensor perturbation equations and then, by using the solution of $\tilde{v}(k,\eta)$, we move on to determine the electromagnetic mode function from Eq.(3.38). However, for solving For the scalar and tensor perturbation variables, one needs an explicit form of c_s^2, c_T^2, and z^2 in terms of conformal time. In the present context, we consider, $c_s^2 = 1, c_T^2 = 1$, which in turn put certain conditions on the EFT coefficients. However, at this point, let us point out that such conditions are supported by various modified gravity theories, such as canonical scalar-tensor theory, F(R) higher curvature theory or more generally $F(\phi, R)$ theory etc. Moreover, the unit gravitational wave speed, i.e, $c_T^2 = 1$, is also compatible with LIGO's recent gravitational wave observation. With $c_s^2 = 1$, the scalar power spectrum becomes $exactly$ scale invariant if $z(\eta)$ behaves as $z(\eta) \propto \eta^{-1}$, which is not consistent with the Planck observations. Thereby, in order to make the theoretical predictions compatible with the Planck results, We consider $z(\eta) = \kappa^\gamma(-1/\eta)^{1+\gamma}$, with γ, a small parameter, making the scalar power spectrum compatible with the latest PLANCK observations. With those forms, the EFT coefficients will take the following form,

$$\frac{1}{c_1(\eta)}\left(\frac{c_3'(\eta)}{a^2} - \frac{1}{\kappa^2}\right) = 1 \ , \ \frac{1}{1 + 2\big(\kappa m_4(\eta)\big)^2} = 1 \ , \ c_1(\eta) = H^2\kappa^{2\gamma}\left(\frac{-1}{\eta}\right)^{2\gamma} \tag{3.41}$$

Correspondingly, one of the possible choices on m_3, m_4, M_2 and $\tilde{m}_4$ by which Eq.(3.41) is satisfied are given by,

$$\begin{aligned} m_3 = 0 \ , \ m_4 = 0 \ , \ M_2(\eta) = \frac{1}{2^{1/4}} H\kappa^{\gamma/2}\left(\frac{-1}{\eta}\right)^{\gamma/2} \\ 4\tilde{m}_4\frac{d\tilde{m}_4}{d\eta} + 2\tilde{m}_4^2\left(\frac{-1}{\eta}\right) = H^2\kappa^{2\gamma}\left(\frac{-1}{\eta}\right)^{1+2\gamma}, \end{aligned} \tag{3.42}$$

where it may be observed that $\tilde{m}_4$ obeys a first order differential Eq.(3.42). With these choices of EFT parameters, the scalar Mukhanov-Sasaki equation takes the following form,

$$\tilde{v}''(k,\eta) + \left(k^2 - \frac{2\big(1+3\gamma/2\big)}{\eta^2}\right)\tilde{v}(k,\eta) = 0, \tag{3.43}$$

which can be exactly solved as,

$$\tilde{v}(k,\eta) = \sqrt{-k\eta}\Big[D_1\ J_\nu(-k\eta) + D_2\ J_{-\nu}(-k\eta)\Big], \tag{3.44}$$

where $\nu = \sqrt{\frac{9}{4} + 3\gamma}$, J_ν is the Bessel function of the first kind. D_1, D_2 are two integration constants which are determined by setting the Bunch-Davies initial condition at in the infinite past $|k\eta| >> 1$,

$$D_1 = \frac{1}{2}\sqrt{\frac{\pi}{k}}\,\frac{e^{-i\frac{\pi}{2}(\nu+\frac{1}{2})}}{\cos\left[\pi(\nu+1/2)\right]} \quad , \quad D_2 = \frac{1}{2}\sqrt{\frac{\pi}{k}}\,\frac{e^{i\frac{\pi}{2}(\nu+\frac{3}{2})}}{\cos\left[\pi(\nu+1/2)\right]}, \tag{3.45}$$

and, consequently, the final solution of the scalar Mukhanov-Sasaki variable becomes

$$\tilde{v}(k,\eta) = \frac{\sqrt{-k\eta}}{2}\left\{\sqrt{\frac{\pi}{k}}\,\frac{e^{-i\frac{\pi}{2}(\nu+\frac{1}{2})}}{\cos\left[\pi(\nu+1/2)\right]}\,J_{\nu}(-k\eta) + \sqrt{\frac{\pi}{k}}\,\frac{e^{i\frac{\pi}{2}(\nu+\frac{3}{2})}}{\cos\left[\pi(\nu+1/2)\right]}\,J_{-\nu}(-k\eta)\right\} \tag{3.46}$$

Finally, in the superhorizon limit, when the modes are going outside the Hubble radius, i.e, $k < \frac{1}{\mathcal{H}}$ (recall $\mathcal{H}$ is the Hubble parameter), the $\tilde{v}(k,\eta)$ can be expressed as

$$\lim_{|k\eta|\ll 1} \tilde{v}(k,\eta) = \left\{\frac{D_1}{2^{\nu}\Gamma(\nu+1)}\,\big(-k\eta\big)^{\nu+\frac{1}{2}} + \frac{D_2}{2^{-\nu}\Gamma(-\nu+1)}\,\big(-k\eta\big)^{-\nu+\frac{1}{2}}\right\}, \tag{3.47}$$

where we have used the power law expansion of the Bessel function given by

$$\lim_{|k\eta|\ll 1} J_{\nu}(-k\eta) = \frac{1}{2^{\nu}\Gamma(\nu+1)}(-k\eta)^{\nu},$$

and similarly for $J_{-\nu}(-k\eta)$. However due to the fact $\nu > 1/2$, the second term containing $\big(-k\eta\big)^{-\nu+\frac{1}{2}}$ in the above expression becomes dominant over the other one and thus $\tilde{v}(k,\eta)$ effectively behaves as $\tilde{v}(k,\eta) \sim \big(-k\eta\big)^{-\nu+\frac{1}{2}}$ in the superhorizon limit. Consequently, the scalar power spectrum is determined as,

$$P_{\Psi}(k,\eta) = \frac{k^3}{2\pi^2}\left|\frac{\tilde{v}(k,\eta)}{z(\eta)}\right|^2 \tag{3.48}$$

with $\tilde{v}(k,\eta)$ is given in Eq.(3.46). In view of Eq.(3.47), the scalar power spectrum goes as $P_{\Psi} \sim \big(k|\eta|\big)^{3-2\nu}$ in the superhorizon scale, which in turn provides the scalar spectral index as $n_s = 4 - 2\nu$. With the help of the solution of $\tilde{v}(k,\eta)$, we will solve the electromagnetic mode function from Eq.(3.38). However, before going to the electromagnetic mode function, for the sake of completeness, let us determine the tensor power spectrum which can be obtained from the solution of the perturbation Eq.(3.40),

$$\tilde{v}_T(k,\eta) = \frac{\sqrt{-\pi\eta}}{2} H^{(2)}\left[\frac{3}{2}, -k\eta\right] \tag{3.49}$$

where $H^{(2)}\left[\frac{3}{2}, -k\eta\right]$ symbolizes the Hankel function of second kind with order $3/2$. In the infinite past the above solution matches with the Bunch-Davies initial condition, $\lim_{|k\eta|\gg 1}\tilde{v}_T(k,\eta) = \frac{1}{\sqrt{2k}}e^{-ik\eta}$. Thus, the tensor power spectrum comes with the following expression,

$$P_T(k,\eta) = 2\times\frac{k^3}{2\pi^2}\left|\frac{\tilde{v}_T(k,\eta)}{z_T(\eta)}\right|^2 = \frac{k^3}{4\pi^2}\left|\frac{\sqrt{-\pi\eta}}{z_T(\eta)}\,H^{(2)}\left[\frac{3}{2}, -k\eta\right]\right|^2 \quad . \tag{3.50}$$

The multiplicative factor 2 arises from the two polarization waves in the gravity wave. Now we can confront the model at hand with the latest Planck observational data [?], so we shall calculate the spectral index of the primordial curvature perturbations n_s and the tensor-to-scalar ratio $r_{\mathrm{t/s}}$, which are defined as follows,

$$n_s = 1 + \left.\frac{\partial \ln P_\Psi}{\partial \ln k}\right|_*\,, \quad r_{\mathrm{t/s}} = \left.\frac{P_T(k,\eta)}{P_\Psi(k,\eta)}\right|_*\,, \tag{3.51}$$

where the suffix $*$ corresponds to the horizon crossing instant of the CMB scale (afterwards in the paper, a suffix $*$ with a quantity represents that quantity when the CMB scale crosses the horizon). Eqs.(3.48) and (3.50) immediately lead to the explicit forms of n_s and $r_{\mathrm{t/s}}$ as follows,

$$\begin{aligned} n_s &= 4 - 3\sqrt{1+\frac{4\gamma}{3}} \\ r_{\mathrm{t/s}} &= \left|\frac{z(\eta_*)}{z_T(\eta_*)}(\sqrt{-\pi\eta_*})\tilde{v}(k,\eta_*)\;H^{(2)}\left[\frac{3}{2}, -k\eta_*\right]\right|^2 \end{aligned} \tag{3.52}$$

with $\tilde{v}(k,\eta)$ is given in Eq.(3.46). It may be noticed that n_s and $r_{\mathrm{t/s}}$ depend on the dimensionless parameter γ. Here we would like to mention that in the context of EFT, the spectral index can be expressed as [59],

$$n_s = 1 + 4\frac{\dot{H}_*}{H_*^2} - \frac{\ddot{H}_*}{H_*\dot{H}_*} \tag{3.53}$$

Comparing Eqs.(3.52) and (3.53) immediately connects γ with $\dot{H}_*$ and $\ddot{H}_*$, as given by the following relation

$$\gamma = -\frac{2\dot{H}_*}{H_*^2} + \frac{\ddot{H}_*}{2H_*\dot{H}_*} \quad . \tag{3.54}$$

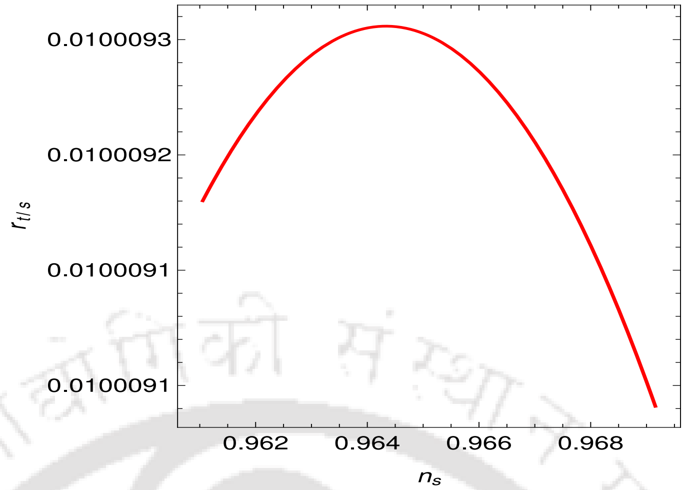

Figure 3.1: Parametric plot of n_s vs $r_{\rm t/s}$ for $0.0155 \leq \gamma \leq 0.0196$.

Having obtained Eq.(3.52), we can now directly confront the spectral index and the tensor-to-scalar ratio with the Planck 2018 constraints [88], which constrain the observational indices as follows,

$$n_s = 0.9649 \pm 0.0042 \,, \qquad r_{\rm t/s} < 0.064 \,. \tag{3.55}$$

In the present context, the theoretical expectations of n_s and $r_{\rm t/s}$ lie within the Planck constraints for the following ranges of parameter value: $0.0155 \leq \gamma \leq 0.0196$, and this behaviour is depicted in Fig. 3.1. Now we can solve for the electromagnetic perturbation by using the solution of $\tilde{v}(k,\eta)$. By using the dimensionless variables $x = k\eta$, $\bar{A}_{\pm}(k,\eta) = \sqrt{k}A_{\pm}(k,\eta)$ and $V(k,\eta) = \sqrt{k}\tilde{v}(k,\eta)$, and using Eqs.(3.20) and (3.21), the electromagnetic equation (3.38) becomes,

$$\mathcal{A}_1 \frac{d^2\bar{A}_{\pm}}{dx^2} + \mathcal{A}_2 \frac{d\bar{A}_{\pm}}{dx} \pm \mathcal{A}_3 \bar{A}_{\pm} = \mathcal{S}_{\pm}, \tag{3.56}$$

where the coefficients are,

$$\mathcal{A}_1 = \frac{1}{a_f^2}\left(\frac{k}{H}\right)^{4+m} + 2(-1)^m x^{4+m} \,;\; \mathcal{A}_2 = -\frac{2}{x^2 a_f^2}\left(\frac{k}{H}\right)^{4+m} + (4+2m)(-1)^m x^{3+m} \tag{3.57}$$

$$\mathcal{A}_3 = \frac{1}{a_f^2}\left(\frac{k}{H}\right)^{4+m} + 2(-1)^r(2+r)\left(\frac{k}{H}\right)^{m-r} x^{3+r} - 8s(-1)^s\left(\frac{k}{H}\right)^{m-s+2} x^{s+1} \tag{3.58}$$

$$\mathcal{S}_{\pm} = \pm 2\sqrt{2}\left(\frac{h_0 x^5}{H}\right)\left(\frac{k}{H}\right)^{m-1}\left[(5+2\gamma)\left(\frac{dV}{dx}+\left(\frac{1+\gamma}{x}\right)V\right)+x\left(\frac{d^2V}{dx^2}-\frac{(2+3\gamma)}{x^2}V\right)\right] \tag{3.59}$$

Here, it may be mentioned that we solve the above equation numerically due to its complicated nature. For this we will consider values of m, r and s which lead to a scale invariant magnetic power spectrum in the superhorizon limit. For the modes lying outside the horizon, the scalar Mukhanov-Sasaki variable behaves as $\tilde{v}(k,\eta) \sim (-k\eta)^{-\nu+\frac{1}{2}} = (-k\eta)^{-1-\gamma}$ (see Eq.(3.47)), which indicates that $\tilde{v}(k,\eta)$ becomes proportional to $z(\eta)$ at the scale $-k\eta \to 0$. Furthermore the factor $\frac{k}{H}$ present in Eq.(3.56) is considered to be less than unity, which is indeed true for the CMB scale modes $\sim 10^{-40}\mathrm{GeV}^{-1}$ - the scale of interest to estimate the magnetic strength at the current Universe. In consideration of these arguments, Eq.(3.56) in the superhorizon scale can be written as,

$$\begin{aligned}\frac{d^2\bar{A}_{\pm}}{dx^2} &+ \left(\frac{2+m}{x}\right)\frac{d\bar{A}_{\pm}}{dx}\\ &\pm (-1)^{r-m}\left\{\left(\frac{k}{H}\right)^{m-r}\left(\frac{2+r}{x^{1+m-r}}\right) - 4s\,(-1)^{-2-r}\left(\frac{k}{H}\right)^{2+m-s} x^{3+m-s}\right\}\bar{A}_{\pm}\end{aligned} \tag{3.60}$$

Where it can be shown that $\mathcal{S}_{\pm}$ vanishes due to the superhorizon solution of $\tilde{v}(k,\eta)$ given in Eq.(3.46). The above equation may not be solved analytically; thus, we consider $m = r \geq s$ (later, we will show that such choices of the coupling parameters lead to the scale-invariant electric as well as the scale-invariant magnetic power spectrum for specific values of m, respectively). In effect, the term containing $(k/H)^{2+m-s}$ within the curly bracket becomes subdominant compared to the other one, since $k/H \ll 1$ for the CMB scale modes, in particular $k/H \sim 10^{-54}$ for $H \sim 10^{14}\mathrm{GeV}$. As a consequence, Eq.(3.60) turns out to be

$$\frac{d^2\bar{A}_{\pm}}{dx^2} + \left(\frac{2+m}{x}\right)\frac{d\bar{A}_{\pm}}{dx} \pm \left(\frac{2+m}{x}\right)\bar{A}_{\pm} = 0 \tag{3.61}$$

Eq.(3.61) has the following solution for $\bar{A}_{\pm}(k,\eta)$,

$$\bar{A}_{+}(k,\eta) = \big(-k\eta\big)^{\frac{1-m}{2}}\Big\{C_1\mathrm{I}_{-m-1}\big[\sqrt{-(8+4m)x}\big] + D_1\mathrm{I}_{m+1}\big[\sqrt{-(8+4m)x}\big]\Big\} \quad (3.62)$$

$$\bar{A}_{-}(k,\eta) = \big(-k\eta\big)^{\frac{1-m}{2}}\Big\{C_2\mathrm{I}_{-m-1}\big[\sqrt{(8+4m)x}\big] + D_2\mathrm{I}_{m+1}\big[\sqrt{(8+4m)x}\big]\Big\} \quad (3.63)$$

respectively, with $C_{1,2}$ and $D_{1,2}$ are integration constants. Here $\mathrm{I}_n(w)$ symbolizes the modified Bessel function of first kind having order n and argument w, which, in the limit $w \ll 1$, has a power law form as $\mathrm{I}_n(w) = w^{n/2}$. Thus due to the presence of the modified Bessel function in Eq.(3.63), the term containing C_1 in the expression of $\bar{A}_+$ dominate over the other one containing D_1, i.e we may write $\lim_{|k\eta|\ll 1}\bar{A}_+ \approx C_1(-k\eta)^{-m}$. Similar argument can also be drawn for $\bar{A}_-$, i.e $\lim_{|k\eta|\ll 1}\bar{A}_- \approx C_2(-k\eta)^{-m}$. As a result, Eq.(3.34) immediately leads to the electric Moreover, magnetic spectra in the superhorizon limit are as follows:

$$P^{(E)}(k,\eta) = \frac{m^2}{2\pi^2}\{|C_1|^2+|C_2|^2\}\left[f_1(\eta)+\frac{6f_2(\eta)}{a^2}\right]H^4\big(-k\eta\big)^{2-2m}$$
$$P^{(B)}(k,\eta) = \frac{f_1(\eta)}{2\pi^2}\{|C_1|^2+|C_2|^2\}H^4\big(-k\eta\big)^{4-2m} \quad . \quad (3.64)$$

Furthermore, as the two polarization modes evolve differently, the magnetic field generated through this mechanism will be helical, and the helicity power spectrum during inflation comes as,

$$P^{(h)}(k,\eta) = \left(\frac{k^3}{2\pi^2 a^3}\right)\big(-k\eta\big)^{-2m}\Big\{\big|C_1\big|^2 - \big|C_2\big|^2\Big\} \quad . \quad (3.65)$$

Specifically, the $(-k\eta)^{-2m}$ factor in the above expression depicts that the comoving helicity spectra increase with time for a given mode for any positive value of m during the inflationary era.

Eq.(3.64) points out that the scale dependence of the electric and the magnetic power spectra are different, in particular, $P^{(E)} \sim (-k\eta)^{2-2m}$ and $P^{(B)} \sim (-k\eta)^{4-2m}$. The electric power spectrum becomes scale invariant for $m = 1$ while, in the magnetic case, $m = 2$ leads to a scale invariant power spectrum. The coupling exponents are consistent with a scale-invariant magnetic power spectrum and are constrained by $m = 2$, $r = 2$, and $s \leq 2$. In contrast, the corresponding constraint is given by $m = 1$, $r = 1$, and $s \leq 1$ for the scale-invariant electric power spectrum. Hence, in the following section, we will solve the electromagnetic mode functions and discuss the possible implications for the two cases. Before we embark on estimating the magnetic field strength at a large scale in the next section, we would like to address the strong coupling problem for general values of m, r, and s in the spirit of EFT. For this purpose, we need to start with the action of the EM and Dirac field, which in the present context, can be expressed by,

$$\begin{aligned} \mathcal{S}_{em} + \mathcal{S}_{\Psi} \;\; &= \int d^4x\sqrt{-g}\Big[-\frac{1}{4}f_1(\eta)F_{\mu\nu}F^{\mu\nu} + f_2(\eta)F^0_i F^{0i} + f_3(\eta)\epsilon^{ijk}F^0_i F_{jk} + f_4(\eta)\epsilon^{\mu\nu\alpha\beta}F_{\mu\nu}F_{\alpha\beta}\Big] \\ &+ \int d^4x\sqrt{-g}\Big[\alpha(\eta)\bar{\Psi}\, i\,\gamma^{\mu}\mathbf{D}_{\mu}\Psi \;+\; \beta(\eta)\bar{\Psi}\, i\,\gamma^0\mathbf{D}_0\Psi\Big] \end{aligned} \tag{3.66}$$

where Ψ is the Dirac field and $\mathbf{D}_{\mu} = \nabla_{\mu} - ieA_{\mu}$ is the covariant derivative. The part of the EM field in the above action has been considered earlier in Eq.(3.7), however in regard to the Dirac field, S_{Ψ} contains two terms with EFT coefficients $\alpha(\eta)$ and $\beta(\eta)$. The underlying spatial diffeomorphism symmetry allows the coefficients $\alpha(\eta)$ and $\beta(\eta)$ to depend on η only. Moreover the term $\beta(\eta)\bar{\Psi}i\gamma^0\mathbf{D}_0\Psi$ behaves as a scalar quantity under spatial diffeomorphism symmetry transformation can thus be a possible term in S_{Ψ} in the context of EFT of cosmology [89]. By expanding the S_{Ψ} in terms of temporal and spatial parts over the FRW spacetime, we get,

$$\mathcal{S}_{\Psi} = \int d^4x a^4\Big[i(\alpha(\eta)+\beta(\eta))\bar{\Psi}\gamma^0\mathbf{D}_0\Psi + i\alpha(\eta)\bar{\Psi}\gamma^i\mathbf{D}_i\Psi\Big] \tag{3.67}$$

which makes the Dirac field non-canonical. Therefore, in order to make the Dirac field canonical, we redefine the field as,

$$\Psi \longrightarrow \widetilde{\Psi} = a^2\sqrt{\alpha(\eta)+\beta(\eta)}\;\Psi \;\; . \tag{3.68}$$

Similarly due to the presence of the coupling functions $f_i(\eta)$ ($i = 1, 2, 3, 4$), the electromagnetic kinetic part becomes non-canonical, in particular,

$$\mathcal{S}_{em}^{(kin)} = \frac{1}{2}\int d^4x \left[\left(f_1(\eta) + \frac{2f_2(\eta)}{a^2} \right) (A_i')^2 \right] . \tag{3.69}$$

Thus, we redefine the EM field as,

$$A_i \longrightarrow \widetilde{A}_i = \left(f_1(\eta) + \frac{2f_2(\eta)}{a^2} \right) A_i \tag{3.70}$$

which in turn restores the canonicity of the EM field. In terms of such canonical variables, Eq.(3.66) immediately leads to the U(1) interaction between the EM and the Dirac fields as,

$$\mathcal{S}_{int} = \int d^4x \left[\frac{e\,\alpha(\eta)}{(\alpha(\eta)+\beta(\eta))\sqrt{f_1(\eta) + \frac{2f_2(\eta)}{a^2}}} \right] \bar{\widetilde{\Psi}} i\,\gamma^i \widetilde{A}_i \widetilde{\Psi} = \int d^4x \left(e\,\lambda_{\text{eff}} \right) \bar{\widetilde{\Psi}} i\,\gamma^i \widetilde{A}_i \widetilde{\Psi} \tag{3.71}$$

here λ_{eff} defines an effective electric charge as

$$e_{eff} = e\lambda_{\text{eff}} = \frac{e}{\left(1 + \frac{\beta(\eta)}{\alpha(\eta)}\right)\sqrt{f_1(\eta) + \frac{2f_2(\eta)}{a^2}}} \tag{3.72}$$

In order to avoid the strong coupling problem, we need to have $\lambda_{\text{eff}} \leqslant 1$, which leads to the following condition on the EFT parameters,

$$\left(1 + \frac{\beta(\eta)}{\alpha(\eta)}\right) \geqslant \frac{1}{\sqrt{f_1(\eta) + \frac{2f_2(\eta)}{a^2}}} . \tag{3.73}$$

Thus, in the context of EFT magnetogenesis, the strong coupling problem can be naturally resolved provided the functions $a(\eta)$, $\beta(\eta)$, $f_1(\eta)$ and $f_2(\eta)$ satisfy Eq.(3.73) during inflation. In the present work, we consider $f_1(\eta) = \left(a/a_{\text{f}}\right)^2$ and $f_2(\eta) = \left(a_{\text{i}}/a\right)^m$ (see Eqs.(3.20) and (3.21)), due to which the above equation becomes,

$$\left(1 + \frac{\beta(\eta)}{\alpha(\eta)}\right) \geqslant \frac{1}{\sqrt{\left(\frac{a}{a_f}\right)^2 + \frac{2f_2}{a^2}\left(\frac{a_i}{a}\right)^m}} . \tag{3.74}$$

As mentioned earlier, we are interested in two distinct cases, depending on whether the magnetic power spectrum or the electric power spectrum becomes scale invariant, for which the corresponding parametric regimes are given by $m = 2$, $r = 2$, $s \leq 2$ or $m = 1$,

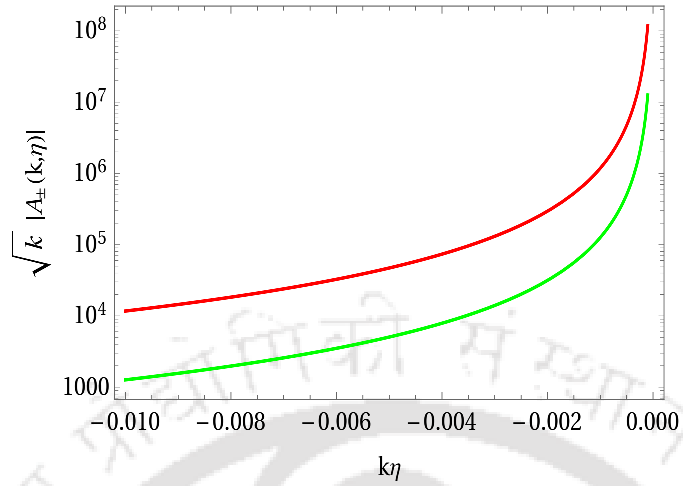

Figure 3.2: The red line represents $\sqrt{k}A_{+}(k,\eta)$ versus $k\eta$ and the green line represents $\sqrt{k}A_{-}(k,\eta)$ versus $k\eta$. Both the plots are for $k = 0.05\text{Mpc}^{-1} \approx 2 \times 10^{-40}\text{GeV}$, $H = 10^{14}\text{GeV}$ and $m = r = s = 2$ respectively.

$r = 1$, $s \leq 1$. Thereby, depending on such values of m along with $a(\eta) = (-H\eta)^{-1}$, the functions $\alpha(\eta)$ and $\beta(\eta)$ can be chosen properly so that Eq.(3.74) holds true during the inflation, which in turn leads to the resolution of the strong coupling problem.

3.4 Case-I: Scale invariant magnetic power spectrum

In this section, we consider the case where the magnetic power spectrum is scale invariant for the choices of the parameters $m = 2$, $r = 2$ and $s \leq 2$. Considering these set of parameter values we numerically solve Eq.(3.56) for $\bar{A}_{\pm}(k,\eta)$ which are depicted in Fig.3.2. During the numerical analysis, we take the Bunch-Davies initial condition for the electromagnetic mode functions. Furthermore, the initial conditions are set for the modes when they are well within the horizon length scale (i.e, $-k\eta = 10$). Moreover, the numerical solutions are obtained up to the epoch when the modes are well outside the horizon ($-k\eta = 10^{-4}$ has been used in our calculation).

Fig.[3.2] demonstrates that the A_{+} mode dominates over the A_{-} mode and thus the electromagnetic energy density in the superhorizon limit is effectively determined by that of the contribution of the A_{+} mode.

3.4.1 Present magnetic strength and backreaction problem

In this section, we will concentrate on the strength of the magnetic field in the present epoch. Conventionally, one considers high electrical conductivity in the post-inflationary epoch within the instantaneous reheating scenario, where the inflaton suddenly jumps from the inflationary phase to a radiation-dominated phase. Due to the large electrical conductivity, the electric field quickly vanishes, and the magnetic field freezes, evolving into a large-scale magnetic field. As we mentioned earlier for our analysis, coupling functions $f_1(\eta) = 1$, $f_2(\eta) \approx f_3(\eta) \approx f_4(\eta) \approx h(\eta) \approx 0$, are assumed which will restore the conformal symmetry and the electromagnetic field will follow the standard Maxwell's equations. Hence, the frozen-in magnetic field energy density evolves as $1/a^4$. The magnetic field strength at the present epoch is related to that at the end of inflation by the expression

$$\left.\frac{\partial\rho(\vec{B})}{\partial\ln k}\right|_0 = \left(\frac{a_f}{a_0}\right)^4 \left.\frac{\partial\rho(\vec{B})}{\partial\ln k}\right|_{\eta_f}, \tag{3.75}$$

where η_f is the conformal time at the end of inflation and the suffix '0' denotes the present time. With Eq.(3.34), the above equation yields the present magnetic strength (B_0)

$$B_0 = \frac{1}{2\pi}\left\{\sqrt{\left|\bar{A}_+(k,\eta_f)\right|^2 + \left|\bar{A}_-(k,\eta_f)\right|^2}\right\}\left(\frac{a_f}{a_0}\right)^2 H^2\big(-k\eta_f\big)^2, \tag{3.76}$$

where we recall that $\bar{A}_\pm = \sqrt{k}A_\pm$ and k denotes the CMB scale ($\simeq 0.02\mathrm{Mpc}^{-1}$) We will estimate the current magnetic strength at this time. In order to estimate B_0 from Eq.(3.76), we need to know $\frac{a_0}{a_f}$. The factor $\frac{a_0}{a_f}$ can be determined from the entropy conservation relation, i.e., from $gT^3a^3 = \mathrm{constant}$, where g is the effective relativistic degrees of freedom and T denotes the temperature of the relativistic fluid, which finally yields $\frac{a_0}{a_f} \approx 10^{30}\big(H/10^{-5}M_{Pl}\big)^{1/2}$, with H being the Hubble parameter during inflation and, in particular, we consider $H = 10^{-5}M_{Pl}$. Moreover, by using the numerical solution of $\bar{A}_\pm k,\eta)$ from Fig.[3.2], we get, $\bar{A}_+(k,\eta_f) \simeq 10^8$ and $\bar{A}_-(k,\eta_f) \simeq 10^7$ for $-k\eta_f = 10^{-4}$. With such ingredients of $\frac{a_0}{a_f}$ and $\bar{A}_\pm k,\eta_f)$, we estimate the magnetic strength at the present epoch from Eq.(3.76) to be

$$B_0\Big|_{CMB} = 0.82 \times 10^{-13}\text{G}, \tag{3.77}$$

where we use the conversion $1\text{G} = 1.95\times 10^{-20}\text{GeV}^2$. The above result gives us a typical value for the magnetic field at the present epoch in our present framework. It may be noticed that B_0 indeed depends on the inflationary Hubble parameter; in particular, if we consider $H = 10^{-6}M_{Pl}$, then B_0 will be estimated as $B_0 \simeq 10^{-14}\text{G}$ which, in comparison with Eq.(3.77), clearly argue that the current magnetic strength for $H = 10^{-6}M_{Pl}$ gets 1 order lower than that of the case where $H = 10^{-5}M_{Pl}$. However, from the observational [23, 90, 91] results a constraint on the current magnetic strength of $10^{-10}G \lesssim B_0 \lesssim 10^{-22}G$ is obtained around the CMB scales. Therefore, the theoretical prediction of B_0 lies within the observational constraints where the magnetic power spectrum is scale invariant.

At this stage, it deserves mentioning that the present case (i.e, $m = 2$), despite having compatibility with the observational strength of B_0 hinges on the backreaction problem. In particular, for $m = 2$, we have from Eq.(3.64) $P^{(E)}(k,\eta) \propto (-k\eta)^{-2}$. In this case, as $-k\eta \to 0$ (i.e., towards the end of inflation), the electric energy density increases rapidly as $P^{(E)} \propto (-k\eta)^{-2} \to \infty$. The model runs into *difficulties* as the electric energy density would eventually exceed the inflaton energy density in the Universe even before inflation ends. Thus, the scenario where the magnetic power spectrum becomes scale invariant can lead to the required value of magnetic strength; however, it suffers from the backreaction problem. On the contrary, the situation becomes different when the electric power spectrum becomes scale invariant (i.e, for $m = 1$), as discussed in the following section.

3.5 Case-II: Scale invariant electric power spectrum

Eq.(3.64) shows that the electric power spectrum becomes scale invariant for the parametric space satisfying $s \leq m = r = 1$. Thereby, considering a particular set of

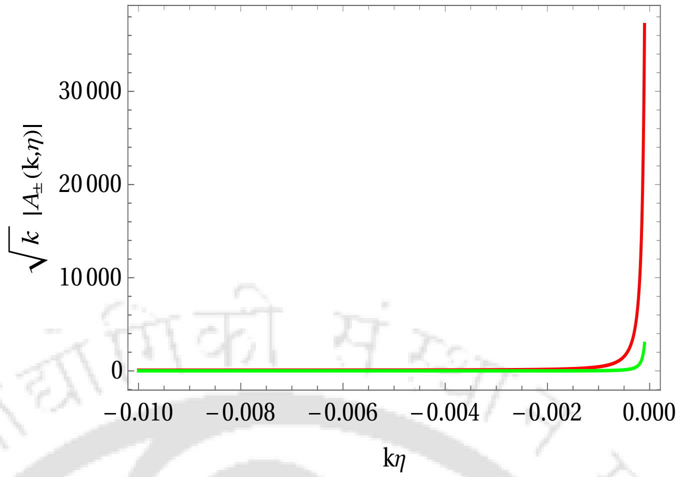

Figure 3.3: The red line represents $\sqrt{k}A_+(k,\eta)$ versus $k\eta$ and the green line represents $\sqrt{k}A_-(k,\eta)$ versus $k\eta$. Both the plots are for $k = 0.05\text{Mpc}^{-1} \approx 2\times10^{-40}\text{GeV}$, $H = 10^{14}\text{GeV}$ and $m = r = s = 1$ respectively.

parameter values, in particular $m = r = s = 1$, we solve the electromagnetic mode functions from Eq.(3.56) with the Bunch-Davies initial condition. However due to the complicated nature, Eq.(3.56) is solved numerically and they are depicted in Fig.[3.3]. The numerical analysis is performed for $k = 0.05\text{Mpc}^{-1}$ within the same same range $-10 < k\eta < 10^{-4}$ from sub to super Hubble scale.

Fig.3.3 depicts that similar to the previous case, the A_+ mode is slightly dominated over the A_- mode towards the end of inflation, and thus the electromagnetic energy density in the superhorizon limit is effectively determined by the contribution of A_+ mode. The solutions of $A_\pm$ immediately lead to the evolution of the helicity density during the inflationary era. This is depicted in Fig.3.4, demonstrating that the comoving helicity density during inflation increases with time. The scenario, where the electric power spectrum becomes scale invariant (i.e, for $s \leq m = r = 1$), leads to the electric and magnetic power spectra in the superhorizon scale as,

$$
\begin{aligned}
P^{(E)}(k,\eta) &= \frac{m^2}{2\pi^2}H^4\{|C_1|^2+|C_2|^2\}\left[f_1(\eta)+\frac{6f_2(\eta)}{a^2}\right] \\
P^{(B)}(k,\eta) &= \frac{f_1(\eta)}{2\pi^2}H^4\{|C_1|^2+|C_2|^2\}\big(-k\eta\big)^2 \quad . \qquad (3.78)
\end{aligned}
$$

TH-3815_1861231026

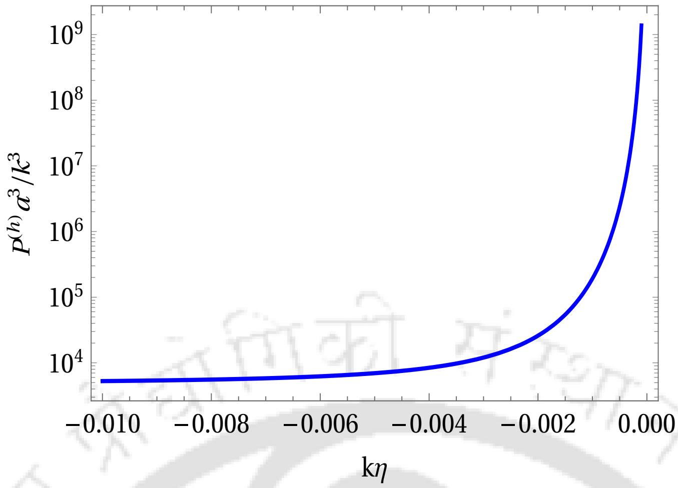

Figure 3.4: $P^{(h)}a^3/k^3$ versus $k\eta$ during inflationary epoch.

respectively, where we use Eq.(3.64). Thereby, the spectral indices of the electric and magnetic spectra, defined by $n(E) = \frac{\partial \ln P^{(E)}}{\partial \ln k}$ and $n(B) = \frac{\partial \ln P^{(B)}}{\partial \ln k}$, become $n(E) = 0$ and $n(B) = 2$ respectively. In the scenario where the electric power spectrum becomes scale invariant, the spectral index for the magnetic power becomes positive, which hints at the resolution of the backreaction problem. However, in order to investigate whether the backreaction of the electromagnetic field stays small during inflation, we shall first consider the energy stored in the electric field at a given time η_c, which is

$$\rho(\vec{E}, \eta_c) = \int_{k_i}^{k_c} \frac{\partial \rho(\vec{E})}{\partial \ln k} d\ln k = \frac{1}{2\pi^2}\left[e^{-2\left(N_f - N_c\right)} + 6e^{-3N_c}\right]\{|C_1|^2 + |C_2|^2\}H^4 N_c \ , \quad (3.79)$$

Here, k_i and k_c denote the modes that cross the horizon at the beginning of inflation and at $\eta = \eta_c$, respectively, and thus k_i is considered to be the CMB scale. Moreover, N_f is the total e-folding number of the inflation era. $N_c = \ln\left(\frac{a_c}{a_i}\right)$, with $a_i = a(\eta_i)$ and $a_c = a(\eta_c)$, is the e-fold number associated with conformal time $\eta = \eta_c$ during inflation. We also have the relation $|\eta_c| = k_c^{-1}$ and k_c is obviously greater than the CMB mode momentum $k_{CMB} \approx 10^{-40}\text{GeV} \approx 0.05\text{Mpc}^{-1}$. Similarly, we determine the energy density coming from the magnetic fields, which yields

$$\rho(\vec{B}, \eta_c) = \int_{k_i}^{k_c} \frac{\partial \rho(\vec{B})}{\partial \ln k} d\ln k = \frac{1}{4\pi^2} e^{-2\left(N_f - N_c\right)}\{|C_1|^2 + |C_2|^2\}H^4\left(1 - e^{-2N_c}\right) \ . \quad (3.80)$$

To derive the above two expressions, we use the form of the coupling functions at $\eta = \eta_c$ in terms of the e-folding number, as $f_1(\eta_c) = \left(a_c/a_f\right)^2 = e^{-2\left(N_f - N_c\right)}$ and $f_2(\eta) = \left(a_i/a_c\right) = e^{-N_c}$. The total electromagnetic energy density at $\eta = \eta_c$ becomes

$$\begin{aligned} \rho_{em}(\eta_c) = \rho(\vec{E}, \eta_c) + \rho(\vec{B}, \eta_c) &= \frac{1}{4\pi^2}\{|C_1|^2 + |C_2|^2\}H^4\Big\{N_c\left(2e^{-2\left(N_f - N_c\right)} + 12e^{-3N_c}\right) \\ &+ e^{-2\left(N_f - N_c\right)}\left(1 - e^{-2N_c}\right)\Big\} \end{aligned} \tag{3.81}$$

where $C_{1,2}$ are integration constants as mentioned in Eq.(3.64). In order to avoid the backreaction issue, we have to ensure that the electromagnetic energy density is less than that of the background energy density. In particular, we have to show $\rho_{em} < 3M_{Pl}^2 H^2$ during inflation. The above expression, along with the consideration of $N_c \leq N_f \approx 60$, clearly indicate that the electromagnetic energy density during inflation is of the order of H^4, i.e.

$$\rho_{em}(\eta_c) \sim H^4 \quad . \tag{3.82}$$

The inflationary energy scale is less than the Planck scale; in particular, we consider $H = 10^{-5} M_{Pl}$ and, thus, Eq.(3.82) leads to the inequality $\rho_{em} \ll M_{Pl}^2 H^2$. It confirms that the electromagnetic field has a negligible backreaction on the background inflationary spacetime, leading to the resolution of the backreaction problem in the present magnetogenesis scenario.

3.5.1 Present magnetic strength

Following the same methodology discussed for the scale-invariant magnetic case (Sec.[3.4.1]), and using Eqs. (3.63) with $m = 1$, the expression of the current magnetic strength turns out to be,

$$B_0 = \frac{1}{2\pi}\left\{\sqrt{|C_1|^2 + |C_2|^2}\right\}\left(\frac{a_f}{a_0}\right)^2 H^2(-k\eta_f), \tag{3.83}$$

Here $C_{1,2}$ are integration constants appeared in Eq.(3.64) and k symbolizes the momentum of the CMB scale $\approx 0.05\mathrm{Mpc}^{-1}$. As discussed earlier, by using the entropy conservation, we get $\frac{a_0}{a_f} = 10^{30}\left(H/10^{-5}M_{Pl}\right)^{1/2}$ with H being the inflationary Hubble scale. Moreover, regarding $-k\eta_f$, we have the relation $|\eta_f| = \frac{1}{k_f}$ where k_f is the mode which crosses the horizon at the end of inflation and thus $-k\eta_f$ is given by $-k\eta_f = \exp\left(N_f\right)$. With such expressions of $\frac{a_0}{a_f}$ and $-k\eta_f$, along with $H = 10^{-5}M_{Pl}$, we estimate the magnetic strength at the present epoch from Eq.(3.83) to be,

$$B_0\Big|_{CMB} \sim 10^{-40}\text{G} \tag{3.84}$$

where we use $N_f = 60$ and the conversion $1\text{G} = 1.95 \times 10^{-20}\text{GeV}^2$ may be useful. The above result estimates the current epoch's magnetic field, as obtained from the framework. However, the observational results put a constraint on the current magnetic strength as $10^{-10}\text{G} \lesssim B_0 \lesssim 10^{-22}\text{G}$ around the CMB scales. Therefore, it is clear from Eq.(3.84) that the theoretical prediction of B_0 lies far below the range of the observational expectation.

Thus, as a whole, by comparing Secs.[3.4] and [3.5], it is evident that the scenario where the magnetic power spectrum is scale invariant (let us call it S1) gets distinct features in comparison to that of where the electric spectrum is scale invariant (let us call it S2). In particular, the scenario S1 is observationally compatible with the present magnetic strength but suffers from the backreaction problem. On the other hand, the scenario S2 is free from the backreaction problem, but does not predict sufficient magnetic field strength in the present Universe. Such distinctions between S1 and S2 are depicted in Table[3.1]. However, scenarios S1 and S2 can resolve the strong coupling problem as indicated earlier in Eq.(3.74). The above issues motivated us to

Scenario	First feature	Second feature
S1	Compatible with observation	Suffers from backreaction problem
S2	Not compatible with observation	Free from backreaction problem

Table 3.1: Comparison between the scenarios S1 and S2

look for physical solutions that can be theoretically and observationally viable concurrently. Furthermore, the case when reheating plays an important role. It deserves mentioning that our discussions on scenarios. S1 and S2 are based on the fact that radiation domination starts immediately after the inflation ends, which we call the *instantaneous reheating* case. However, a more physical approach would be if, during the cosmic evolution, the Universe experiences a reheating phase with *non zero* e-fold number. In the following sections, we will discuss this possibility and its implications. We further assume that the conductivity will be vanishingly small during reheating, as it is known that during the entire reheating period, the dynamics are mostly oscillating and inflaton-dominated. During the cosmological expansion of the Universe, the EM field eventually evolves through the reheating phase. Thus, the evolution of the electric and magnetic field(s) is considerably affected compared to the instantaneous reheating case. As a consequence, there is a possibility that such an elongated reheating phase may make the models viable which we will investigate in Sec.[3.6]. However, our analysis shows that the presence of a reheating phase will not cure the difficulty of the scenario S1, because S1 suffers from the backreaction problem during inflation, which a reheating phase can not rescue after inflation. Thus, in the following, we will consider the scenario S2 with an elongated reheating phase, and depending on the background reheating dynamics, two cases will arise: (i) when the Kamionkowski-like mechanism characterizes the reheating phase and (ii) where the reheating dynamics follow the perturbative mechanism.

3.6 Scenario with scale invariant electric field and reheating phase

The presence of a reheating phase with non-zero e-folding number considerably affects the magnetic field evolution compared to the instantaneous reheating case we have considered in Sec.[3.5]. Actually, in the instantaneous reheating scenario, the conductivity becomes huge after the end of inflation. Consequently, the magnetic field evolves as $1/a^4$ from the end of inflation to the present epoch. However, suppose the reheating phase is considered to have a non-zero e-fold number (a natural consideration). In that case, there is no reason to consider a large conductivity immediately after the inflation. In particular, the conductivity remains non-zero and small during the reheating epoch and consequently, the strong electric field induces the magnetic field [92]. Due to such Faraday's induction from electric to magnetic field, the red-shift of the magnetic field becomes lesser as compared to $1/a^4$ in the reheating epoch, and thus the magnetic field's present strength may become larger than estimated in Eq.(3.84). Motivated by this situation, we aim to determine the magnetic field's current strength in the present magnetogenesis model by considering the reheating phase to have a non-zero e-fold number.

To this end, let us point out that an extended reheating phase is known to affect the evolution of the magnetic field at the background level [93, 94]. However, the importance of the Faraday effect during this phase has not been critically explored until recently in the context of the magnetogenesis scenario [70, 92, 95]. Furthermore, the effect of reheating is independent of our EFT construction, which is only applied during inflation. The most important point is that accounting for the EM Faraday effect can put interesting constraints on the reheating parameters, such as reheating temperature, inflaton equation of state, and reheating efolding number. Those constraints will propagate into constraints on the EFT parameters in a model-independent way. The constraints on the reheating and EFT inflationary parameters can be observed to be intertwined due to this reheating phase. We will discuss these in detail in the following sections.

3.6.1 Electromagnetic field evolution and the corresponding power spectrum during reheating

The effective theory parameters are so chosen, $f_1(\eta) = 1$, $f_2(\eta) = f_3(\eta) = f_4(\eta) = h(\eta) = 0$. After the end of inflation, the conformal symmetry coupling of the electromagnetic field (EM) is restored; hence, the EM field evolution will follow the standard Maxwell's equations in vacuum [92]. In particular, the equations of motion of $A_{\pm}(k, \eta)$

are given by,

$$A''^{(re)}_{\pm}(k,\eta) + k^2 A^{(re)}_{\pm}(k,\eta) = 0, \tag{3.85}$$

where $A^{(re)}_{\pm}(k,\eta)$ represents the electromagnetic mode function during reheating (i.e, the superscript 're' denotes the reheating era). As a consequence of the restored conformal symmetry, the further quantum production of the gauge field stops during the reheating stage, particularly the absolute value of the Bogoliubov coefficient in the post-inflation becomes time independent. At this stage, it deserves mentioning that we consider the universe a poor conductor; in particular, the universe has zero conductivity during the reheating era. However, due to the Schwinger production, such consideration of zero conductivity needs an investigation, which, in the context of EFT, is expected to be studied in the near future. Coming back to Eq.(3.85), the corresponding solution of the mode functions are,

$$A^{(re)}_{\pm}(k,\eta) = \frac{1}{\sqrt{2k}}\left[\alpha_{\pm}(k)\, e^{-ik(\eta-\eta_f)} + \beta_{\pm}(k)\, e^{ik(\eta-\eta_f)}\right], \tag{3.86}$$

with $\alpha_{\pm}(k)$, $\beta_{\pm}(k)$ being two integration constants and η_f is the end instant of inflation. The integration constants can be determined by matching the EM mode functions and their derivative (with respect to the conformal time) at the junction of inflation-to-reheating; in particular,

$$A^{(re)}_{\pm}(k,\eta_f) = A_{\pm}(k,\eta_f) \quad \text{and} \quad A'^{(re)}_{\pm}(k,\eta_f) = A'_{\pm}(k,\eta_f), \tag{3.87}$$

here $A_{\pm}(k,\eta)$ represents the mode function during inflation and follows Eq.(3.38) (note, the EM mode function during inflation is symbolized without any superscript, while the EM mode function during reheating is designated by the superscript 're'). Eqs.(3.86) and (3.87) immediately lead to $\alpha_{\pm}(k)$ and $\beta_{\pm}(k)$ as,

$$\begin{aligned}
\alpha_{\pm}(k) &= \sqrt{\frac{k}{2}}\, A_{\pm}(k,\eta_f) + \frac{i}{\sqrt{2k}}\, A'_{\pm}(k,\eta_f) \\
\beta_{\pm}(k) &= \sqrt{\frac{k}{2}}\, A_{\pm}(k,\eta_f) - \frac{i}{\sqrt{2k}}\, A'_{\pm}(k,\eta_f)
\end{aligned} \tag{3.88}$$

$A_{\pm}(k,\eta_f)$ can be obtained from their superhorizon solution as obtained in Eqs. (3.63) and (3.63), by putting $\eta = \eta_f$. If we think in terms of particle production during inflation, the above integration constants $\alpha_{\pm}(k)$ and $\beta_{\pm}(k)$ can be identified with the Bogoliubov coefficients at time $\eta = \eta_f$ for the incoming and outgoing modes, respectively. Naturally, those remain constants during the subsequent evolution. $|\beta_k(\eta)|$ represents the total number of produced particles (having momentum k) at time η_f from the Bunch-Davies vacuum defined at $\eta \to -\infty$. Hence, the time independence of the Bogoliubov coefficients during the reheating phase directly result from the fact that the conformal symmetry of the electromagnetic field is restored after inflation. Nonetheless, by plugging back the solution of $A_{\pm}^{(re)}(k,\eta)$ into Eq.(3.34) and by using the conformal invariance of the electromagnetic field (i.e $f_1(\eta) = 1$, $f_2(\eta) = 0$), We determine the magnetic and electric power spectra during the reheating epoch, as follows

$$\frac{\partial\rho(\vec{B})}{\partial\ln k} = \frac{1}{2\pi^2}\sum_{r=\pm}\frac{k^5}{a^4}\left|A_r^{(re)}(k,\eta)\right|^2$$
$$= \frac{1}{2\pi^2}\sum_{r=\pm}\left(\frac{k^4}{a^4}\right)\left[|\alpha_r|^2 + |\beta_r|^2 + 2|\alpha_r||\beta_r|\cos\left\{\theta_1^{(r)} - \theta_2^{(r)} - 2k(\eta-\eta_f)\right\}\right] \quad (3.89)$$

$$\frac{\partial\rho(\vec{E})}{\partial\ln k} = \frac{1}{2\pi^2}\sum_{r=\pm}\frac{k^2}{a^4}\left|A_r'^{(re)}(k,\eta)\right|^2$$
$$= \frac{1}{2\pi^2}\sum_{r=\pm}\left(\frac{k^4}{a^4}\right)\left[|\alpha_r|^2 + |\beta_r|^2 - 2|\alpha_r||\beta_r|\cos\left\{\theta_1^{(r)} - \theta_2^{(r)} - 2k(\eta-\eta_f)\right\}\right] \quad (3.90)$$

respectively, with r being the electromagnetic polarization index and runs from $r = \pm$, and furthermore $\theta_1^{(r)} = \mathrm{Arg}[\alpha_r(k,\eta_f)]$ and $\theta_2^{(r)} = \mathrm{Arg}[\beta_r(k,\eta_f)]$. Consequently, the total electromagnetic power spectrum is

$$\frac{\partial\rho_{em}}{\partial\ln k} = \frac{\partial\rho(\vec{B})}{\partial\ln k} + \frac{\partial\rho(\vec{E})}{\partial\ln k} = \frac{1}{\pi^2}\sum_{r=+,-}\left(\frac{k^4}{a^4}\right)\left[\left|\alpha_r(k,\eta_f)\right|^2 + \left|\beta_r(k,\eta_f)\right|^2\right]. \quad (3.91)$$

Furthermore, during the reheating epoch, the helicity spectrum evolves as,

$$P^{(h)}(k,\eta) = \left(\frac{k^3}{\pi^2 a^3}\right)\left\{\left|\beta_+\right|^2 - \left|\beta_-\right|^2 + \sqrt{1+\left|\beta_+\right|^2}\,\left|\beta_+\right|\,\cos\left\{\theta_1^{(+)} - \theta_2^{(+)} - 2k(\eta-\eta_f)\right\}\right.$$
$$\left. - \sqrt{1+\left|\beta_-\right|^2}\,\left|\beta_-\right|\,\cos\left\{\theta_1^{(-)} - \theta_2^{(-)} - 2k(\eta-\eta_f)\right\}\right\}, \quad (3.92)$$

where we use $|\beta_\pm|^2 - |\alpha_\pm|^2 = 1$. It can be observed from the above equations that the individual electric and magnetic spectrum depends on the phase factor evolution, which is the well-known Faraday effect. However, the comoving total electromagnetic power spectrum is independent of time and behaves as a standard radiation field. Furthermore, the helicity spectrum also evolves with the phase factor during reheating due to zero electrical conductivity. Moreover, the relative phase factors between the Bogoliubov coefficients, from the numerical solutions of $A_\pm(k,\eta)$, are determined as,

$$\begin{aligned} \theta_1^{(+)} - \theta_2^{(+)} &= \mathrm{Arg}\left[\alpha_+(\eta_f)\beta_+^*(\eta_f)\right] \simeq 3.141 \\ \theta_1^{(-)} - \theta_2^{(-)} &= \mathrm{Arg}\left[\alpha_-(\eta_f)\beta_-^*(\eta_f)\right] \simeq 3.141 \quad . \end{aligned} \tag{3.93}$$

This can also be understood from the analytic solutions of $A_\pm(k,\eta)$ in the superhorizon limit. In particular we obtained $\lim_{|k\eta|\ll 1} A_\pm \sim (-k\eta)^{-m}$ which leads to $\lim_{|k\eta|\ll 1} A'_\pm \sim (-k\eta)^{-m-1}$. Therefore for $m = 1$ (i.e the parametric value for the scenario S2), $A'_\pm(k,\eta)$ dominates over the corresponding mode functions $A_\pm(k,\eta)$ at the limit $|k\eta| \to 0$ i.e towards the end of inflation. As a result,

$$\alpha_\pm(k,\eta_f) \simeq \frac{i}{\sqrt{2k}} A'_\pm(k,\eta_f) \qquad , \qquad \beta_\pm(k,\eta_f) \simeq \frac{-i}{\sqrt{2k}} A'_\pm(k,\eta_f) \quad . \tag{3.94}$$

The above expressions, due to the presence of the $\pm i$ factor, immediately lead to the relative phase between the respective Bogoliubov coefficients as $\theta_1^{(\pm)} - \theta_2^{(\pm)} = \pi$, which is in agreement with the numerical estimation in Eq.(3.93).

Now we need to know the unknown part of the phase factor "$\eta - \eta_f$" which is defined as

$$\eta - \eta_f = \int_{a_f}^{a} \frac{da}{a^2 H} \quad . \tag{3.95}$$

The presence of the Hubble parameter in Eq.(3.95) indicates that in order to determine $\eta - \eta_f$ during the reheating phase, we need to state the background reheating dynamics, in particular how the inflaton energy density converts to other matter forms. In the present context, we will consider two simple reheating mechanisms: (1) An effective time-independent equation of state describes it, and (2) a perturbative reheating scenario.

3.6.2 Reheating with time independent equation of state: Evolution of Ectromagnetic field

Regarding the reheating process, as the first consideration, we follow the conventional reheating mechanism proposed by Kamionkowski et al. [66], where the reheating phase is parametrized by a constant equation of state ω_{eff}. The reheating equation of state parameter (i.e, ω_{eff}) remains constant during the entire reheating epoch. Finally, it makes a sharp transition to the vale $1/3$ at the end of it, which in turn indicates the beginning of the radiation epoch. Due to the constant equation of state, the Hubble parameter during the reheating evolves as $H \propto a^{-\frac{3}{2}(1+\omega_{\text{eff}})}$. Moreover, the reheating e-fold number N_{re}, and the reheating temperature (T_{re}) can be expressed in terms of the ω_{eff} and of some inflationary parameters by the following relations [66,67],

$$N_{re} = \frac{4}{3\omega_{\text{eff}} - 1}\left[\frac{1}{4}ln(\rho_f) - \frac{1}{4}ln\left(\frac{\pi^2 g_{re}}{30}\right) - \frac{1}{3}\left(\frac{43}{11 g_{s,re}}\right) - ln\left(\frac{a_0 T_0}{k}\right) - ln(H_*) + N_f\right] \quad (3.96)$$

$$T_{re} = \left(\frac{43}{11 g_s, re}\right)^{\frac{1}{3}}\left(\frac{a_0 T_0}{k}\right) H_* e^{-N_f} e^{-N_{re}}, \quad (3.97)$$

where, recall, the subscript '*' denotes the value of a quantity at the horizon crossing instant of CMB scale and N_f is the e-fold number of the inflation epoch. Moreover, ρ_f denotes the inflaton energy density at the end of inflation. The present CMB temperature is taken as $T_0 = 2.725\text{K}$, $k \approx 0.05\text{Mpc}^{-1}$ is the pivot scale and a_0 denotes the present time scale factor. The symbols $g_{s,re}$ and g_{re} represent the degrees of freedom for entropy at reheating and the effective number of relativistic species upon thermalization respectively, and they are taken to be the same, particularly $g_{s,re} = g_{re} \approx 100$. It may be observed from the above equations that both N_{re} and T_{re} depend on the inflationary parameters, in particular on H_* and N_f. For the inflationary quantities, we first consider the scalar spectral index (n_s) and the scalar perturbation amplitude ($\mathcal{A}_s$), which, in the context of EFT, takes the following forms [59],

$$n_s = 1 + \frac{4\dot{H}_*}{H_*^2} - \frac{\ddot{H}_*}{\dot{H}_* H_*} \quad , \quad \mathcal{A}_s = \frac{H_*^2}{4\epsilon_* M_{Pl}^2} \tag{3.98}$$

with $\epsilon_* = -\dot{H}_*/H_*^2$ and an overdot represents the differentiation with respect to the cosmic time. The first and second derivatives of H_* (appearing in the expression of n_s) are connected to the first and second slow-roll parameters, respectively. To determine N_f, we expand the Hubble parameter around $t = t_*$ (i.e, the horizon crossing instant of the CMB scale) as follows,

$$H(t) = H_* + \dot{H}_*(t - t_*) + \frac{1}{2}\ddot{H}_*(t - t_*)^2 \tag{3.99}$$

where we retain the terms up to $\mathcal{O}(\ddot{H}_*)$, that means we consider up to the second slow roll parameter. If the duration of inflation is designated by Δt, then the Hubble parameter at the end of inflation (H_f) is given by,

$$H_f = H_* + \dot{H}_*\Delta t + \frac{1}{2}\ddot{H}_*\left(\Delta t\right)^2 \ . \tag{3.100}$$

Inverting the above equation, we get the duration of inflation in terms of H_*, H_f, $\dot{H}_*$, and $\ddot{H}_*$ as,

$$\Delta t = \frac{|\dot{H}_*|}{\ddot{H}_*}\left(1 - \sqrt{1 - \frac{2\ddot{H}_*}{|\dot{H}_*|^2}(H_* - H_f)}\right) \tag{3.101}$$

with $|\dot{H}_*| = -\dot{H}_*$. Using the above expressions, we determine the inflationary e-folding number, which is given by,

$$\begin{aligned}
N_f &= \int_{t_*}^{t_f} H(t)dt \\
&= \frac{H_*|\dot{H}_*|}{\ddot{H}_*}\left(1 - \sqrt{1 - \frac{2\ddot{H}_*}{|\dot{H}_*|^2}(H_* - H_f)}\right) - \frac{|\dot{H}_*|^3}{2\ddot{H}_*^2}\left(1 - \sqrt{1 - \frac{2\ddot{H}_*}{|\dot{H}_*|^2}(H_* - H_f)}\right)^2 \\
&+ \frac{|\dot{H}_*|^3}{6\ddot{H}_*^2}\left(1 - \sqrt{1 - \frac{2\ddot{H}_*}{|\dot{H}_*|^2}(H_* - H_f)}\right)^3
\end{aligned} \tag{3.102}$$

in the second line, we use the expression of Δt from Eq.(3.101). Furthermore, Eq.(3.98) leads to $\dot{H}_*$ and $\ddot{H}_*$ in terms of n_s, $\mathcal{A}_s$ as follows

$$|\dot{H}_*| = \frac{H_*^4}{4\mathcal{A}_s M_{Pl}^2} \quad , \quad \ddot{H}_* = \frac{H_*^5}{4\mathcal{A}_s M_{Pl}^2}\left(\frac{H_*^2}{\mathcal{A}_s M_{Pl}^2} - (1-n_s)\right) \tag{3.103}$$

respectively. Here we would like to mention that, as depicted in Fig.3.1, the observable quantities like scalar spectral index and tensor-to-scalar ratios are indeed compatible with the Planck constraints in the present EFT context, where the EFT coefficients satisfy Eq.(3.42). Thereby using the viable value(s) of n_s and $\mathcal{A}_s$, in particular we will consider $n_s = 0.9649$ and $\ln[10^{10}\mathcal{A}_s] = 3.044$ (i.e the central values of n_s and $\mathcal{A}_s$ in respect to the Planck constraints), one can determine $\dot{H}_*$ and $\ddot{H}_*$ from Eq.(3.103), which in turn will evaluate the inflationary e-fold number from Eq.(3.102).

Returning to the quantity $\eta - \eta_f$, we first consider the behaviour of the Hubble parameter during the reheating stage. Because the effective EoS remains constant, the Hubble parameter behaves as $H \propto a^{-\frac{3}{2}(1+\omega_{\text{eff}})}$, and as a result, the term $\eta - \eta_f$ boils down to the following simple form:

$$\eta - \eta_f = \frac{2}{(1+3\omega_{\text{eff}})}\left[\frac{1}{aH} - \frac{1}{a_f H_f}\right], \tag{3.104}$$

where we use Eq.(3.95). Due to the above expression of $\eta - \eta_f$ along with the fact that $\left|\beta_{\pm}(\eta_f)\right|^2 \gg 1$, the magnetic power spectrum during the reheating era becomes [92]

$$\frac{\partial\rho(\vec{B})}{\partial \ln k} = \frac{1}{\pi^2}\left(\frac{k^4}{a^4}\right)\sum_{r=+,-}|\beta_r|^2\left\{\text{Arg}\left[\alpha_r\beta_r^*\right] - \pi - \left(\frac{4k}{3\omega_{\text{eff}}+1}\right)\left(\frac{1}{aH} - \frac{1}{a_f H_f}\right)\right\}^2 \tag{3.105}$$

The above equation indicates that the magnetic power evolution during reheating scales by two different terms: (1) the conventional one that goes as $1/a^4$ and (2) the term that redshifts as $\propto a^{-6}H^{-2}$, emerging from $\frac{1}{aH}$ in the right-hand side of Eq.(3.105). Because the universe undergoes deceleration, the EoS follows $\omega_{\text{eff}} > -\frac{1}{3}$, and thus the magnetic power effectively scales by the component $\propto a^{-6}H^{-2}$. In the context of instantaneous reheating, the magnetic power evolves as a^{-4} from the end of inflation until today, whereas if one considers an intermediate reheating phase with negligible conductivity, the evolution of magnetic power will be as described above. Due to this fact, the magnetic field's present strength can be larger than that for the instantaneous reheating case. This phenomenon can make the S2-like magnetogenesis scenario viable, which we will elaborate on next. The electric power in the reheating epoch evolves as,

$$\frac{\partial \rho(\vec{E})}{\partial \ln k} = \frac{1}{\pi^2}\left(\frac{k^4}{a^4}\right) \sum_{r=+,-} \left|\beta_r(\eta_f)\right|^2 \tag{3.106}$$

Hence, electric power evolves exactly like radiation during reheating on a large scale. Finally, the behavior of the helicity spectrum takes the following form in the large $|\beta(k, \eta_f)|$ limit,

$$\begin{aligned} P^{(h)} &= \left(\frac{k^3}{\pi^2 a^3}\right)\left\{\left|\beta_+(k,\eta_f)\right|^2 - \left|\beta_-(k,\eta_f)\right|^2\right\}\left\{\frac{4k}{3\omega_{\rm eff}+1}\left(\frac{1}{aH} - \frac{1}{a_f H_f}\right)\right\}^2 \propto \frac{1}{a^5 H^2} \\ &+ \cdots \end{aligned} \tag{3.107}$$

During reheating the Hubble parameters behaves as $H = a^{-\frac{3}{2}(1+\omega_{\rm eff})}$. Hence, from Eq.(3.107), the leading behaviour of the helicity density will be, $a^3 P^{(h)} \sim a^{1+3\omega_{\rm eff}}$. For all reheating equation of state $\omega_{\rm eff} > -\frac{1}{3}$, the comoving helicity during the reheating era monotonically grows with time.

3.6.2.1 Present day magnetic field and constraints on reheating parameters, ω_{eff}

Here, we may recall that the scenario S2 with an instantaneous reheating mechanism does not predict a sufficient magnetic strength in the present epoch, in particular it predicts $B_0 = 10^{-40}$G as shown in Eq.(3.84). Given the characteristic difference in the evolution of the magnetic power spectrum during reheating, we see how those models can be made viable with the CMB observations. With this motivation in mind, we are now in a position to constrain such a model with respect to the observation. For this, let us first express the Hubble parameter at the end of reheating (H_{re}) in terms of that of the end of inflation (H_f) as

$$H_{re} = H_f \left(\frac{a_{re}}{a_f}\right)^{-\frac{3}{2}(1+\omega_{eff})}, \tag{3.108}$$

where the suffix *'re'* denotes the end point of reheating and the scale factor a_{re} can be identified as $a_{re}/a_f = e^{N_{\rm re}}$ with $N_{\rm re}$ being the e-fold number of the reheating epoch and given in Eq.(3.96). Consequently, from Eq.(3.105), we evaluate the magnetic power spectrum at the end instant of reheating, as

$$\left.\frac{\partial\rho(\vec{B})}{\partial\ln k}\right|_{re} = \left(\frac{k^4}{a_{re}^4\pi^2}\right)\sum_{r=\pm}|\beta_r|^2\left\{\text{Arg}\left[\alpha_r\beta_r^*\right] - \pi - \left(\frac{4k}{(3\omega_{\rm eff}+1)a_f H_f}\right)\left[\left(\frac{H_f}{H_{re}}\right)^{\delta} - 1\right]\right\}^2 \quad (3.109)$$

where, $\delta = (3\omega_{\rm eff}+1)/(3\omega_{\rm eff}+3)$. After the reheating era, the conductivity of the universe is assumed to be sufficiently large so that the electric field dies out very fast. Therefore, Faraday induction will halt. Consequently, the magnetic field begins to evolve according to radiation as a^{-4} till today. The present-day magnetic power spectrum then becomes,

$$\left.\frac{\partial\rho(\vec{B})}{\partial\ln k}\right|_{0} = \left(\frac{a_{re}}{a_0}\right)^4 \left.\frac{\partial\rho(\vec{B})}{\partial\ln k}\right|_{re} \quad (3.110)$$

and, as a result, Eq.(3.109) leads to the current magnetic strength, as

$$B_0 = \frac{\sqrt{2}}{\pi}\left(\frac{k}{a_0}\right)^2\sqrt{\sum_{r=\pm}|\beta_r|^2\left\{\text{Arg}\left[\alpha_r\beta_r^*\right] - \pi - \left(\frac{4}{3\omega_{\rm eff}+1}\right)\left(\frac{k}{a_f H_f}\right)\left[\left(\frac{H_f}{H_{re}}\right)^{\delta} - 1\right]\right\}^2} \quad (3.111)$$

The above expression clearly indicates that the magnetic field's current amplitude explicitly depends on the reheating parameters $(\omega_{\rm eff}, H_{re})$, and inflationary n_s. As a consequence, probing B_0 and its nature open up a new window to look into the reheating phase. Given an inflationary model, the expression in Eq.(3.111) establishes the connection between the current magnetic strength B_0 and the reheating EoS parameter $\omega_{\rm eff}$. Thus, we may argue that the effective equation of state is no longer a free parameter; rather, it is fixed by the B_0 via CMB.

Having obtained the final expression of B_0, now we confront our model with the CMB observations, which put a constraint on the current magnetic strength, as $10^{-10}\text{G} \lesssim B_0 \lesssim 10^{-22}\text{G}$ [23,90,91]. For this purpose, we need H_f/H_{re}, which depends on $N_{\rm re}$, as

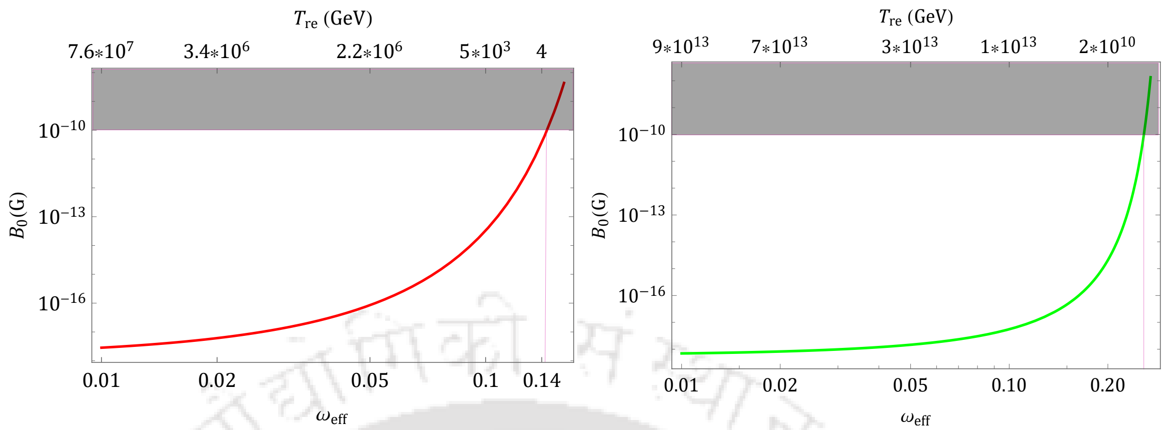

Figure 3.5: B_0 (in Gauss units) vs $\omega_{\rm eff}$ with $k = 0.05{\rm Mpc}^{-1}$ in the Kamionkowski like reheating scenario. The reheating temperature for different values of $\omega_{\rm eff}$ is shown in the upper label of the x-axis. In the left plot: $H_* = 10^{-5}M_{Pl}$, $n_s = 0.9649$, $\ln\left[10^{10}\mathcal{A}_s\right] = 3.044$, $N_f = 50$ and in the right plot: $H_* = 10^{-5}M_{Pl}$, $n_s = 0.9649$, $\ln\left[10^{10}\mathcal{A}_s\right] = 3.044$, $N_f = 55$.

discussed after Eq.(3.108). In our effective theory framework, we have three main input parameters: the inflationary energy scale H^* and the inflationary e-folding number N_f, and the reheating equation of state ω_{eff}. All the other parameters can be computed such as $N_{\rm re}, H_f, \dot{H}_*$ and $\ddot{H}_*$. Given the observed central values $n_s = 0.9649$, $\ln\left[10^{10}\mathcal{A}_s\right] = 3.044$, for our estimation, we consider two different sets of values for (H_*, N_f) particular, we consider - (1) $(H_*, N_f) = (10^{-5}M_{Pl}, 50)$ and (2) $(H_*, N_f) = (10^{-5}M_{Pl}, 55)$. The first and second sets correspond to the Hubble parameter at the end of inflation as $H_f = 3.61 \times 10^{-6}M_{Pl}$ and $H_f = 1.62 \times 10^{-6}M_{Pl}$ respectively, i.e H_f decreases with increasing e-folding number, as expected. With such considerations, we plot B_0 versus $\omega_{\rm eff}$ by using Eq.(3.111) in Fig.3.5. It clearly demonstrates that the theoretical prediction of B_0 lies well within the observational constraints for a certain range of values of the reheating EoS parameter, given by: $0.01 \lesssim \omega_{\rm eff} \lesssim 0.14$ for $N_f = 50$ and $0.01 \lesssim \omega_{\rm eff} \lesssim 0.25$ for $N_f = 55$, which are also consistent with BBN constraint on the minimum reheating temperature $\sim 10^{-2}{\rm GeV}$.

Finally, let us also point out how the helical nature of the magnetic field spectrum evolves, which is shown in the Fig.3.6. The figure depicts that the comoving helicity density grows with time during the reheating stage. However, during the post-

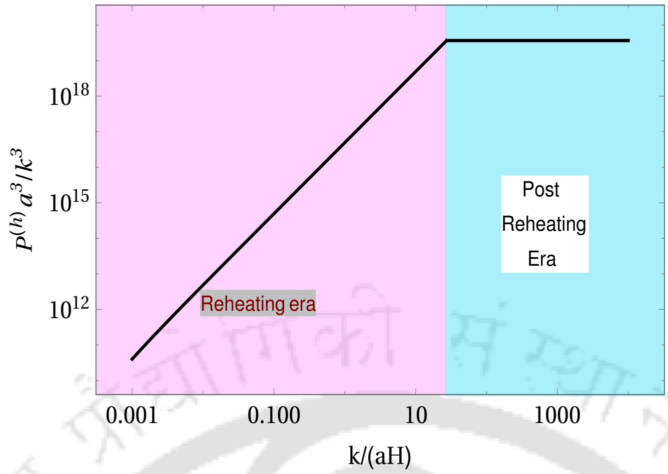

Figure 3.6: $P^{(h)}a^3/k^3$ versus $k/(aH)$ during and after reheating era. The reheating EoS is taken as $\omega_{\rm eff} = 0$ for which $\frac{k}{aH} \propto k\sqrt{a} \propto k\eta$.

reheating phase, the universe is considered to be a very good conductor, which in turn makes the electromagnetic mode functions constant over time. As a result, the helicity goes as $1/a^3$, or equivalently, the comoving helicity becomes constant during the after-reheating phase to the present epoch. Important to realize that the introduction of reheating has increased the comoving helicity density by a manifold compared to that of the helicity density produced for the instantaneous reheating case.

3.6.3 Perturbative reheating with time dependent EoS: Evolution of magnetic field

In this section we consider perturbative reheating scenario [183], where the inflaton energy density (ρ_ϕ) decays into the radiation energy density ($\rho_{\rm R}$) governed by the Boltzmann equations Eqs.(3.113) and (3.114). It essentially leads to the time-dependent effective equation of state (EoS) during the phase, which is defined by

$$\omega_{\rm eff} = \frac{3\omega_\phi \rho_\phi + \rho_R}{3\big(\rho_\phi + \rho_R\big)}. \tag{3.112}$$

Where, ω_ϕ symbolizes the time-averaged EoS of the inflaton field. For example, during reheating, for oscillating canonical inflaton with potential $V(\phi) \propto \phi^p$, assumes the time-averaged EoS, $\omega_\phi = (p-2)/(p+2)$. However, the effective equation of state ω_{eff} naturally [183] depends on time. Initially, $\omega_{\rm eff}$ behaves as approximately equal to ω_ϕ, and after a certain instance of time it smoothly transits to the value $\approx 1/3$, setting the beginning of the radiation epoch. This scenario is different from that of the earlier one, where the inflaton energy density is assumed to be instantaneously converted into radiation energy density at the end of reheating.

The set of Boltzmann equations governing the evolution of ρ_ϕ and ρ_R are given by,

$$\frac{d\Phi}{d\xi} + \frac{\sqrt{3}M_{Pl}\Gamma_\phi}{H_f^2}(1+\omega_\phi)\frac{\xi^{1/2}\Phi}{\Phi\xi^{-3\omega_\phi} + R\xi^{-1}} = 0 \tag{3.113}$$

and

$$\frac{dR}{d\xi} - \frac{\sqrt{3}M_{Pl}\Gamma_\phi}{H_f^2}(1+\omega_\phi)\frac{\xi^{\frac{3(1-2\omega_\phi}{2}}\Phi}{\Phi\xi^{-3\omega_\phi} + R\xi^{-1}} = 0 \quad , \tag{3.114}$$

respectively. The Boltzmann equations are expressed in terms of a rescaled scale factor $\xi(a) = a/a_f$ for convenience, with a_f being the scale factor at the end of inflation. Furthermore Γ_ϕ symbolizes the decay rate from inflaton to radiation energy density and the comoving densities are rescaled in terms of the dimensionless variable as,

$$\Phi = \left(\frac{\rho_\phi}{H_{\rm f}^4}\right)\xi^{3\left(1+\omega_\phi\right)} \quad ; \quad R = \left(\frac{\rho_R}{H_{\rm f}^4}\right)\xi^4 \ . \tag{3.115}$$

For solving the above Boltzmann equations, the natural initial conditions will be set at the end of inflation as follows,

$$\Phi(\xi = 1) = \rho_f/H_f^4 \quad \text{and} \quad R(\xi = 1) = 0 \,, \tag{3.116}$$

ρ_f is the inflaton energy density at $\xi = 1$. Furthermore, the reheating temperature is identified from the radiation temperature $T_{\rm rad}$ at the point of $H(t_{\rm re}) = \Gamma_\phi$ ($t_{\rm re}$ denotes the end of reheating), when maximum inflaton energy density is transferred into radiation.

$$T_{re} = T_{rad}^{end} = \left(\frac{30}{\pi^2 g_{re}}\right)^{1/4}\left[\rho_R(\Gamma_\phi, \xi_{re}, n_s)\right]^{1/4} . \tag{3.117}$$

with ξ_{re} being the rescaled factor at the end of reheating i.e $\xi_{re} = a_{re}/a_f$. From the entropy conservation of thermal radiation, the relation among $T_{\rm rad} = T_{\rm re}$ at equilibrium,

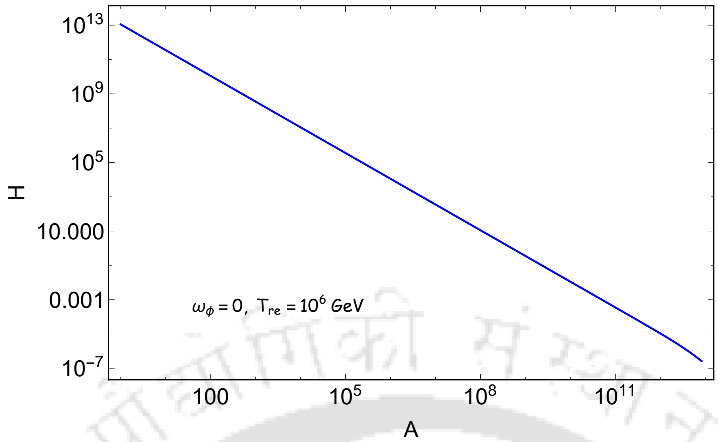

Figure 3.7: The background Hubble parameter $H(\xi)$ versus ξ during the reheating era i.e for $1 \leq \xi \leq \xi_{re}$. The plot corresponds to $\omega_\phi = 0$ and $T_{\rm re} = 10^6$GeV.

and $(T_0, T_{\nu 0} = (4/11)^{1/3} T_0)$, the temperature of the CMB photon and neutrino background at the present day, respectively, can be written as

$$g_{re} T_{re}^3 = \left(\frac{a_0}{a_{re}}\right)^3 \left(2T_0^3 + 6\frac{7}{8} T_{\nu 0}^3\right). \tag{3.118}$$

Using the above equation, one arrives at the following well-known relation

$$T_{re} = \left(\frac{43}{11 g_{re}}\right)^{\frac{1}{3}} \left(\frac{a_0 T_0}{k}\right) H_* e^{-N_{\rm f}} e^{-N_{\rm re}} \ , \tag{3.119}$$

where N_{re} is the e-folding number of the reheating era. To establish one to one correspondence between $T_{\rm re}$ and Γ_ϕ, we combine the equations (3.117) and (3.119). To fix the values of decay width Γ_ϕ in terms of spectral index (n_s), we use one further condition at the end of the reheating

$$H^2(\xi_{re}) = \frac{1}{\xi_{\rm re}^2}\left(\frac{d\xi_{\rm re}}{dt}\right)^2 = \frac{\rho_\phi(\Gamma_\phi, \xi_{\rm re}, n_s) + \rho_R(\Gamma_\phi, \xi_{re}, n_s))}{3M_{\rm Pl}^2} = \Gamma_\phi^2 \ . \tag{3.120}$$

With the above equipments, we solve the Hubble parameter ($H^2(\xi) = \frac{1}{3M_{Pl}^2}(\rho_\phi + \rho_R)$) numerically along with the coupled Boltzmann differential equations (3.113) and (3.114). The numerical solutions of $H(\xi)$ is depicted in Fig.3.7 which corresponds to a particular set: $T_{\rm re} = 10^6$GeV and $\omega_\phi = 0$ respectively. In the perturbative reheating scenario, the quantity $\eta - \eta_f$ of Eq.(3.95) can be expressed as,

$$\eta - \eta_f = \left(\frac{1}{a_f H_{\rm f}}\right) \int_1^{\xi} \frac{d\xi}{\xi^2} \frac{\sqrt{3} M_{Pl} H_{\rm f}}{\sqrt{\rho_r(\xi) + \rho_\phi(\xi)}} \,, \tag{3.121}$$

where ρ_ϕ and ρ_R are governed by the coupled Eqs.(3.113) and (3.114). Due to the complicated nature of the Boltzmann equations, the integral in Eq.(3.121) may not be performed in a closed form; however, we will perform it numerically for various values of ω_ϕ. The above expression of $\eta - \eta_f$ immediately leads to the magnetic power spectrum during the reheating era as follows,

$$\frac{\partial \rho(\vec{B})}{\partial \ln k} = \frac{1}{\pi^2}\left(\frac{k^4}{a^4}\right) \sum_{r=\pm} \left|\beta_r\right|^2 \left\{ \mathrm{Arg}\left[\alpha_r \beta_r^*\right] - \pi - 2\left(\frac{k}{a_f H_{\rm f}}\right) \int_1^{\xi} \frac{d\xi}{\xi^2} \frac{\sqrt{3} M_{Pl} H_{\rm f}}{\sqrt{\rho_r(\xi) + \rho_\phi(\xi)}} \right\}^2 \tag{3.122}$$

Furthermore, due to the fact that $\left|\beta_r(\eta_f)\right| \gg 1^2$, the electric power spectrum during the reheating phase goes as,

$$\frac{\partial \rho(\vec{E})}{\partial \ln k} = \frac{1}{\pi^2}\left(\frac{k^4}{a^4}\right) \sum_{r=\pm} \left|\beta_r(\eta_f)\right|^2 \,. \tag{3.123}$$

The above expressions will be used to investigate whether scenario S2, with a reheating phase, characterized by a perturbative mechanism, will predict sufficient magnetic strength in the present Universe. We will analyze this for different values of ω_ϕ in Sec.3.6.3.1, which in turn will help to probe various information about the reheating phase.

3.6.3.1 Present day magnetic field and constraints on perturbative reheating

Following this same methodology considered for the earlier reheating scenario, we will see that the present value of the magnetic field constrains the perturbative reheating dynamics. During the perturbative reheating, the effective EoS $\omega_{\rm eff}$ is time-dependent. However, to set constraints, we may introduce an average effective EoS defined by,

$$\langle \omega_{\rm eff} \rangle = \frac{1}{\xi_{re} - 1} \int_1^{\xi_{re}} \omega_{\rm eff}\, d\xi = \frac{1}{\xi_{re} - 1} \int_1^{\xi_{re}} \left\{ \frac{3\omega_\phi \rho_\phi + \rho_R}{3\left(\rho_\phi + \rho_R\right)} \right\} d\xi \tag{3.124}$$

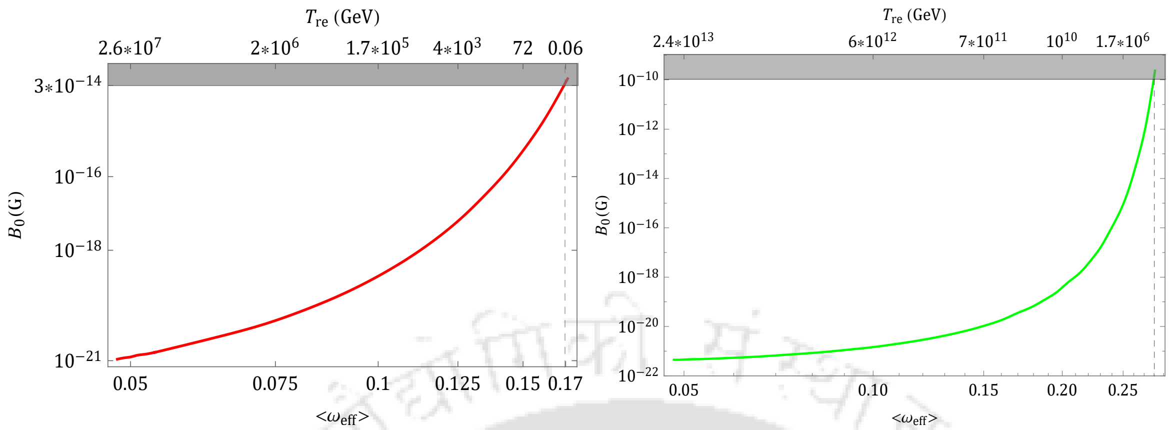

Figure 3.8: B_0 (in Gauss units) vs $\langle\omega_{\rm eff}\rangle$ with $k = 0.05\text{Mpc}^{-1}$ in the perturbative reheating scenario. The reheating temperature for different values of $\langle\omega_{\rm eff}\rangle$ is shown in the upper label of the x-axis. In the left plot: $H_* = 10^{-5}M_{Pl}$, $n_s = 0.9649$, $\ln\left[10^{10}\mathcal{A}_s\right] = 3.044$, $N_f = 50$ and in the right plot: $H_* = 10^{-5}M_{Pl}$, $n_s = 0.9649$, $\ln\left[10^{10}\mathcal{A}_s\right] = 3.044$, $N_f = 55$.

where we use Eq.(3.112) and recall, $\xi = 1$ to $\xi = \xi_{re}$ denotes the reheating phase. It may be observed from Eq.(3.124) that $\langle\omega_{\rm eff}\rangle$ contains the information of background evolution of ρ_ϕ and ρ_R, and also depends on the inflaton EoS (ω_ϕ). Following Eq.(3.122), and the detailed procedure discussed in the previous section, one obtains the magnetic field strength at the present epoch as,

$$B_0 = \frac{\sqrt{2}}{\pi}\left(\frac{k}{a_0}\right)^2 \sqrt{\sum_{r=\pm}|\beta_r|^2\left\{\text{Arg}\left[\alpha_r\,\beta_r^*\right] - \pi - \left(\frac{2kM_{pl}}{a_f H_{\rm f}}\right)\int_1^{\xi_{re}}\frac{d\xi}{\xi^2}\frac{\sqrt{3}H_{\rm f}}{\sqrt{\rho_r(\xi)+\rho_\phi(\xi)}}\right\}^2} \tag{3.125}$$

For this purpose, we will take the same set of parameter values as before for our numerical computation, $(H_*, N_f) = (10^{-5}M_{Pl}, 50)$ and (2) $(H_*, N_f) = (10^{-5}M_{Pl}, 55)$. Given those values, we first need to evaluate ξ_{re} appearing in the upper limit of the integral, which is done by simultaneously satisfying the following equations:

$$H(\xi_{re}) = \Gamma_\phi \;\; , \;\; T_{re} = \left(\frac{30}{\pi^2 g_{re}}\right)^{1/4}\rho_R^{1/4} \;\; , \;\; T_{re} = \left(\frac{43}{11 g_s, re}\right)^{\frac{1}{3}}\frac{a_0 T_0}{k}H_* e^{-N_f}e^{-N_{re}} \tag{3.126}$$

Using ξ_{re} and the numerical solutions of ρ_ϕ and ρ_R from the Boltzmann equations, we get the variation of B_0 with ω_ϕ, which is depicted in Fig.3.8. It is with respect to the average effective EoS of the reheating era, i.e, in respect to $\langle\omega_{\rm eff}\rangle$ defined in Eq.(3.124). As we may observe, similar to the earlier reheating case, the current magnetic strength in the perturbative reheating mechanism increases with the average effective EoS (i.e $\langle\omega_{\rm eff}\rangle$, defined in Eq.(3.124)) and lies within the observational constraints for a suitable regime of reheating parameters. However, the viable range of the reheating parameters differs in the two reheating mechanisms . In particular, the compatibility of the scenario S2, with a reheating phase characterized by a perturbative mechanism, both with the CMB observations on B_0 and with the BBN constraint on the reheating temperature, leads to a constraint on $\langle\omega_{\rm eff}\rangle$ as: $0.05 \lesssim \langle\omega_{\rm eff}\rangle \lesssim 0.17$ for $N_f = 50$ and $0.04 \lesssim \langle\omega_{\rm eff}\rangle \lesssim 0.27$ for $N_f = 55$ respectively.

3.7 Conclusion

Effective field theory is a powerful tool in various branches of physics. In this chapter, we studied inflationary magnetogenesis in this EFT framework in detail. In the cosmological Universe, four-dimensional diffeomorphism symmetry is generically broken down to spatial diffeomorphism. In this framework, the electromagnetic sector automatically breaks conformal invariance, which plays the crucial role in producing the gauge field from the quantum vacuum. We have also considered the parity-violating term, which further gives rise to the helical magnetic field, which has great observational significance. The form of the coupling functions has been considered in such a way that during inflation, the electromagnetic field evolves non-trivially; however, at late times (in particular after the end of inflation), the conformal symmetry of the EM field is restored and consequently the standard Maxwellian evolution is restored.

We have explored the evolution of the EM, scalar, and tensor perturbations and determined the primordial power spectrum taking into account PLANCK and large-scale magnetic field observations. In regard to the cosmological evolution of the electric and magnetic fields, we discussed the possibilities of a scale-invariant magnetic or electric power spectrum, particularly at the superhorizon scale. If we consider instantaneous reheating after inflation, it is observed that the scale-invariant magnetic field scenario is observationally compatible, but it suffers from the backreaction problem. On the other hand, the scale-invariant electric field scenario is indeed free from the backreaction problem. However, it does not predict a sufficient amount of magnetic strength in the present Universe.

To cure this problem, we next introduce a reheating phase with non-trivial evolution dynamics and a non-zero e-folding number. Two different reheating mechanisms are considered: (i) Reheating dynamics is [66] governed by a time independent effective equation of state ($\omega_{\rm eff}$). (ii) As a second possibility, we consider a perturbative reheating scenario where the effective equation of state is time-evolving due to non-trivial decay of the inflaton into the radiation. Because of the reheating phase, the post-inflation dynamics of the EM field become non-trivial. The most interesting case arises when one considers vanishing electrical conductivity during this phase, which induces an additional magnetic field from the non-vanishing electric field due to the well-known Faraday effect. However, after the end of reheating, this effect ceases to exist as the Universe becomes a good conductor and, hence, the electric field vanishes. Specifically, the magnetic field energy density evolves as $a^{-6}H^{-2}$ during the reheating era, and after the reheating, as a^{-4}. Furthermore, we observed that reheating also helps increase the helicity of the magnetic field if parity violation is introduced in the system, as shown in Fig.3.6. Reheating phase, therefore, helps enhance the present value of magnetic field as compared to the ordinary instantaneous reheating case. Our detailed analysis shows that this is precisely the mechanism that can provide the right magnitude of the present magnetic field for the scale-invariant electric field scenario. However, this mechanism does not help to cure the problem for the scale-invariant magnetic case. The reason is that the backreaction problem occurs during inflation and thus can not be rescued by any post-inflationary phase. We will discuss the possible resolution of this problem in our forthcoming paper.

Most importantly, introducing the reheating era not only helps to obtain the right magnitude of the large-scale magnetic field, It allows one to obtain valuable information about the reheating EoS parameter ($\omega_{\rm eff}$), which in turn can potentially constrain the inflationary model itself, which has been discussed before in some of our recent works [70, 95]. Therefore, probing a large-scale magnetic field opens up a new probe to look into the reheating phase, which is otherwise very difficult to constrain. Combining CMB, presently observed constraint on B_0, and the BBN constraint, our analysis restricts the value of of $\omega_{\rm eff}$ as follows: (i) $0.01 \lesssim \omega_{\rm eff} \lesssim 0.14$ for $N_f = 50$ and $0.01 \lesssim \omega_{\rm eff} \lesssim 0.25$ for $N_f = 55$ for the reheating scenario where EoS is constant. and (ii) $0.05 \lesssim \langle\omega_{\rm eff}\rangle \lesssim 0.17$ for $N_f = 50$ and $0.04 \lesssim \langle\omega_{\rm eff}\rangle \lesssim 0.27$ for $N_f = 55$ for the perturbative reheating scenario (recall, N_f is the inflationary e-folding number and $\langle\omega_{\rm eff}\rangle$ is the average effective EoS during the reheating era defined in Eq.(3.124). The reheating era provides a viable constraint on the reheating EoS parameter from CMB observations.

4

Magnetogenesis from Anisotropic Inflation

Contents

Based on *"Magnetogenesis from an anisotropic universe"* by S. Pal, D. Maity and T. Q. Do, **Phys. Rev. D 109, no.8, 083507 (2024)** [arXiv:2311.07685].

As we had discussed in Chapter 1, it is well known that our Universe is magnetized on all observational scales. Starting from the planets and stars to large-scale galaxies and galaxy clusters, and even to the intergalactic medium (IGM). In particular, the magnetic field strength for galaxies and galaxy clusters has been observed to be $\sim \mu G$. A few G of magnetic field is hosted by planets. Furthermore, in the case of neutron stars, a magnetic field strength of $10^{12} G$ has been measured. From Gamma-ray observations and Faraday rotation measurements, the magnetic field in the intergalactic medium (IGM) has also been shown to be bounded with the strength ranging from $10^{-10} - 10^{-22}\ G$ [23, 50, 90, 91, 96]. The presence of magnetic fields on a large scale ($\sim 1\ MPc$), especially in the IGM, suggests that they are primordial, having been generated during the Big Bang or later and surviving until today as a relic. Magnetohydrodynamic processes can successfully explain the magnetic fields in galaxies and galaxy clusters, where the dynamo mechanism amplifies the seed magnetic field. However, the origin of primordial magnetic fields is still an active area of research. Various mechanisms for generating large-scale primordial magnetic fields have been proposed, which can be found in Refs. [31, 34, 36, 93, 97–108]. Among all the proposed models, the inflationary magnetogenesis model is the most accepted one [31], where the electromagnetic fields are generated during the inflationary period. Here, the conformal invariance of the Maxwell term, i.e., $F_{\mu\nu}F^{\mu\nu}$ under a spatially flat background, is broken through non-minimal coupling(s) with other fields, such as scalar fields.

Following the inflationary magnetogenesis mechanism provided in refs. [30, 31, 33, 93, 103, 109], we propose a novel mechanism for generating the primordial magnetic fields through anisotropic spacetime. In particular, the Maxwell field experiences the existence of the anisotropies of spacetime during the inflationary era, and therefore, the conformal invariance is not protected. In cosmology, there exists a nice classification of homogeneous but anisotropic spacetimes called the Bianchi universe [110–114]. We work with the Bianchi type I metric, which is the simplest one and can be regarded as a straightforward extension of the Friedmann-Lemaitre–Robertson–Walker (FLRW) spacetime. Therefore, we study the evolution of the electromagnetic field during the inflationary era.

Remarkably, it has long been argued that the very early Universe, which is close to the initial singularity, should be strongly anisotropic [115–117]. During an inflationary phase of the early Universe, all spatial anisotropies, which could have happened in a pre-inflationary phase, should decrease very quickly such that the Universe speedily approaches a locally isotropic state, as pointed out in Refs. [118, 119]. It should be noted that this scenario is consistent with the so-called cosmic no-hair conjecture, which claims that all initial anisotropies and inhomogeneities should disappear in a late-time universe [120,121]. Very interestingly, some recent unavoidable anomalies in the cosmic microwave background (CMB)radiations confirmed by the Planck [88,122], such as the cold spot and hemispheric asymmetry, have challenged the standard inflationary universe models, which are based on the cosmological principle stating, the Universe should be homogeneous and isotropic on large scales. In addition, other interesting observational evidence, which has called the validity of the cosmological principle into question, has been listed in a recent interesting review [123]. These remarkable points lead us to a possible scenario of an anisotropic inflationary universe in early times. Many papers have been working on anisotropic inflation, e.g., see Refs. [110–112] as well as Refs. [124–129].

Here, we do not discuss the origin of anisotropies in spacetime; rather, we study the effect of this anisotropy. We treat the anisotropies as a perturbation over the FLRW background. As the spatial anisotropy breaks the conformal flatness of the background in the electromagnetic (EM) field, we do not need any explicit coupling with the scalar field as proposed in the literature [93, 103–105, 108] for gauge field production during inflation. In this context, it is important to mention the challenges in inflationary magnetogenesis, namely the strong-coupling problem and the backreaction problem [35, 36, 89, 93]. In the literature, several mechanisms and different types of coupling [35] have been introduced to overcome these problems. However, in our formalism, the strong coupling problem is readily solved in this paper since no explicit coupling is involved with the gauge field. However, there might still be a possibility of backreaction, which we will discuss in detail in the next sections.

4.1 Bianchi I type spacetime and Quantization of the Electromagnetic field

We introduce the spatial anisotropy in the background through the homogeneous but anisotropic Bianchi type I metric. In general, this type of metric can be written as

$$ds^2 = a^2(\eta)\left[-d\eta^2 + b^2(\eta)dx^2 + dy^2 + dz^2\right], \tag{4.1}$$

where η is the conformal time, $a(\eta)$ is the overall scale factor and $b(\eta)$ is the anisotropic factor along the x-direction. In our phenomenological model, we impose the condition that the anisotropy in the spacetime exists only in the inflationary era, although the spacetime remains continuous. This ansatz guarantees that the conformal flatness is restored after inflation. These conditions can be satisfied by various models of the anisotropic factor $b(\eta)$. However, we take a particular model that satisfies all the necessary conditions

$$b(\eta) = 1 + \alpha\, e^{-\left(\frac{\eta}{\eta_m}\right)^2}, \tag{4.2}$$

In the above Eq. (4.2), α is a dimensionless parameter that determines the strength of the anisotropy. Furthermore, η_m is a parameter that dictates the overall behavior of the anisotropic background. An example of the anisotropic background is shown in Fig. 4.1. Here, α and η_m are free parameters of the anisotropic model. In this paper, we do not discuss the origin of such anisotropies. However, the anisotropy, particularly near the end of inflation, may be a combined effect of quantum field theory and the sudden breakdown of slow-roll conditions. We will come back to this issue in the future.

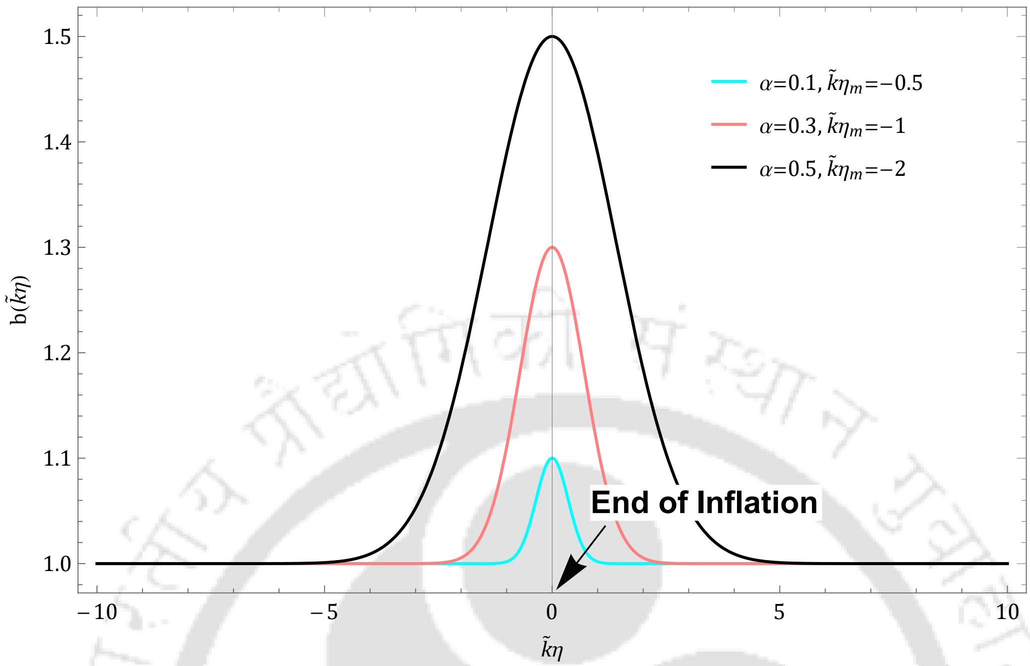

Figure 4.1: Behaviour of the anisotropic factor $b(\tilde{k}\eta)$ with $\tilde{k}\eta$ for anisotropic free parameters α and $\tilde{k}\eta_m$.

The action of Einstein-scalar-vector theory can be given by

$$\mathcal{S} = \int d^4x\sqrt{-g}\left[\frac{1}{16\pi G}R - \frac{1}{2}\partial_\mu\phi\partial^\mu\phi - V(\phi) - \frac{1}{4}F_{\mu\nu}F^{\mu\nu}\right], \tag{4.3}$$

where G is the gravitational constant, ϕ is a scalar field, and $F_{\mu\nu} \equiv \partial_\mu A_\nu - \partial_\nu A_\mu$ is the field strength of the vector field $A_\mu(t, \mathbf{x})$ describing the electromagnetic field. In this paper, the dynamics of the scalar field and the metric itself due to the anisotropies present are beyond our scope. Therefore, we will mainly discuss the dynamics of the EM field during the inflationary era due to the spatially anisotropic background. Therefore, the Lagrangian of interest here is the Lagrangian corresponding to the electromagnetic field, which, according to Eq. (5.1), is given by

$$\mathcal{L}_{em} = \frac{1}{2a^2}g^{jn}A'_jA'_n - \frac{1}{4}g^{im}g^{jn}F_{ij}F_{mn}, \tag{4.4}$$

where the prime denotes a derivative with respect to conformal time. In this paper, all the physical quantities are denoted with the lower index, e.g., the physical momentum is denoted by k_i, and the vector potential is given by A_i. We set $A_0 = 0$ as the choice of gauge, and unlike the case of conformally flat spacetime, the $\nu = 0$ component satisfies the modified constraint equation,

$$\tilde{g}^{im}\partial_i A'_m = 0, \tag{4.5}$$

where we have defined $\tilde{g}^{ij} = a^2 g^{ij}$ for simplicity of calculation. It can be further shown that the above equation boils down to the usual Coulomb condition for the conformally flat case. However, the raising (and lowering) of the indices is done through the metric component $g^{ij}(g_{ij})$. Similarly, the dynamical equation of motion for the magnetic vector potential A_i can be calculated from the $\nu = j$ component, which boils down to

$$A''_n + \frac{b'}{b}A'_n + \tilde{g}_{jn}\tilde{g}'^{jk}A'_k - \tilde{g}^{im}\partial_i F_{mn} = 0. \tag{4.6}$$

It is important to note that the metric components play a crucial role in the dynamics of the field. In the case of a standard conformally flat background, the term with the metric component's derivative vanishes, giving us the regular plane wave solutions. Now, we will promote the fields and their conjugates as operators. The conjugate momentum operator corresponding to the field operator A_i turns out to be

$$\Pi^i = \frac{\partial \mathcal{L}_{em}}{\partial A'_i} = \frac{1}{a^2}g^{im}A'_m. \tag{4.7}$$

To quantize the field, we decompose the magnetic vector potential A_i as,

$$A_i(\eta, \mathbf{x}) = \sum_p \int \frac{d^3k}{(2\pi)^3}\left(a^{(p)}_{\mathbf{k}} u^{(p)}_i(\eta)e^{ik_n x^n} + a^{\dagger(p)}_{\mathbf{k}} u^{*(p)}_i(\eta)e^{-ik_n x^n}\right). \tag{4.8}$$

In the above Eq. (4.8), (p) is the polarization index, $a^{(p)}_{\mathbf{k}}$ and $a^{\dagger(p)}_{\mathbf{k}}$ are the annihilation and creation operators corresponding to the polarization mode (p). They follow the general commutation relation,

$$\left[a^{(p)}_{\mathbf{k}}, a^{(q)}_{\mathbf{k}'}\right] = \delta^{pq}(2\pi)^3\delta^3(\mathbf{k} - \mathbf{k}'). \tag{4.9}$$

In this article, the boldface letters represent vector quantities.

In this context, it is important to discuss the commutation relation of the magnetic vector potential A_i and its conjugate momentum Π^i. We impose the commutation relation, such that they satisfy the constraint Eq. (4.5) on vector potential A_i,

$$\begin{aligned} [A_i(\eta,\mathbf{x}), A_j(\eta,\mathbf{y})] &= 0; \; [\Pi_i(\eta,\mathbf{x}), \Pi_j(\eta,\mathbf{y})] = 0, & (4.10) \\ \left[A_i(\eta,\mathbf{x}), \Pi^j(\eta,\mathbf{y})\right] &= \frac{i}{\sqrt{-g}} \int \frac{d^3k}{(2\pi)^3} e^{ik_n(x^n-y^n)} \times \left(\delta_i^j - \frac{k_i k^j}{k_n k^n}\right). & (4.11) \end{aligned}$$

With the quantization of the field, we now get the mode function equations using Eq. (4.6). The mode functions satisfy the relation,

$$u_n'' + \frac{b'}{b} u_n' + \tilde{g}'^{jl} \tilde{g}_{jn} u_l' + \tilde{g}^{im} \left(k_m k_i u_n - k_n k_i u_m\right) = 0. \tag{4.12}$$

The polarization index is omitted here, as all the polarization modes follow the same equation of motion. Similarly, the constraint Eq. (4.5) in terms of the mode function becomes

$$\tilde{g}^{in} k_i u_n' = 0. \tag{4.13}$$

Interestingly, Eq. (4.12) contains the derivative of the metric coefficients, which works as the source of particle production during the inflationary era. As the mode function equation contains the derivative of the metric components, substituting the metric components, we get the modified mode function equations as,

$$\begin{aligned} & u_1'' - \frac{b'}{b} u_1' + k_2^2 u_1 + k_3^2 u_1 - k_1 k_2 u_2 - k_1 k_3 u_3 = 0, \\ & u_2'' + \frac{b'}{b} u_2' + \frac{k_1^2}{b^2} u_1 + k_3^2 u_2 - \frac{k_1 k_2}{b^2} u_1 - k_2 k_3 u_3 = 0, \\ & u_3'' + \frac{b'}{b} u_3' + \frac{k_1^2}{b^2} u_3 + k_2^2 u_3 - \frac{k_1 k_3}{b^2} u_1 - k_2 k_3 u_2 = 0. \end{aligned} \tag{4.14}$$

Moreover, all the mode functions u_1, u_2, and u_3 satisfy the constraint in Eq. (4.13) which explicitly boils down to

$$\frac{k_1}{b^2} u_1' + k_2 u_2' + k_3 u_3' = 0. \tag{4.15}$$

The mode functions follow the normalization condition,

$$\left(u_i^{(p)}\tilde{g}^{jm}u_m^{*\prime(p)} - u_i^{*(p)}\tilde{g}^{jm}u_m^{\prime(p)}\right) = \frac{i}{2b}\left(\delta_i^j - \frac{k_ik^j}{k_nk^n}\right). \tag{4.16}$$

Utilizing the above formalism of quantization along with the constraint relation, we evolve the mode function in different phases of the universe until the present epoch.

4.2 Evolution of Electromagnetic field during inflationary era

According to our model in Eq.(4.1), the anisotropy in the spacetime exists only towards the end of inflation. After the end of inflation, within a short period, the spacetime becomes FLRW. again, as seen from Fig. 4.1. However, it is important to mention that the large-scale production of the EM field is not affected due to this short presence of anisotropy after inflation. It is also evident that $b \to 1$ towards past infinity ensures that the Bunch-Davis vacuum condition is satisfied in the infinite past. Furthermore, we assume the background spacetime is de Sitter in nature, i.e., $a = -1/(H\eta)$, where H is the Hubble parameter during inflation and remains constant throughout the entire inflation. Following these initial conditions, we numerically solve the mode function equations shown in Eq. (4.14). We consider $k_1 = k_2 = k_3 = \tilde{k} \sim 1$ Mpc^{-1} for simplification and the Hubble parameter $H = 10^{-5}M_{\rm pl}$ remains constant throughout the inflationary era. Here $M_{\rm pl} = \sqrt{1/(8\pi G)}$ is the reduced Planck mass. We redefine the conformal time η as a dimensionless parameter $x = \tilde{k}\eta$. In terms of this new variable, Eq. (4.2) can be rewritten as,

$$b(x) = 1 + \alpha e^{-\left(\frac{x}{x_m}\right)^2}, \tag{4.17}$$

where the parameters α and $\tilde{k}\eta_m$ are chosen accordingly to avoid the backreaction from anisotropy, which essentially means that the anisotropy acts as a perturbation over the FLRW universe. A detailed discussion of the anisotropic backreaction is done in the later section. In terms of the redefined variables $x = \tilde{k}\eta$, $\tilde{u}_i = \sqrt{\tilde{k}}u_i$, and $\tilde{k} = k_1 = k_2 =$

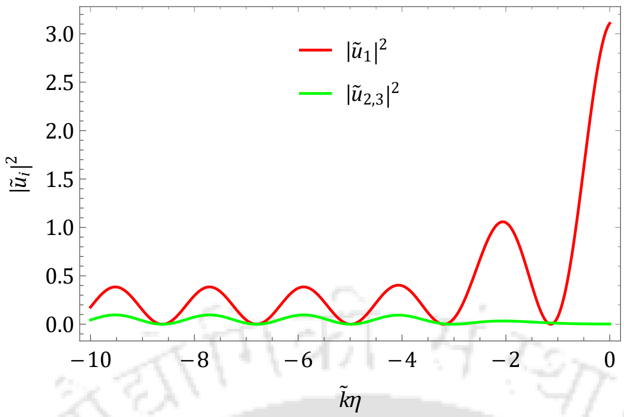

Figure 4.2: Evolution of the mode functions $\tilde{u}_1$, $\tilde{u}_2$, and $\tilde{u}_3$ with $x = \tilde{k}\eta$ for the value of anisotropic parameter $\alpha = 3$ and $x_m = -2$. As the anisotropy exists only along the x-direction, the mode function equation corresponding to the x-direction $(\tilde{u}_1)$ behaves differently than the other two $(\tilde{u}_2, \tilde{u}_3)$.

k_3, the mode function equations can be written as,

$$\begin{aligned} \frac{d^2\tilde{u}_1}{dx^2} - \frac{1}{b}\frac{db}{dx}\frac{d\tilde{u}_1}{dx} + 2\tilde{u}_1 - \tilde{u}_2 - \tilde{u}_3 &= 0, \\ \frac{d^2\tilde{u}_2}{dx^2} + \frac{1}{b}\frac{db}{dx}\frac{d\tilde{u}_2}{dx} + \frac{\tilde{u}_2 - \tilde{u}_1}{b^2} - \tilde{u}_3 &= 0, \\ \frac{d^2\tilde{u}_3}{dx^2} + \frac{1}{b}\frac{db}{dx}\frac{d\tilde{u}_3}{dx} + \frac{\tilde{u}_3 - \tilde{u}_1}{b^2} - \tilde{u}_2 &= 0, \end{aligned} \tag{4.18}$$

along with the constraint equation,

$$\frac{1}{b^2}\frac{d\tilde{u}_1}{dx} + \frac{d\tilde{u}_2}{dx} + \frac{d\tilde{u}_3}{dx} = 0. \tag{4.19}$$

By solving Eq. (4.18), we can obtain the mode function solution for different choices of the parameters α and x_m as shown in Fig. 4.2. The above figure shows that the mode function grows in time due to anisotropy, particularly near the end of inflation. For values $\alpha < 0.03$, field production stops altogether. Hence, we get a lower bound on the anisotropic parameter $\alpha \geq 0.03$. The upper bound on α is discussed in the later sections.

4.2.1 Power spectrum of the electromagnetic field during inflationary era

The stress energy-momentum tensor corresponding to the produced EM field is given by

$$T_{\mu\nu} = -\frac{2}{\sqrt{-g}}\frac{\delta[\sqrt{-g}\mathcal{L}]}{\delta g^{\mu\nu}}. \tag{4.20}$$

As a result, the energy-momentum tensor corresponding to the electromagnetic part of the Lagrangian boils down to

$$T_{mn} = -\frac{1}{4}g_{mn}g^{\mu\alpha}g^{\nu\beta}F_{\mu\nu}F_{\alpha\beta} + g^{\mu\nu}F_{m\mu}F_{n\nu}. \tag{4.21}$$

The total energy density of the system is given by the T_{tt} component of the energy-momentum tensor. Therefore, the total electromagnetic energy density of the system is

$$\rho = -\langle T^0_0\rangle = \frac{1}{2a^2}g^{ij}\langle A'_i A'_j\rangle + \frac{1}{4}g^{ij}g^{ab}\langle F_{ia}F_{jb}\rangle. \tag{4.22}$$

Thus, we have the electric field and magnetic field energy densities as,

$$\begin{aligned}\rho_E(x,\eta) &= \frac{1}{2a^2}g^{ij}\langle A'_i A'_j\rangle,\\ \rho_B(x,\eta) &= \frac{1}{4}g^{ij}g^{mn}\langle F_{ij}F_{mn}\rangle,\end{aligned} \tag{4.23}$$

respectively, where the expectation values are taken with respect to the initial Bunch-Davies (BD) vacuum. In the momentum space, these energy densities can be written as

$$\rho_E(k,\eta) = \frac{1}{2a^4}\sum_p\int\frac{d^3k}{(2\pi)^3}u_i^{(p)}\tilde{g}^{ij}u_j^{*\prime(p)}, \tag{4.24}$$

$$\begin{aligned}\rho_B(k,\eta) = \frac{1}{4a^4}\sum_p\int\frac{d^3k}{(2\pi)^3}\tilde{g}^{ij}\tilde{g}^{mn}\times&\left[\left(k_ik_nu_m^{(p)}u_j^{*(p)} - k_ik_ju_m^{(p)}u_n^{*(p)}\right)\right.\\ &\left.+\left(k_mk_ju_i^{(p)}u_n^{*(p)} - k_mk_nu_iu_j^{*(p)}\right)\right].\end{aligned} \tag{4.25}$$

In order to determine the strength of the magnetic field in the present era, we first define the power spectrum of the electromagnetic field as

$$\mathcal{P}_{E/B}(k,\eta) = \frac{\partial \rho_{E/B}}{\partial \ln k}, \tag{4.26}$$

As already stated earlier, each polarization mode follows the same equation of motion. Therefore, all the polarization modes have equal contributions. Summing over all the polarization modes and using the assumption that the amplitude of all the momenta $k_1 = k_2 = k_3 = \tilde{k}$ is the same, we calculate the power spectrum of the electric and magnetic fields as

$$\mathcal{P}_E(\eta,\tilde{k}) = \frac{\tilde{k}^3}{2\pi^2 a^4}\left(\frac{|u_1'(\eta)|^2}{b^2} + |u_2'(\eta)|^2 + |u_3'(\eta)|^2\right), \tag{4.27}$$

$$\begin{aligned}\mathcal{P}_B(\eta,\tilde{k}) = \frac{\tilde{k}^5}{2\pi^2 a^4}\Bigg[&\frac{1}{b^2}\left(2|u_1|^2 + |u_2|^2 + |u_3|^2 - 2\Re(u_1 u_2^*) - 2\Re(u_1 u_3^*)\right)\\ &+ \left(|u_2|^2 + |u_3|^2 - 2\Re(u_2 u_3^*)\right)\Bigg].\end{aligned} \tag{4.28}$$

With these forms of the power spectrum, our goal would be to calculate its strength at present. However, before that, we will calculate the condition for which the produced electromagnetic field should not backreact to the background during inflation.

4.2.2 Backreaction of anisotropic background and generated EM field

In the previous section, we briefly discussed the backreaction and strong coupling problem of inflationary magnetogenesis. In a general large-scale gauge field production scenario, a scalar field is coupled to the EM field to break the conformal invariance. Depending on the choice of the coupling function, it is possible to have a strong coupling problem, and different scenarios have been discussed in the literature [35,36,89, 93]. For the sake of completeness, we discuss it here briefly. In order to have a sustainable production of the electromagnetic field during inflation, the coupling function is often chosen to be an increasing function of time. However, it needs to revert to unity to restore the regular Maxwellian electromagnetism at the end of inflation. Hence, it needs to be very small at the start of the inflationary era, so the effective charge of electrons will be very large, and we cannot treat the gauge field as a free field during the inflationary era. In this proposal, there is no such direct coupling between the inflaton field and the EM field. Therefore, we do not need to worry about the strong coupling issue in this scenario. However, we must ensure that the anisotropy energy density or the generated EM field does not jeopardize the inflation. To this extent, we calculate the energy density produced by the anisotropic background and get a lower bound on the anisotropic parameter $\tilde{k}\eta_m$ and α introduced in Eq. (4.17). The energy-momentum tensor of the background $T_{\mu\nu}$ is dictated by the Einstein equation in terms of the Einstein tensor $G_{\mu\nu}$ as

$$G_{\mu\nu} = 8\pi G T_{\mu\nu}. \tag{4.29}$$

In the case of Bianchi type I background as introduced in Eq. (5.3), the 00 component of the Einstein tensor can be calculated as

$$G_{00} = \frac{a'(3a'b + 2ab')}{a^2 b}. \tag{4.30}$$

Thanks to this result, we can calculate the energy density corresponding to the anisotropic background. It turns out as

$$\begin{aligned} \rho_{\text{total}} &= -T^0_0 = -\frac{1}{8\pi G} G^0_0 = \frac{1}{8\pi G}\left(3\frac{a'^2}{a^4} + 2\frac{a'}{a^3}\frac{b'}{b}\right) \\ &= 3H^2 M_{\text{pl}}^2 + 2H M_{\text{pl}}^2 \frac{b'}{ab}, \end{aligned} \tag{4.31}$$

where $H \equiv a'/a^2$ is the Hubble parameter in conformal time during the inflation, a is the scale factor in de Sitter spacetime ($a = -1/(H\eta)$). From the dynamics of the inflaton field during inflation, we already know that the total energy of the inflaton field is given by $\rho_{\text{inf}} = 3H^2 M_{\text{pl}}^2$. Therefore, the total background energy density in Eq. (4.31) consists of two parts. The first part we call inflationary energy density, and the second part is the energy density due to anisotropy in the background,

$$\rho_{\text{inf}} = 3H^2 M_{\text{pl}}^2, \ \rho_{\text{anis}} = 2H M_{\text{pl}}^2 \frac{b'}{ab}. \tag{4.32}$$

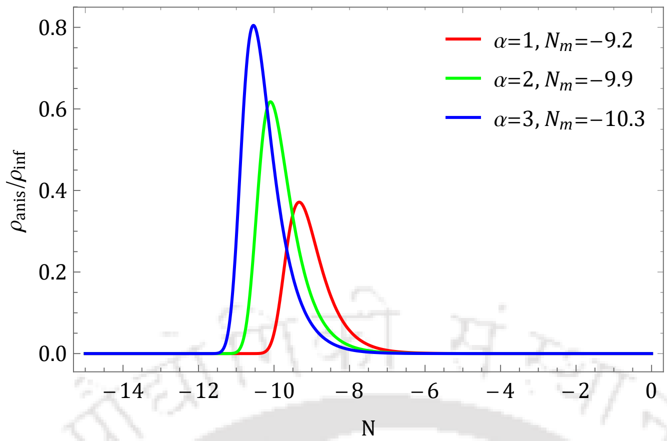

Figure 4.3: Evolution of the ratio of anisotropic energy density to inflationary energy density with the e-folding number N with different anisotropic parameters α and N_m.

In our proposition, we have mentioned earlier that the anisotropy should act as a perturbation. Therefore, we must ensure that the anisotropic energy density must be much lower than the inflaton energy density. Furthermore, the electromagnetic energy density has to be lower than the anisotropic and inflaton energy densities. From the PLANCK data [88], we know that the temperature anisotropy in CMB is $\frac{\Delta T}{T} \sim 10^{-5}$. If the anisotropic energy is closer to the perturbative limit towards the end of the inflationary era, it will not affect the CMB map, as observed by the PLANCK. We define e-folding number during the inflationary era as $N = \ln\left(\frac{a}{a_{\rm end}}\right)$, where $a_{\rm end}$ is the scale factor at the end of inflation. By this definition, the e-folding number at the end of inflation $N_{\rm end} = 0$. Moreover, the total e-folding number during the inflation is $N_{\rm tot} \simeq 60$. The anisotropic factor b in terms of e-folding number can be written as

$$b(N) = 1 + \alpha \exp\left[-e^{2(N_m - N)}\right], \tag{4.33}$$

here N_m is the e-folding number corresponding to the conformal time η_m. We can calculate the ratio of the anisotropic energy density and the inflationary energy density in terms of the e-folding number N as follows

$$\left|\frac{\rho_{\rm anis}}{\rho_{\rm inf}}\right| = \left|\frac{2}{3H}\frac{b'}{ab}\right| = \left|\frac{2}{3}\frac{db}{dN}\frac{1}{b}\right|. \tag{4.34}$$

In order to have sustainable inflation, such that the anisotropic energy density does not affect the inflation energy density, we need to have $\left|\frac{\rho_{\rm anis}}{\rho_{\rm inf}}\right| < 1$ throughout the entirety of the inflation. Thus, the ratio gives us an upper bound on α, which dictates the strength of the anisotropy. In Fig. 4.3, we can see that the ratio of the energy densities reaches its maximum towards the end of inflation. Thus, we can choose our parameters such that the ratio is up to the perturbative level (~ 0.5). It gives us the upper bound $\alpha \leq 1.48$. Still, the CMB remains unaffected due to the presence of spatial anisotropies. However, it is worth mentioning here that we do not consider the dynamics of the anisotropy in the background. In order to make sure that the anisotropic background comes in towards the end of inflation, we take the upper limit on the parameter $\tilde{k}\eta_m \geq -2$. Furthermore, during inflation, the EM field is also produced. It is also necessary to ensure that the generated gauge field energy density does not violate the inflationary energy density. We can see that the maximum production occurs towards the end of inflation from the nature of the coupling function introduced in Eq. (4.17). Thus, to avoid the backreaction problem, it is sufficient to satisfy

$$\rho_E + \rho_B \leqslant \rho_{\rm inf}.$$

We can obtain the values of the energy densities of the electric and magnetic fields from Eq. (4.23) and integrate over all the modes inside the horizon during the inflationary era. Which finally boils down to,

$$\rho_E = \frac{H^4}{2\pi^2}\int_{x_i}^{x_f} dx x^3 \left[\frac{1}{b^2}\left|\frac{d\tilde{u}_1}{dx}\right|^2 + \left|\frac{d\tilde{u}_2}{dx}\right|^2 + \left|\frac{d\tilde{u}_3}{dx}\right|^2\right], \tag{4.35}$$

$$\rho_B = \frac{H^4}{\pi^2}\int_{x_i}^{x_f} dx x^3 \left[\frac{1}{b^2}\Big(2|\tilde{u}_1|^2 + |\tilde{u}_2|^2 + |\tilde{u}_3|^2 - 2\Re(\tilde{u}_1\tilde{u}_2^*) - 2\Re(\tilde{u}_1\tilde{u}_3^*)\Big) + \Big(|\tilde{u}_2|^2 + |\tilde{u}_3|^2 - 2\Re(\tilde{u}_2\tilde{u}_3^*)\Big)\right]. \tag{4.36}$$

Where we recall the variables $x = \tilde{k}\eta$, $\tilde{u}_i = \sqrt{\tilde{k}}u_i$, evaluating the integrations numerically, the ratio of the energy densities turns out to be $\frac{\rho_{\rm E}+\rho_{\rm B}}{\rho_{\rm inf}} \sim 10^{-9}$, for the anisotropic parameter $\tilde{k}\eta_m = -1$ and $\alpha = 1.45$. As the generated electromagnetic energy density is very low compared to the background inflaton energy density, the backreaction problem is also avoided. Therefore, with this formalism, we can sustainably produce the EM field during inflation without worrying about the strong coupling or backreaction problem. On the other hand, ensuring that the generated EM field does not surpass the energy density of the inflationary background is also necessary. Eq. (4.17) shows that the maximum energy density occurs at $\eta = 0$. However, we have taken that the inflation ends at η_f, so there is no production of the large-scale magnetic field in the post-inflationary era. If the electromagnetic energy density is less than the anisotropic energy density at the end of inflation, all the sufficient conditions for no backreaction are satisfied. To this end, we reiterate that the anisotropic parameter α is so chosen that the anisotropic energy density remains subdominant compared to the inflaton energy density. We further show that the produced energy density of the electromagnetic field is less than the anisotropic energy density. In conclusion, the produced electromagnetic field affects neither the inflationary nor the anisotropic background. Therefore, this formalism effectively produces a magnetic field without special coupling to avoid the backreaction effect.

4.3 Post inflationary evolution

The anisotropic factor b goes to unity after the end of inflation, and the spacetime becomes conformally flat. Afterward, the EM field evolved into a usual Maxwellian field. However, depending on the evolution of the universe, we can have two different scenarios of field evolution: (i) In the first scenario, it is assumed that the universe instantly goes into radiation domination, i.e., the inflaton field instantly decays and produces radiation. (ii) In the second scenario, the inflaton decays within a finite time, and therefore, it goes through a brief period of reheating, having a non-zero e-folding number and very low conductivity. The dynamics of the subsequent evolution of the universe dictate the present strength of the observed magnetic field. We will discuss both scenarios in the next subsections.

4.3.1 The case of instantaneous reheating

In this section, we will find the strength of the magnetic field at present, considering an instantaneous reheating scenario. In this case, after the end of the inflationary era, the universe instantly thermalizes and goes to the radiation-dominated era. As the conductivity of the universe becomes very large, the electric field dies out instantly. However, the magnetic field produced during the inflationary era decays as a radiation density $\mathcal{P}_B \propto a^{-4}$. Therefore, by incorporating the conservation of entropy, we can compute the strength of the magnetic field, which relates to the field strength at the end of inflation. We have already calculated the power spectra of the magnetic field during the inflationary era in Eq. (4.28). In terms of the mode functions, the explicit expression for the present-day magnetic field turns out to be

$$B_0 = \left(\frac{-\tilde{k}\eta_f a_f H}{\pi^2 a_0}\right)^2 \sqrt{|\tilde{u}_1(x_f)|^2 + |\tilde{u}_2(x_f)|^2 + |\tilde{u}_3(x_f)|^2}. \tag{4.37}$$

The above expression is in the GeV^2 unit. Here, we recall the variable $\tilde{u}_i = \sqrt{\tilde{k}}u_i$ (with $i = 1, 2, 3$), H is the Hubble parameter during inflation, and $\tilde{k}$ is the scale under consideration in which we will estimate the strength of the magnetic field. Furthermore, in order to calculate the value of B_0 from Eq. (4.37), we first need to evaluate the value of the ratio $\frac{a_f}{a_0}$. We evaluate the value to be $\frac{a_0}{a_f} \approx 10^{30}(H/10^{-5}M_{\rm pl})^{1/2}$. Here, in particular, we have taken the value of the Hubble parameter to be $H = 10^{-5}M_{\rm pl}$. With the numerical solution of the mode functions from Fig. 4.2 at the end of inflation $\tilde{k}\eta_f = -0.0001$ and Eq. (4.37) we can evaluate the strength of the magnetic field at present-day using the conversion 1 G $= 1.95 \times 10^{-20}$ GeV^2 for different values of the anisotropic parameters α and $\tilde{k}\eta_m$. In Fig. 4.4, we can see the variation of the present-day magnetic field B_0 with α for a fixed value of $\tilde{k}\eta_m$ as well as the variation of magnetic field strength with $\tilde{k}\eta_m$. The maximum value of B_0 obtained in the instant reheating scenario for fixed value of $\tilde{k}\eta_m$ is $B_0 = 2.86 \times 10^{-21}$ G varying α. Similarly for a fixed value of α, the maximum value of B_0 obtained is $B_0 = 3.24 \times 10^{-21}$ G. Experiments like Faraday

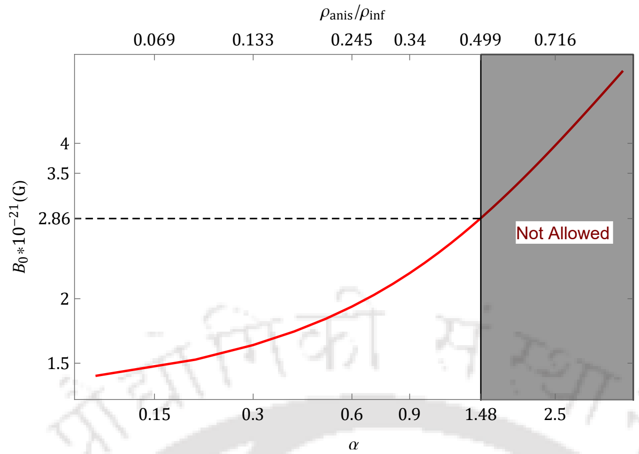

(a)

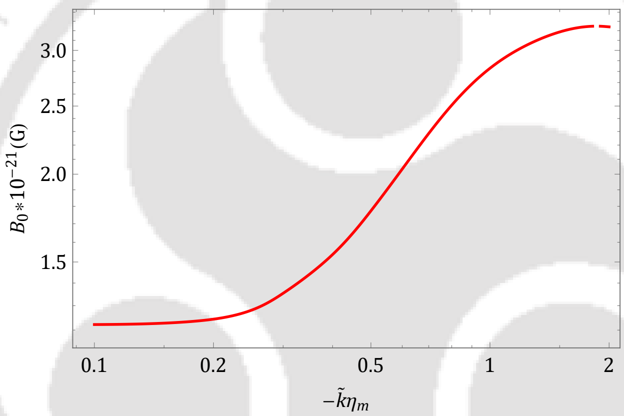

(b)

Figure 4.4: **(a)** Variation of the present strength of the magnetic field B_0 with α for a fixed value of the anisotropic parameter $\tilde{k}\eta_m = -1$. **(b)** Variation of the present strength of the magnetic field B_0 with $\tilde{k}\eta_m$ for a fixed value of the anisotropic parameter $\alpha = 1.45$, the ratio of the anisotropic energy density in this case remains constant at $\rho_{\rm anis}/\rho_{\rm inf} = 0.492$.

rotation and gamma-ray observation impose a bound on the present strength of the primordial magnetic field 10^{-10} G $\lesssim B_0 \lesssim 10^{-22}$ G [23]. Therefore, this proposal can generate a large-scale magnetic field within the experimental bounds of the present-day intergalactic magnetic field. With the choice of the anisotropic parameter in the range $0.03 \leq \alpha \leq 1.48$, the backreaction or the strong coupling problem is also avoided.

4.3.2 The case of prolonged reheating with constant equation of state

In the last section, we saw that we can generate the required strength of the magnetic field in the instant reheating scenario. However, if we consider a reheating phase with a non-zero e-folding number, then the conductivity of the universe does not reach infinity instantly. Instead, during this period, the conductivity of the universe may remain very low. As a result, the electric field does not go to zero immediately and induces a magnetic field during this period. This conversion of the electric field into the magnetic field during the reheating phase occurs through Faraday induction [92]. This conversion of an electric field to a magnetic field makes it diluted slowly during the reheating era compared to the previous case of $\mathcal{P}_B \propto a^{-4}$. Thus, a finite reheating era further strengthens the magnetic field on a large scale and gives us bounds on the EoS during the reheating era. After the inflation ends, the anisotropic factor b goes to unity after a very short period, and the EM field evolves in the usual manner. Following the regular Maxwellian evolution, the equation of motion of the mode functions $u_i(\tilde{k},\eta)$ during the reheating becomes

$$u_i^{\prime\prime(re)}(\tilde{k},\eta) + 3\tilde{k}^2 u_i^{(re)}(\tilde{k},\eta) = 0, \tag{4.38}$$

where $i = 1,\ 2,\ 3$ are the indices corresponding to three spatial components of the gauge field and $u_i^{(re)}(\tilde{k},\eta)$ are the mode functions during reheating. Furthermore, we consider the universe a poor conductor during this period. To be precise, we take the conductivity to be zero. The solution of the mode function from Eq. (4.38), along with the proper normalization condition, gives us

$$\begin{aligned} u_1^{(re)}(\tilde{k},\eta) &= \frac{1}{\sqrt{6\sqrt{3}\tilde{k}}}\left[\alpha_1(\tilde{k})e^{-i\sqrt{3}\tilde{k}(\eta-\eta_f)} + \beta_1(\tilde{k})e^{i\sqrt{3}\tilde{k}(\eta-\eta_f)}\right], \\ u_{2,3}^{(re)}(\tilde{k},\eta) &= -\frac{1}{2\sqrt{6\sqrt{3}\tilde{k}}}\left[\alpha_{2,3}(\tilde{k})e^{-i\sqrt{3}\tilde{k}(\eta-\eta_f)} + \beta_{2,3}(\tilde{k})e^{i\sqrt{3}\tilde{k}(\eta-\eta_f)}\right], \end{aligned} \tag{4.39}$$

with α_i and β_i are the integration constants, and η_f denotes the end of inflation. the integration constants are evaluated at the end of inflation η_f by equating the junction conditions of inflationary and reheating era

$$u_i^{(re)}(\tilde{k},\eta_f) = u_i(\tilde{k},\eta_f) \ \text{ and } \ u_i^{\prime(re)}(\tilde{k},\eta_f) = u_i^{\prime}(\tilde{k},\eta_f). \tag{4.40}$$

In the above Eq. (4.40), $u_i(\tilde{k},\eta)$ are mode functions during the inflationary era which follow Eq. (4.14) and $u_i^{(re)}$ are mode functions during the reheating era following Eq. (4.38). This immediately leads to the integration constants,

$$
\begin{aligned}
\alpha_1(\tilde{k}) &= \sqrt{\frac{3\sqrt{3}\tilde{k}}{2}}u_1(\tilde{k},\eta_f) + i\sqrt{\frac{\sqrt{3}}{2\tilde{k}}}u_1'(\tilde{k},\eta_f), \\
\beta_1(\tilde{k}) &= \sqrt{\frac{3\sqrt{3}\tilde{k}}{2}}\tilde{u}_1(\tilde{k},x_f) - i\sqrt{\frac{\sqrt{3}}{2\tilde{k}}}u_1'(\tilde{k},\eta_f), \\
\alpha_{2,3}(\tilde{k}) &= -\sqrt{6\sqrt{3}\tilde{k}}u_{2,3}(\tilde{k},\eta_f) - i\sqrt{\frac{2\sqrt{3}}{\tilde{k}}}u_{2,3}'(\tilde{k},\eta_f), \\
\beta_{2,3}(\tilde{k}) &= -\sqrt{6\sqrt{3}\tilde{k}}u_{2,3}(\tilde{k},\eta_f) + i\sqrt{\frac{2\sqrt{3}}{\tilde{k}}}u_{2,3}'(\tilde{k},\eta_f).
\end{aligned} \tag{4.41}
$$

With all these, we can now compute the time-evolving power spectrum during reheating as

$$
\begin{aligned}
\mathcal{P}_B(\eta,\tilde{k}) &= \frac{\tilde{k}^5}{\pi^2 a^4}\left(|u_1^{(re)}|^2 + |u_2^{(re)}|^2 + |u_3^{(re)}|^2\right) \\
&= \sum_i \frac{\tilde{k}^4}{\pi^2 a^4}|\tilde{u}_i^{(re)}|^2 \\
&= \frac{\tilde{k}^4}{\pi^2 a^4}\Bigg[\frac{1}{6\sqrt{3}}\left(|\alpha_1|^2 + |\beta_1|^2 + 2|\alpha_1||\beta_1| \times \cos[Arg(\alpha_1\beta_1^*) - 2\sqrt{3}\tilde{k}(\eta-\eta_f)]\right) \\
&+ \frac{1}{24\sqrt{3}}\left(|\alpha_2|^2 + |\beta_2|^2 + 2|\alpha_2||\beta_2| \times \cos[Arg(\alpha_2\beta_2^*) - 2\sqrt{3}\tilde{k}(\eta-\eta_f)]\right) \\
&+ \frac{1}{24\sqrt{3}}\left(|\alpha_3|^2 + |\beta_3|^2 + 2|\alpha_3||\beta_3| \times \cos[Arg(\alpha_3\beta_3^*) - 2\sqrt{3}\tilde{k}(\eta-\eta_f)\right)\Bigg].
\end{aligned} \tag{4.42}
$$

In order to estimate the strength of the magnetic field during the reheating era, we first need to evaluate the term $\eta - \eta_f$. Following Ref. [92] the term is calculated as

$$
\eta - \eta_f = \int_{a_f}^{a} \frac{da}{a^2 H}. \tag{4.43}
$$

As the Hubble constant H is present in the above equation, it is evident that the quantity $\eta - \eta_f$ depends on the background's evolution during the inflationary era. In particular, how the inflaton energy density is converted into radiation energy density. In general, there are two scenarios

- Evolution through time-independent, effective equation of state.
- Perturbative decay of inflaton into radiation (perturbative reheating scenario).

Here in this paper, we will only discuss evolution through an independent constant effective EoS. In this context, we follow the methodology proposed by Kamionkowski et al. in Ref. [66]. Here, the evolution of the background is parametrized by a constant effective EoS ω_{eff}. Therefore, the Hubble parameter during the reheating evolves as $H \propto a^{-\frac{3}{2}(1+\omega_{eff})}$. The physical parameters of reheating, like the e-folding number of the reheating era N_{re} and the reheating temperature T_{re}, can be expressed in terms of the inflationary parameters and effective EoS ω_{eff} as [67]

$$\begin{aligned} N_{re} &= \frac{1}{3\omega_{\rm eff}-1}\Bigg[\ln(\rho_f) - \ln\left(\frac{\pi^2 g_{re}}{30}\right) - \frac{1}{3}\ln\left(\frac{43}{11 g_{s,re}}\right) - 4\ln\left(\frac{a_0 T_0}{k}\right) \\ &+ 4\ln(H_k) + 4N_k\Bigg], \end{aligned} \tag{4.44}$$

$$T_{re} = \left(\frac{43}{11 g_{s,re}}\right)^{1/3}\left(\frac{a_0 T_0}{k} H_k e^{-N_k} e^{-N_{re}}\right), \tag{4.45}$$

where H_k denotes the Hubble parameter at the time of horizon crossing, $k/a_0 = 0.05\,\text{Mpc}^{-1}$ is the pivot scale, g_{re} is the degrees of freedom during reheating, and N_k is the total e-folding number from the end of inflation till horizon crossing. As we have not considered any particular inflation potential in this paper, we develop a model-independent way to determine N_k following Ref. [184]. In the calculation of N_k, we have taken the central values of scalar spectral index $n_s = 0.9649$ and scalar perturbation amplitude $\ln[10^{10}\mathcal{A}_s] = 3.044$, considering the constraints provided by the PLANCK data [88] and as an input parameter we have chosen $N_k = 50$. With this choice of n_s, N_k, we get an upper bound on the effective EoS $\omega_{eff} < 0.164$ from the BBN bound of reheating temperature $T_{re} \sim 10^{-2}$ GeV. Now, in order to connect the reheating parameters N_{re}, T_{re} to the strength of the primordial magnetic field, we need to evaluate the quantity $\eta - \eta_f$ in Eq. (4.43). It is evaluated following the evolution of the Hubble parameter during the reheating era. As the EoS is constant ω_{eff}, the variation of the Hubble parameter during the reheating era (H_{re}) is related to the Hubble parameter at the end of inflation

(H_f) as

$$H_{re} = H_f \left(\frac{a_{re}}{a_f}\right)^{-\frac{3}{2}(1+\omega_{eff})}, \tag{4.46}$$

where the subscript "re" represents the end of reheating. Thus, a_{re} and H_{re} are the scale factor and Hubble parameter at the end of reheating, respectively. Following the above relation, the term in Eq. (4.43) boils down to

$$\eta - \eta_f = \frac{2}{1+3\omega_{eff}}\left(\frac{1}{aH} - \frac{1}{a_f H_f}\right). \tag{4.47}$$

Substituting the value of the extra reheating term $\eta - \eta_f$, we can calculate the present strength of the magnetic field as a function of the effective EoS ω_{eff}. After the end of reheating, the conductivity of the universe goes to infinity. Therefore, the electric field goes to zero, and the Faraday conversion of the electric field into the magnetic field stops at the end of reheating. And the magnetic field decays as radiation (a^{-4}) until now. From the conservation of magnetic energy density, the present strength of the magnetic field can be calculated from the relation as follows

$$\left.\frac{\partial \rho_B}{\partial \ln k}\right|_0 = \left(\frac{a_{re}}{a_0}\right)^4 \left.\frac{\partial \rho_B}{\partial \ln k}\right|_{\rm re}. \tag{4.48}$$

Evolving through the reheating era, the strength of the magnetic field in the present era turns out as

$$B_0 = \frac{\sqrt{2}}{6\pi\sqrt{3}}\left(\frac{\tilde{k}}{a_0}\right)^2 \left[\mathcal{I}_1 + \frac{1}{4}(\mathcal{I}_2 + \mathcal{I}_3)\right]^{1/2}, \tag{4.49}$$

where,

$$\begin{aligned} \mathcal{I}_i &= |\alpha_i|^2 + |\beta_i|^2 + 2|\alpha_i|\,|\beta_i| \cos(\mathrm{Arg}(\alpha_i \beta_i^*) - \Phi), \\ \Phi &= \frac{4\tilde{k}\sqrt{3}}{(1+3\omega_{eff})a_f H_f}\left(\left(\frac{H_f}{H_{re}}\right)^\delta - 1\right). \end{aligned} \tag{4.50}$$

In the above Eq. (4.49), $\delta = (3\omega_{eff}+1)/(3\omega_{eff}+3)$. Varying the EoS ω_{eff}, we get the present-day strength of the magnetic field of $B_0 \sim 4 \times 10^{-20}$ G, which is one order higher than what was predicted for instantaneous reheating case, which is $\sim 3 \times 10^{-21}$

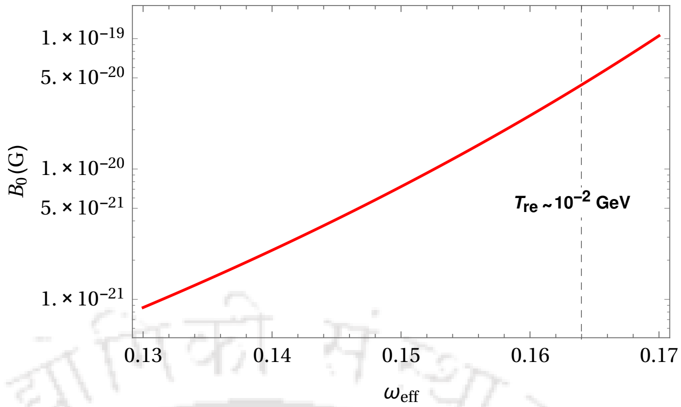

Figure 4.5: Variation of present magnetic strength with effective equation of state ω_{eff} for the choice of anisotropic parameters $\alpha = 1.45$ and $\tilde{k}\eta_m = -1$. With the model independent formalism input parameter $N_k = 50$ and inflationary parameter $n_s = 0.9649$.

G. Furthermore, from the observed strength of the magnetic field, we also get a lower bound of EoS $\omega_{eff} > 0.132$. From Fig. 4.5, we see that the present strength of the magnetic field increases due to the Faraday conversion of the electric field into the magnetic field; such an increment is quite insensitive to the reheating EoS. This increment is small since the strength of the electric field compared to the magnetic field at the end of inflation is not significantly higher.

4.4 Conclusions

In this work, we propose a new formalism to generate large-scale magnetic fields during the inflationary era. The novelty of the work lies in the generation of fields during inflation. The previous works done in the context of inflationary magnetogenesis rely on breaking the conformal invariance by coupling the EM field to some scalar field or gravity. In the present case, we have taken the underlying background to be anisotropic (Bianchi type I) so that the EM field action is not conformally invariant under the anisotropic background. Due to the absence of any explicit coupling of the EM field, it does not suffer from the usual strong coupling problem. In the process, we have introduced two parameters α and η_m to characterize the behavior of the anisotropic scale factor $b(\eta)$. By appropriately tuning those anisotropic parameters, we further addressed the backreaction problem and successfully circumvented it. The constraints on the anisotropic parameter is obtained from the backreaction energy condition, which suggests that the ratio of the energy densities $\rho_{\rm anis}$ and the inflaton energy density $\rho_{\rm inf}$ to be $\rho_{\rm anis}/\rho_{\rm inf} \leqslant 0.5$. We get an upper bound on the anisotropic parameter $\alpha \leq 1.48$. Furthermore, to ensure that an electromagnetic field gets produced during the inflationary era, we get a lower bound on the parameter $\alpha \geq 0.03$. The parameter η_m is so chosen that the anisotropy appears towards the end of inflation. For this, we have taken $\tilde{k}\eta_m \geq -2$, ensuring that the anisotropy is localized and short-lived. With this choice of parameters, we find that the ratio of the energy density of the generated EM field to the total inflaton energy density is $\sim 10^{-9}$, which implies that the electromagnetic energy density is also lower than the anisotropic energy density. Therefore, the generated electromagnetic field neither back-reacts on the inflaton field nor on the anisotropic background. Finally, this set of parameters gives us a present strength of magnetic field $B_0 \sim 3 \times 10^{-21}\ G$, for $\alpha = 1.45$ and $\tilde{k}\eta_m = -2$, which is well in between the latest bound on present-day magnetic field strength. However, if we consider an elongated reheating period followed by inflation, the magnetic field strength further increases. This increase in strength occurs due to Faraday's conversion of the electric field to the magnetic field. By this prolonged reheating era, we get the present strength of the magnetic field $B_0 \sim 4 \times 10^{-20}\ G$. Through the introduction of the reheating era, we also get a tight constraint on the range of equation of state $0.132 < \omega_{eff} < 0.164$ for the particular choice of inflationary parameter n_s and N_k. Due to the presence of anisotropies, there might be interesting signatures of the anisotropies on gravitational waves at small scales. Further, the most interesting would be investigating the origin of such anisotropies, particularly near the end of inflation, which is part of the future aspect of this work.

5

Application of Quantum Information theory in cosmological scenarios

Contents

Based on *"Probing non-classicality of primordial gravitational waves and magnetic field through quantum Poincare sphere"* by D. Maity and S. Pal,**Phys.Lett.B 835 (2022) 137503**

The Universe is believed to have originated from quantum fluctuations. As discussed in Chapter 1, the small-scale perturbations in the early Universe evolved into the large-scale structure we observe today. However, any experimental verification of this quantumness would be pivotal to understanding the underlying principle of nature. Therefore, finding any quantum signatures embedded in the Universe has gained much interest in the recent past. One of the recent endeavors toward understanding this question has been to set up experiments to understand the large-scale structure of our Universe and look for observable quantum signatures in it. Inflation [43, 130–134] is the most successful theory that can explain the observed large-scale structure of our Universe to a great precision, and is essentially assumed to be a quantum mechanical phenomenon. Although quantum fluctuations during inflation can successfully explain the observed matter fluctuation distribution, any classical statistical origin of such fluctuations can not be ruled out. Therefore, looking for an unambiguous signature of quantumness encoded in the distribution of matter would be a pivotal step toward establishing the inflationary paradigm itself. Cosmic Microwave Background (CMB) anisotropy directly corresponds to the matter distribution of the Universe, and it is related to the scalar quantum fluctuations during inflation. Therefore, in recent years, it has been considered as a potential test-bed to look for quantum signatures in the early universe [51–55]. Primordial gravitational waves (PGW) can also be produced from the tensor fluctuations during the inflationary era. Hence, further studies have been performed in the context of gravitational waves [135]. The primordial magnetic field (PMF) is also believed to have originated from inflation [34, 36, 93, 99–102, 136]. Therefore, primordial gravitational waves and the primordial magnetic field can also play a crucial role as observables that may encode the quantum signature of the early Universe. In this work, we aim to find the quantum signatures embedded in the primordial fields by defining an appropriate observable called the quantum Poincaré sphere. We will consider both gravitational and electromagnetic fields in a unified framework for our present discussion.

Measurement of gravitational waves and large-scale magnetic fields is a long-standing endeavor with resounding successes. However, the detection of gravitational waves over the last few years by LIGO and Virgo [137–150] has opened up a new era in the experimental front of understandintg the origin of our Universe in the near future. Magnetic fields of order a few micro-Gauss (μG) with coherence length of hundred kilo-parsecs (Kpc) scale [50, 90, 151] have been observed in galaxies and galaxy clusters, and for neutron stars, the magnetic field strength is quite high. The intergalactic void also hosts a weak $\sim 10^{-16}$ Gauss magnetic field, with the coherence length as large as Mpc scales [23]. The origin of magnetic fields with a Mpc coherence scale is difficult to explain by any known classical processes. At the astrophysical scale, to generate a magnetic field of μG order, a very weak seed magnetic field is needed. However, to explain the origin of such a magnetic field at large scales, inflationary magnetogenesis [31, 33, 35, 37, 92] is believed to be the most successful mechanism. Similar to the scalar and tensor perturbations, the quantum electromagnetic fluctuations of the vacuum during inflation can be amplified to produce a large-scale magnetic field. Apart from explaining the presence of a magnetic field in the intergalactic media, such a magnetic field can then act as a seed magnetic field at small scales and get enhanced to the galactic scale of μG order by the well-known *Galactic dynamo* mechanism [151–153].

Our primary goal in this work is to construct appropriate observables for both PGWs and PMFs, which can be measured in the present Universe and provide important quantum signatures. Our analysis will be along the lines of the squeezed state formalism [51–53]. Furthermore, by constructing appropriate observables measured in this state, we will solidify our proposal for quantum signatures.

5.1 Magnetogenesis in squeezed state formalism

We begin with a detailed account of the primordial magnetogenesis in the squeezed state formalism. The conformal symmetry broken electromagnetic (EM) Lagrangian is taken as [31],

$$S = -\frac{1}{4}\int d^4x\sqrt{-g}I^2(\eta)F_{\mu\nu}F^{\mu\nu}, \tag{5.1}$$

where, $F_{\mu\nu} = \partial_\mu A_\nu - \partial_\nu A_\mu$ is EM field strength tensor with A_μ being the vector potential. $I(\eta)$ is an arbitrary EM coupling which breaks the conformal invariance of the EM field. Generally, in the case of inflationary magnetogenesis, this coupling is taken as a function of the inflaton field, which goes to 1 at the end of inflation. Following the literature, it can be written as

$$I(\eta) = \begin{cases} \left(\frac{a_{end}}{a}\right)^{2n}, & \text{if } \eta < \eta_{end} \\ 1, & \eta \geq \eta_{end} \end{cases} \tag{5.2}$$

Where a is the scale factor at any arbitrary time η, a_{end} is the scale factor at the end of inflation, and n is the coupling parameter. The background is taken to be spatially flat FLRW metric with scale factor $a(\eta)$,

$$ds^2 = a(\eta)^2(-d\eta^2 + dx^2 + dy^2 + dz^2), \tag{5.3}$$

Because of spatial flatness, components of the vector potential can be defined in terms of irreducible components as $A_\mu = (A_0, \partial_i S + V_i)$ with the traceless condition $\delta^{ij}\partial_i V_j = 0$. In terms of these components, the action Eq.(5.1) becomes,

$$S = \frac{1}{2}\int d\eta d^3x I(\eta)(V_i' V^{i'} - \partial_i V_j \partial^i V^j). \tag{5.4}$$

It is important to note that the action does not depend on the scale factor explicitly because of the inherent conformal invariance of free electrodynamics. The spatial index will be raised or lowered by the usual Kronecker delta function. The Fourier expansion of V_i is taken as

$$V_i(\eta, x) = \sum_{p=1,2} \int \frac{d^3k}{(2\pi)^3} \epsilon_i^{(p)}(\mathbf{k}) e^{i\mathbf{k.x}} u_k^{(p)}(\eta), \tag{5.5}$$

where the reality condition of the field implies $u_{-k}^p = u_k^{p*}$. Here, $\epsilon_i^{(p)}(k)$ is the polarization vectors corresponding to two modes $p = 1, 2$, which satisfy $\epsilon_i^{(p)}(\mathbf{k})k_i = 0$ and $\epsilon_i^{(p)}(\mathbf{k})\epsilon_i^{(q)}(\mathbf{k}) = \delta_{pq}$. The following mode function equation will govern the dynamics of the field,

$$u_k^{(p)\prime\prime} + \frac{I'}{I} u_k^{(p)\prime} + k^2 u_k^{(p)} = 0 \tag{5.6}$$

Where the prime denotes derivative with respect to the proper time η. In terms of u_p^k and its associated conjugate momentum $\pi_k^p = I u_k^{p\prime}$, the Hamiltonian becomes,

$$\mathcal{H} = \frac{1}{2} \sum_{p=1,2} \int \frac{d^3k}{(2\pi)^3} \left(\frac{\pi_k^p \pi_k^{p*}}{I} + I k^2 u_{p*}^k u_p^k \right). \tag{5.7}$$

Treating the above canonically conjugate variables as operators, we express those in terms of creation and annihilation operators,

$$\pi_k^p = -i\sqrt{\frac{k}{2}}(a_k^p - a_{-k}^{\dagger(p)}) \; ; \; u_k^p = \sqrt{\frac{1}{2k}}(a_k^p + a_{-k}^{\dagger(p)}), \tag{5.8}$$

with $[a_k^{(p)}, a_h^{\dagger(q)}] = (2\pi)^3 \delta^{pq} \delta^{(3)}(\mathbf{k}\text{-}\mathbf{h})$ being the fundamental commutation relation. In terms of the operators, the Hamiltonian of each mode k becomes,

$$H_k = k \sum_p \left(\frac{\mathcal{I}_1}{2} \left(a_k^{p\dagger} a_k^p + a_{-k}^p a_{-k}^{p\dagger} \right) + \frac{\mathcal{I}_2}{2} \left(a_k^p a_{-k}^p + a_{-k}^{p\dagger} a_k^{p\dagger} \right) \right)$$

where, $\mathcal{I}_1 = (I + 1/I)$, $\mathcal{I}_2 = (I - 1/I)$. To incorporate the time evolution of the creation and annihilation operators, we employ the Bogoliubov transformation as, $a_k^p(\eta) = \alpha_k(\eta) a_k^p(0) + \beta_k(\eta) a_{-k}^{p\dagger}(0)$, where Bogoliubov coefficients satisfy the relation $|\alpha_k|^2 - |\beta_k|^2 = 1$, which is parametrized by,

$$\alpha_k = e^{i\theta_k} \cosh(r_k) \; ; \; \beta_k = -e^{-i\theta_k + 2i\phi_k} \sinh(r_k) \tag{5.9}$$

(r_k, ϕ_k) symbolize the squeezing parameter and squeezing angle of the quantum state, respectively. They satisfy

$$\begin{aligned}\phi_k' &= -\frac{k\mathcal{I}_1}{2} + \frac{k\mathcal{I}_2}{2}\cos 2\phi_k\ \coth 2r_k, \\ r_k' &= \frac{k\mathcal{I}_2}{2}\sin 2\phi_k\ ;\ \theta_k' = -\frac{k\mathcal{I}_1}{2} + \frac{k\mathcal{I}_2}{4}\cos 2\phi_k \tanh r_k.\end{aligned} \tag{5.10}$$

If one chooses the Bunch-Davis vacuum with the coupling function mentioned in Eq.(5.2), then the solution of those parameters can be expressed as

$$r_k = \sinh^{-1}|\beta_k|\ ;\ \phi_k = \frac{1}{2}Arg(\alpha_k\beta_k^*)$$

If we calculate the Bogoliubov coefficients with the Bunch-Davies condition, it turns out to be

$$\begin{aligned}\beta_k^* &= \left(\frac{\pi z}{8I}\right)^{\frac{1}{2}}\left(H^1_{-n+1/2}(z) + iIH^1_{-n-1/2}(z)\right) \\ \alpha_k &= \left(\frac{\pi z}{8I}\right)^{\frac{1}{2}}\left(H^1_{-n+1/2}(z) - iIH^1_{-n-1/2}(z)\right)\end{aligned} \tag{5.11}$$

Where $z = k\eta$. In this parametrization, we have assumed that the Hubble constant (H) remains constant throughout the inflationary era. Furthermore, it is taken as H_{end}. We can find out the time evolution of the squeezing parameter (r_k) from Eqs.(5.11). The evolution of r_k with $z = k\eta$ is shown in Fig.5.1 for different values of the coupling parameter n. To this end, let us give a connection formula with the observable quantities such as electric and magnetic correlation function with the aforementioned squeezing parameters as

$$\begin{aligned}< E_\mu(x)E^\mu(y) >&= \int \frac{d^3k}{4\pi k^3}e^{ik\cdot(x-y)}\mathcal{P}_E(\eta,k) \\ < B_\mu(x)B^\mu(y) >&= \int \frac{d^3k}{4\pi k^3}e^{ik\cdot(x-y)}\mathcal{P}_B(\eta,k)\end{aligned} \tag{5.12}$$

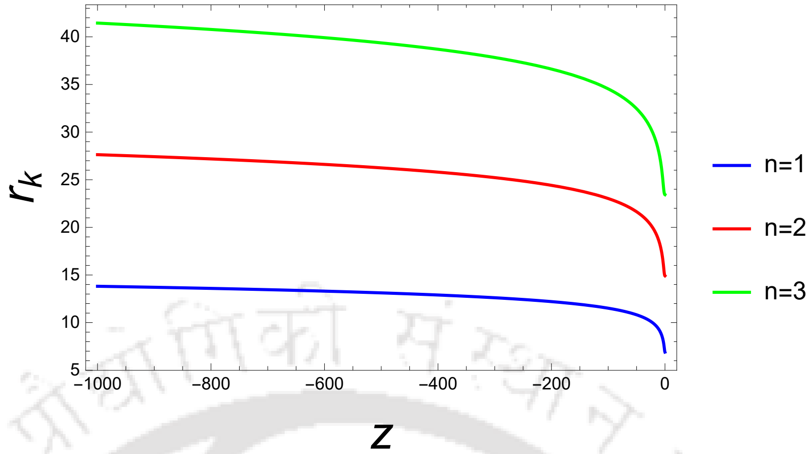

Figure 5.1: Evolution of the squeezing parameter r_k with $z = k\eta$ for different values of the coupling parameter n

Where, electric and magnetic power spectrum defined in momentum space turned out to be

$$\begin{aligned}
\mathcal{P}_E(\eta, k) &= \frac{k^4}{4\pi^2 a^4 I^2} \sum_{p=1,2} |\alpha_k^{(p)} - \beta_k^{(p)}|^2 \\
&= \frac{k^4}{4\pi^2 a^4 I^2} \sum_{p=1,2} (\cosh 2r_k^p - \sinh 2r_k \cos 2\phi_k^p) \\
\mathcal{P}_B(\eta, k) &= \frac{k^4}{4\pi^2 a^4 I^2} \sum_{p=1,2} |\alpha_k^{(p)} + \beta_k^{(p)}|^2 \\
&= \frac{k^4}{4\pi^2 a^4 I^2} \sum_{p=1,2} (\cosh 2r_k^p + \sinh 2r_k^p \cos 2\phi_k^p)
\end{aligned} \tag{5.13}$$

After the end of inflation, the conformal invariance is restored, and thus there is no further production of the EM field. If we consider the instantaneous reheating scenario, the universe readily transforms into a plasma state. Which makes the electric field vanish due to the high conductivity of the medium. This also freezes the magnetic field produced in the inflationary era. As there is no production of magnetic field in the post-inflationary era, the magnetic field power spectrum decays as a^{-4}. At present, the magnetic power spectrum turns out to take the following form,

$$\mathcal{P}_{B0} \propto \left(\frac{k}{a_0}\right)^{6-2n} e^{2(n-1)N} \tag{5.14}$$

Where (N, a_0) are the inflationary e-folding number and the present value of the scale factor, respectively. By this mechanism, therefore, a large-scale magnetic field of order $10^{-15} - 10^{-22}$ Gauss can be generated on Mpc scales [33,154], once an inflation model is considered. The magnetic field generated during the inflationary era is produced from quantum fluctuations. Subsequently, those modes will evolve throughout the entire cosmological evolution. As mentioned earlier, due to the large conductivity, the electric field vanishes, but the magnetic field freezes after the end of inflation. However, the subsequent dynamics of this frozen magnetic field will depend on the individual modes. The magnetic modes that re-enter the Hubble horizon during the radiation era interact with the plasma and further evolve through magneto-hydrodynamic (MHD) evolution. Due to this MHD effect, the information of the inflationary origin of the magnetic field from the Bunch-Davis vacuum will be erased for those magnetic modes. On the other hand, the modes with larger wavelengths will re-enter the horizon during the matter-dominated era and will not interact with the plasma. Hence, no MHD evolution will take place. Therefore, those large-scale magnetic fields are expected to preserve the information of their quantum origin during inflation. The above-mentioned fact is schematically illustrated in Fig.5.1. In the following discussion, we estimate the approximate scale above which information of the quantum origin of the magnetic field will be preserved. We calculate the wavenumber of the mode which re-enters the horizon during matter-radiation equality, where the following relation is satisfied,

$$\frac{T_{eq}}{T_{re}} = \frac{a_{re}}{a_{eq}}, \tag{5.15}$$

where a_{eq} is the scale factor at the matter-radiation equality, and H_{eq} is the Hubble parameter at that point. The temperature at that point is $T_{eq} \approx 10^{-9}$ GeV, T_{re} is the reheating temperature. Considering the instantaneous reheating scenario, it is generically observed that $T_{re} \approx 10^{15}$ GeV. Furthermore, the entropy conservation leads to the

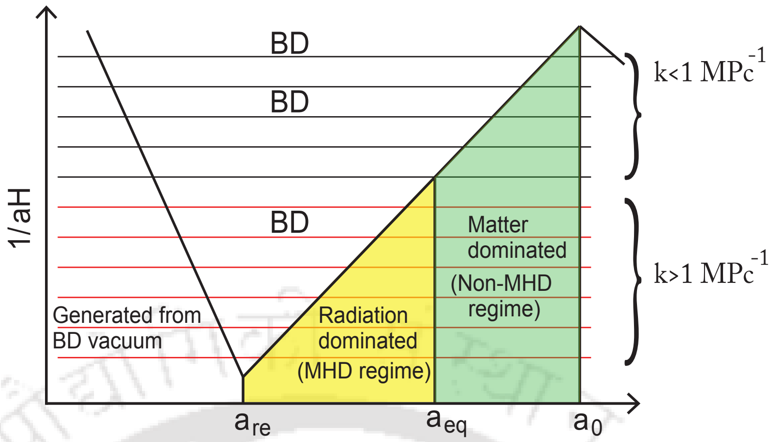

Figure 5.2: $1/aH$ is plotted against a here. The region in yellow shows the radiation-dominated era where the MHD takes over the evolution of the magnetic field, and the modes re-entering the horizon in this era lose the information about the initial quantum production. The green shaded region represents the matter-dominated era, and the modes re-entering the horizon in this era will not undergo MHD processes. BD stands for Bunch-Davis vacuum.

following relation,

$$a_{eq}H_{eq} = a_{re}H_{re}\frac{a_{re}}{a_{eq}} \implies k_{eq} = 10^{-24}k_{re}, \tag{5.16}$$

Where k_{eq} and k_{re} are the modes associated with the radiation-matter equality and the end of reheating. For instantaneous reheating, $k_{re} \sim 10^{-15}$ GeV, which immediately gives $k_{eq} \sim 10^{-39}$ GeV ~ 1 Mpc^{-1}. From this estimation, one observes that any mode $k < k_{eq} \sim 1$ Mpc^{-1} re-enters the horizon during the matter-dominated era, is expected to carry information about its quantum origin, as those are not affected by causal MHD processes. A schematic of the modes that re-enter the horizon during the different eras is given in Fig.5.1. Therefore, from the observation of magnetic field strength and structure for large-scale modes, we can decode the quantum nature of the early universe through observables such as squeezing parameters, which encode the evolution of the field.

5.2 Primordial Gravitational waves in squeezed state formalism

Primordial gravitational wave (GW) has been studied already in the squeezed state formalism [135,155,156]. Hence, we will quote the main results here. Formalism would be the same as discussed in the electromagnetic case. The transverse traceless part of the metric perturbation defines the physical component of the gravitational waves,

$$ds^2 = a^2(\eta)\left[-d\eta^2 + (\delta_{ij} + h_{ij})dx^i dx^j\right] \tag{5.17}$$

The tensor perturbation here h_{ij} satisfies the relation $\partial_i h^{ij} = 0,\ h^i_i = 0$ and $|h_{ij}| \ll \delta_{ij}$.

$$h_{ij}(x,\eta) = \frac{1}{a}\int \frac{d^3k}{(2\pi)^3} e^p_{ij}\, h^p_k\, e^{ik\cdot x} \tag{5.18}$$

Where e_{ij} is the polarization tensor for the GW and it satisfies the relation $e^{m*}_{ij} e^n_{ij} = 2\delta^{mn}$. Here p is the polarization index corresponding to the GW. Like the electromagnetic fields, p assumes two values corresponding to the two polarization modes. The conjugate momentum corresponding to h_k is

$$\pi^{(p)}_k = h'^{(p)}_k - \frac{a'}{a} h^{(p)}_k \tag{5.19}$$

With this in hand, the Hamiltonian turns out as

$$\mathcal{H} = \frac{1}{2}\sum_{p=1,2}\int \frac{d^3k}{(2\pi)^3}\, k\left(a^{(p)}_k a^{\dagger(p)}_k + a^{\dagger(p)}_{-k} a^{(p)}_{-k}\right) + i\frac{a'}{a}\left(a^{\dagger(p)}_k a^{\dagger(p)}_{-k} - a^{(p)}_k a^{(p)}_{-k}\right) \tag{5.20}$$

Now, as in the electromagnetic case, we can calculate the Bogoliubov coefficients as

$$\alpha_k = \left(1 + \frac{i}{k\eta} - \frac{1}{2k^2\eta^2}\right)\ ;\ \beta_k = \frac{1}{2k^2\eta^2} \tag{5.21}$$

Here also, the Bogoliubov coefficients are represented in terms of the squeezing parameter (r_k) and the squeezing angle (ϕ_k) as in Eq.(5.9). The evolution of the squeezing parameter and the squeezing angle in the case of primordial gravitational waves is dictated by the following differential equations:

$$\begin{aligned} \phi'_k &= -k + \frac{a'}{a}\sin(2\phi_k)\coth(2r_k) \\ r'_k &= -\frac{a'}{a}\cos(2\phi_k)\ ;\ \theta'_k = -k + \frac{a'}{a}\sin(2\phi_k)\tanh(r_k) \end{aligned} \tag{5.22}$$

Moreover, the evolution of the squeezing parameter with the conformal time turns out, as shown in Fig.5.3. And the GW power spectra in terms of the squeezing parameter

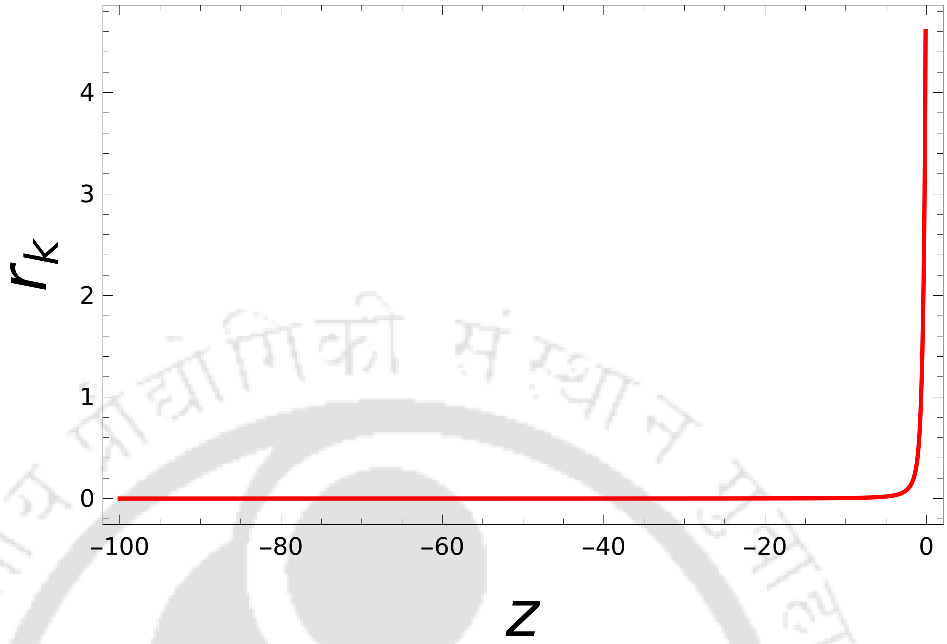

Figure 5.3: Evolution of the squeezing parameter r_k with $z = k\eta$ in case of gravitational waves

(r_k) and squeezing angle (ϕ_k) turn out to be

$$\begin{aligned}\mathcal{P}^{GW}(\eta, k) &= \frac{2k^2}{\pi^2 M_{Pl}^2 a^2} \sum_{p=1,2} |\alpha_k^{(p)} + \beta_k^{(p)}|^2 \\ &= \frac{2k^2}{\pi^2 M_{Pl}^2 a^2} \sum_{p=1,2} \left(\cosh(2r_k^{(p)}) + \sinh(2r_k^{(p)}) \sin(2\phi_k^{(p)}) \right) \end{aligned} \tag{5.23}$$

Where $M_{pl} = (8\pi G)^{-1/2}$ is the reduced Planck mass. From the above expression, it is evident that the power spectra for GW also depend on the squeezing parameter r_k, which can be measured from the strengths. Towards this end, let us point out an important observation regarding the distinct decreasing behavior of the squeezing parameter for the gauge field (see Fig.5.1) from that of the gravitational wave (see Fig.5.3). This distinct behavior of r_k for the gauge field originates from the underlying conformal invariance. Because of this property, the evolution of the squeezing parameter of the gauge field does not depend on the cosmological scale factor, as the background is conformally flat. Hence, it depends only on the gauge coupling parameter $I(\eta)$. The coupling function Eq.5.2 is assumed in such a way that it decreases and becomes unity at the end of inflation, which restores the standard conformal invariant Maxwell's theory. As a result $r_k = \sinh^{-1}|\beta_k|$ also decrease with time. After the end of inflation, the conformal invariance of the EM field is restored, and there will be no more evolution of the squeezing parameter r_k from background expansion. In the asymptotic $k\eta \to 0$ limit, the values of the squeezing parameter turned out to be r_k= 6.9, 14.9, and 23.4 for n= 1, 2, 3, respectively. However, the dynamics of r_k for gravitational waves explicitly depend on the scale factor, which leads r_k to increase in time, as depicted in Fig.5.3. Therefore, for both cases, the information about the quantum origin of the fields should be encoded into the non-zero value of their respective squeezing parameters.

5.3 Modifications due to initial Non Bunch Davies Vacuum

When we solved for the mode functions of gauge fields and the tensor perturbations, in the infinite past, we considered the usual Bunch Davies (BD) vacuum, parametrized by Bogolubov parameter values $\alpha_k = 1$ and $\beta_k = 0$ for $k\eta \to -\infty$. However, generalizing the initial condition to a non-BD vacuum has been studied extensively for scalar and tensor perturbations in the literature [157–162]. Such studies for gauge fields have not been considered before, and we take this opportunity to investigate the effects of a non-BD vacuum on the Primordial magnetic field. For the sake of our present study, we also discuss the non-BD modification of the primordial gravitational waves power spectrum.

5.3.1 Modifications to primordial magnetic field power spectrum due to non-BD vacuum

The time-dependent magnetic field power spectrum can be expressed in terms of the Bogoliubov coefficients as [92]

$$\mathcal{P}_B(k,\eta) = \frac{k^4}{2\pi^2 a^4 I^2}\sum_{p=1,2}|\alpha_k^p + \beta_k^p|^2.$$

In the past infinity, if we take the BD initial condition, i.e., $\alpha_k = 1, \beta_k = 0$, the power spectrum will turn out as

$$\mathcal{P}_B(k)|_{k\eta\to-\infty} = \frac{k^4}{\pi^2 a^4 I^2}. \tag{5.24}$$

Usually, the non-BD initial state is parametrized by non-vanishing β_k for each mode, and the power spectrum at $k\eta \to \infty$ will be,

$$\mathcal{P}_B(k)|_{k\eta\to-\infty} = \frac{k^4}{2\pi^2 a^4 I^2} \sum_{p=1,2} |\alpha_k^{0(p)} + \beta_k^{0(p)})|^2 \tag{5.25}$$

Where $\alpha_k^{0(p)}$ and $\beta_k^{0(p)}$ represents the Bogoliubov coefficients in the limit $k\eta \to -\infty$. For numerical purpose we define a dimensionless ratio $\delta_k^{(p)} = \beta_k^{0(p)}/\alpha_k^{0(p)}$. For the BD vacuum, this ratio goes to zero. The Bogoliubov coefficients follow the relation

$$|\alpha_k|^2 - |\beta_k|^2 = 1 \tag{5.26}$$

In the infinite past also, the Bogoliubov coefficients follow the relation in Eq.(5.26). Thus the quantity $|\alpha_k^{0(p)}|^2$ can be written in terms of $\delta_k^{(p)}$ as

$$\begin{aligned} |\alpha_k^{0(p)}|^2 - |\beta_k^{0(p)}|^2 &= 1 \\ |\alpha_k^{0(p)}|^2 \left(1 - \frac{|\beta_k^{0(p)}|^2}{|\alpha_k^{0(p)}|^2}\right) &= 1 \\ |\alpha_k^{0(p)}|^2 \left(1 - |\delta_k^p|^2\right) &= 1 \end{aligned}$$

Finally, it turns out to be

$$|\alpha_k^{0(p)}|^2 = \frac{1}{1 - |\delta_k^{(p)}|^2} \tag{5.27}$$

Now using Eq.(5.27), the power spectrum can be written in terms of the quantity $\delta_k^{(p)}$ as,

$$\begin{aligned}\mathcal{P}_B(k)|_{k\eta\to-\infty} &= \frac{k^4}{2\pi^2a^4I^2}\sum_{p=1,2}|\alpha_k^{0(p)}|^2|1+\delta_k^{(p)}|^2 \\ &= \frac{k^4}{2\pi^2a^4I^2}\sum_{p=1,2}\frac{|1+\delta_k^{(p)}|^2}{1-|\delta_k^{(p)}|^2} \\ &= \frac{k^4}{2\pi^2a^4I^2}\sum_{p=1,2}(1+g_k^{(p)}).\end{aligned} \tag{5.28}$$

Where $g_k^{(p)}$ encodes the information of the non-BD initial excited state. Here the factor $g_k^{(p)}$ is related to $\delta_k^{(p)}$ as

$$\delta_k^{(p)} = \frac{g_k^{(p)}}{2+g_k^{(p)}}. \tag{5.29}$$

And the Bogoliubov coefficients can be written in terms of $g_k^{(p)}$ as

$$\alpha_k^{0(p)} = \frac{2+g_k^{(p)}}{2\sqrt{1+g_k^{(p)}}} \;;\; \beta_k^{0(p)} = \frac{g_k^{(p)}}{2\sqrt{1+g_k^{(p)}}}. \tag{5.30}$$

For the simplicity of our calculation, we have taken that there is no relative phase difference between the two Bogoliubov coefficients in the past. It is evident from Eq.(5.30) that the values of these coefficients are fixed by a particular choice of the function $g_k^{(p)}$.

5.3.2 Modifications of primordial gravitational wave power spectrum due to Non-BD vacuum

As we discussed in the previous section on primordial magnetic fields, the gravitational waves will also get similar modifications in the non-BD vacuum state. The power spectrum for the PGW can be written in terms of the Bogoliubov coefficients as

$$\mathcal{P}^{GW}(k,\eta) = \frac{2k^2}{\pi^2M_{pl}^2a^2}\sum_{p=1,2}|\alpha_k^{(p)}+\beta_k^{(p)}|^2 \tag{5.31}$$

For the BD initial condition, the power spectrum in the infinite past looks like

$$\mathcal{P}^{GW}(k)|_{k\eta\to-\infty} = \frac{4k^2}{\pi^2M_{pl}^2a^2} \tag{5.32}$$

Now taking into consideration the initial excited state, exactly like in the case of the PMF, we can write it in terms of the ratio $\delta_k^{(p)} = \beta_k^{0(p)}/\alpha_k^{0(p)}$. Following the steps from Eq.(5.26) to Eq.(5.27) we can obtain the power spectrum as

$$\begin{aligned}\mathcal{P}^{GW}(k)|_{k\eta\to-\infty} &= \frac{2k^2}{\pi^2 M_{pl}^2 a^2}\sum_{p=1,2}\frac{|1+\delta_k^{(p)}|^2}{1-|\delta_k^{(p)}|^2} \\ &= \frac{2k^2}{\pi^2 M_{pl}^2 a^2}\sum_{p=1,2}(1+g_k^{(p)}) \qquad (5.33)\end{aligned}$$

The factor $g_k^{(p)}$ is related to $\delta_k^{(p)}$ as described in Eq.(5.29). Moreover, the Bogoliubov coefficients are related to the factor $g_k^{(p)}$ as described in Eq.(5.30). The equations (5.11) and (5.21) show that for the BD initial state, one gets $\beta_k = 0$ in the asymptotic past. However, for the non-BD initial state, β_k is non-vanishing. In our squeezing state formalism, this non-zero β_k in the infinite past suggests that the initial state is squeezed.

In the following, we consider a particular model to show the deviation from the regular BD vacuum. We assume the form of $g_k^{(p)}$ to be a lognormal distribution following from the reference [163].

$$g_k^{(p)} = \frac{\gamma}{\sqrt{2\pi(\Delta_k^{(p)})^2}}\exp\left[-\frac{ln^2(k/k_i)}{2(\Delta_k^{(p)})^2}\right]. \qquad (5.34)$$

Where γ represents the strength of the distribution, Δ_k denotes the width of the Gaussian, and k_i denotes the location of the peak of the distribution. If we set $\gamma = 0$, the non-BD states boil down to the standard Bunch-Davies vacuum state. Furthermore, for the modes $k >> k_i$, $g_k^{(p)} \to 0$, which implies that the small wavelength modes perceive the BD vacuum. For example, suppose we choose a particular value of the parameters of the non-BD state, $k_i = 1$ MPc^{-1}, $k = 0.8$ MPc^{-1}, $\gamma = 4.5$, and Δ_k^p as unity for both polarizations. In that case, the Bogoliubov coefficients turn out to be $\alpha_k = 1.13,\ \beta_k = 0.53$ for both cases. These new values also satisfy the relation $|\alpha_k|^2 - |\beta_k|^2 = 1$. For the case of BD vacuum, the initial value of the squeezing parameter r_k is zero. However, from Eq.(5.11), we can calculate the value of the squeezing parameter at the beginning of the evolution, and the value turns out as $r_0 = 0.51$ for the set of the parameters men-

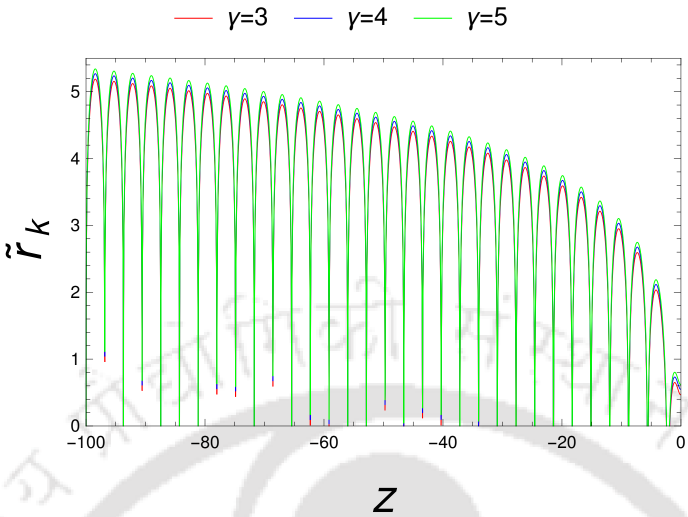

Figure 5.4: Here the evolution of the squeezing parameter (r_k) of the primordial magnetic field for coupling parameter $n = 1$ is plotted against $k\eta$. On the y-axis, we have plotted $(r_k - 9)$ (for scaling), and on the x-axis, $z = k\eta$ is plotted. The three colors correspond to different values of the initial squeezing parameter r_0, the variation in r_0 is obtained by varying the strength of the distribution γ introduced in Eq.(5.34), while keeping the value of k fixed at 0.8 MPc^{-1}.

tioned above. The effect of this initial excited state can be realized from the evolution of the squeezing parameter (r_k) with r_0 as the initial condition. It can, in principle, be observed in the present day. As the r_k is non-zero initially, we numerically solve Eq.(5.10) and study the evolution of the squeezing parameter for magnetic field r_k with $z = k\eta$ as shown in Fig.5.3.2. In the case of primordial gravitational waves, the squeezing parameter asymptotically goes to infinity as $\eta \to 0$, like the BD vacuum. However, we can always calculate the value at a finite but small η, which can be connected with the present-day observation. For a better understanding of the modifications due to initial excitation, we tabulate the values of the squeezing parameter at the end of inflation for the case of primordial magnetic fields. Here we only show the changes in the final values r_k (see Tab.5.1) due to initial squeezing r_0 for the coupling parameter value $n = 1$. To this end, let us briefly discuss the physical interpretation of the excited state. The initial excited state can be regarded as a Bogoliubov transformation of the non-excited BD vacuum state. If u_k is the mode function corresponding to the BD vacuum, then if

Bunch Davies case			Non Bunch Davies case			
Initial value of β_k	Initial value of r_k	Final value of r_k	Parameters (γ, k in MPc^{-1})	Initial value of β_k	Initial value of r_k	Final value of r_k
0	0	6.9	$\gamma = 3,\ k = 0.8$	0.396	0.387	9.468
			$\gamma = 4,\ k = 0.8$	0.487	0.469	9.550
			$\gamma = 5,\ k = 0.8$	0.567	0.540	9.621
			$\gamma = 4,\ k = 0.5$	0.418	0.406	9.487
			$\gamma = 4,\ k = 0.7$	0.474	0.0.458	9.539
			$\gamma = 4,\ k = 0.9$	0.493	0.475	9.556

Table 5.1: The final values of the squeezing parameter in the case of the primordial magnetic field are listed for different r_0. The parameters γ and k are the variables of the initial value of the squeezing parameter r_0. The final value denotes the value of the squeezing parameter at the end of inflation.

we do a transformation as

$$\tilde{u}_k = \alpha_k u_k + \beta_k u_k^*$$

Then the mode $\tilde{u}_k$ is the mode function of the excited state containing $n_k = |\beta_k|^2$ number of particles with momentum k.

5.4 Squeezed quantum states

In order to perform experiments for quantum signatures, following [54], we construct the quantum state generalizing for two polarization states of the photon and graviton. For each polarization mode, we already defined associated squeezing parameters, $(r_k^{1,2}, \phi_k^{1,2})$. A generic quadratic Hamiltonian can always be expressed in terms of those parameters and associated so-called squeezing operator $S\,(r_k, \phi_k) = e^{B_k}$ and rotation operator $R_k = e^{D_k}$ for each individual polarization mode, with [51,52]

$$\begin{aligned} B_k &= r_k e^{-2i\phi_k} a_{-k} a_k - r_k e^{2i\phi_k} a^{\dagger}_{-k} a^{\dagger}_{-k} \\ D_k &= -i\theta_k a^{\dagger}_{-k} a_k - i\theta_k a^{\dagger}_{-k} a_{-k} \end{aligned} \tag{5.35}$$

These are unitary operators It can be shown to form the unitary time evolution operator for the quantum state [54]. During inflation, it is generically assumed that all the quantum states start to evolve from the Bunch-Davies vacuum. Because of the coupling of the fields under study with the classical background, the vacuum state will evolve to a squeezed state, which can be expressed as follows,

$$
\begin{aligned}
|\psi\rangle &= S_2(r_k^2, \phi_k^2) R_2(\theta_k^2)|0\rangle \otimes S_1(r_k^1, \phi_k^1) R_1(\theta_k^1)|0\rangle \\
&= \frac{1}{\mathcal{A}} \sum_{n,m=0}^{\infty} e^{-2i(n\phi_k^1 + m\phi_k^2)} \tanh^n r_k^1 \tanh^m r_k^2 |n_{k,-k}^1, m_{k,-k}^2\rangle .
\end{aligned}
\tag{5.36}
$$

Where, $\mathcal{A} = \cosh(r_k^1)\cosh(r_k^2)$. The position space representation of Eq.(5.36) assume the following form,

$$
\langle q_A^{1,2}, q_B^{1,2} | \Psi \rangle = \frac{1}{\pi} \prod_p \frac{e^{(X_p q_A^p{}^2 + q_B^p{}^2 - Y_p q_A^p q_B^p)}}{\cosh r_k^p \sqrt{1 - e^{4i\phi_k^p} \tanh^2 r_k^p}} \tag{5.37}
$$

Here $X^{1,2}$ and $Y^{1,2}$ are defined as

$$
X_p = \frac{e^{-4i\phi_k^p} \tanh^2 r_k^p + 1}{2\left(e^{-4i\phi_k^p} \tanh^2 r_k^p - 1\right)}; Y_p = \frac{2e^{2i\phi_k^p} \tanh r_k^p}{e^{-4i\phi_k^p} \tanh^2 r_k^p - 1}.
$$

Where the *subscript* 'A' stands for momentum mode $\mathbf{k}$ and 'B' stands for the momentum mode $-\mathbf{k}$. Superscripts $1, 2$ are the polarization index. In the case of a scalar field, we can also see similar product states of the polarization. However, we can see that the state we obtained depends on the squeezing parameter r_k. The evolution of the squeezing parameter depends on the Hamiltonian of the system under consideration. As the evolution of the scalar and gauge fields is totally different, the evolution of the squeezing parameter will also be different. Therefore, it is obvious from the present discussion that the large-scale magnetic field and gravitational waves should be in a highly non-classical state at present. Quantum discord, an important measure of quantumness, is indeed shown to increase [52] for such a state with increasing r_k. However, its measurement in the cosmological setting is not obvious. Therefore, in order to quantify this quantumness, we will perform fuzziness of the quantum Poincaré sphere on this state Eq.(5.36), and to show the concreteness of this proposal, we also perform the well-established Bell test on this state. For this purpose, we consider two sets of observables with their unique algebraic properties.

5.4.1 Effects of initial non-BD vacuum on the squeezed state

In the previous section, we showed the effects of initial excitation on the power spectrum of magnetic fields and primordial gravitational waves. Here, we investigate the effects of the initial excitation on the squeezed state. If we fix the parameters of the function described in Eq.(5.34), then it fixes the value of β_k and thus the excited state $|m_k(\eta_0)\rangle$ also gets fixed, from which the evolution starts. So the final squeezed state will evolve from the state $|m^0_k, m^0_{-k}\rangle$ with a non-zero particle number. As we have taken the factor g_k to be independent of the polarization, this initial state is the same for both polarization modes. In the interaction picture, the state and the operators evolve with time. So the creation and annihilation operators $a_k(0), a^\dagger_k(0)$ defined with respect to the BD vacuum also evolve to some $\hat{b}_k$ and $\hat{b}^\dagger_k$ depending on the Hamiltonian of the system. And the excited state $|m^0_k, m^0_{-k}\rangle$ acts as a vacuum state with respect to the new creation and annihilation operators $\hat{b}_k, \hat{b}^\dagger_k$. So the operator algebra gives $\hat{b}_k\, |m^0_k, m^0_{-k}\rangle = 0$. Therefore the new squeezing and displacement operator is defined with respect to the new creation and annihilation operator $\hat{b}_k, \hat{b}_{-k}$ and $\hat{b}^\dagger_k, \hat{b}^\dagger_{-k}$ respectively as $S'(r'_k, \phi'_k) = e^{B'_k}$ and $R'(\theta'_k) = e^{D'_k}$, where

$$\begin{aligned} B'_k &= r'_k e^{-2i\phi'_k}\hat{b}_{-k}\hat{b}_k - r'_k e^{2i\phi'_k}\hat{b}^\dagger_k\hat{b}^\dagger_{-k} \\ D'_k &= -i\theta'_k\hat{b}^\dagger_k\hat{b}_k - i\theta'_k.\hat{b}^\dagger_{-k}\hat{b}_{-k} \end{aligned} \tag{5.38}$$

Here, we have used a different squeezing parameter r'_k as its value starts from r_0, unlike the case for the general BD vacuum. The final squeezed state will be constructed as

$$\begin{aligned} |\psi\rangle_{exc} &= S'_2(r'^2_k, \phi'^2_k)R'_2(\theta'^2_k)|m^0_k, m^0_{-k}\rangle \otimes S'_1(r'^1_k, \phi'^1_k)R'_1(\theta'^1_k)|m^0_k, m^0_{-k}\rangle \\ &= \frac{1}{\mathcal{A}'}\sum_{n,m=0}^{\infty} e^{-2i(n\phi'^1_k + m\phi'^2_k)}\tanh^n r'^1_k \cdot \tanh^m r'^2_k |n^1_{k,-k}, m^2_{k,-k}\rangle \end{aligned} \tag{5.39}$$

Where, $\mathcal{A}' = \cosh(r'^1_k)\cosh(r'^2_k)$. The squeezed state, which evolved from the initial excited state, can be projected in the real space as described in Eq.(5.37). It can also be noticed that the state described in Eq.(5.39) looks exactly similar to the state in Eq.(5.36), with the only difference being the squeezing parameter r, as in the latter case, it starts to evolve from the value r_0.

5.5 Quantum Stokes operators

The Stokes parameters [164] are known to be an important description of the polarization properties of the electromagnetic field. The same can also be applied to gravitational waves. The quantum Stokes parameters are the operator representations of the polarization that can be applied to non-classical waves. Most interestingly, these operators satisfy an angular momentum-like commutation algebra. Stokes operators are defined as follows,

$$\begin{aligned} \mathcal{S}_k^{(0)} &= a_k^{1\dagger} a_k^1 + a_k^{2\dagger} a_k^2 \;;\; \mathcal{S}_k^{(1)} = a_k^{1\dagger} a_k^1 - a_k^{2\dagger} a_k^2 \\ \mathcal{S}_k^{(2)} &= t_k a_k^{1\dagger} a_k^2 + t_k^* a_k^{2\dagger} a_k^1 \;;\; \mathcal{S}_k^{(3)} = i(t_k^* a_k^{2\dagger} a_k^1 - t_k a_k^{1\dagger} a_k^2) \end{aligned} \tag{5.40}$$

Where $t_k = e^{i\psi_k}$ measures the relative phase between the two modes. According to the above definition, $p = (1, 2)$ corresponds to two different polarization modes associated with electromagnetic and gravitational fields. $\mathcal{S}_k^0$ encodes the intensity of a particular mode k or the total number of photons or graviton. $\mathcal{S}_k^1$ and $\mathcal{S}_k^2$ measures the linear polarization and $\mathcal{S}_k^3$ measures the circular polarization. Interestingly last three Stokes parameters parametrizing the polarization states satisfy $SU(2)$ spin algebra $[\mathcal{S}_k^{(p)}, \mathcal{S}_k^{(q)}] = 2i\epsilon^{pqr}\mathcal{S}_k^{(r)}$, where ϵ^{pqr} is the three dimensional levicivita tensor density. $(p, q, r) \equiv 1, 2, 3$. In order to prove the quantumness of a system through the Stokes parameters, we examine it via the quantum Poincaré sphere [165, 166]. For the classical case, we have the usual relation $\langle(\mathcal{S}_k^1)^2 + (\mathcal{S}_k^2)^2 + (\mathcal{S}_k^3)^2\rangle = \langle(\mathcal{S}_k^0)^2\rangle$ [167, 168]. But in the case of quantum Poincaré sphere, we cannot precisely define the radius of the Poincaré sphere due to the non-commutativity of $\mathcal{S}_k^i$. And we have $\langle(\mathcal{S}_k^1)^2 + (\mathcal{S}_k^2)^2 + (\mathcal{S}_k^3)^2 - (\mathcal{S}_k^0)^2\rangle > 0$. We define the fuzziness of the quantum Poincaré sphere (also called the fuzzy sphere) as a measure of the quantumness

$$Q_{fuzzy} = \langle (\mathcal{S}_k^1)^2 + (\mathcal{S}_k^2)^2 + (\mathcal{S}_k^3)^2 - (\mathcal{S}_k^0)^2 \rangle \tag{5.41}$$

In order to calculate the fuzziness of the Poincaré sphere constructed by the Stokes operators, we need to explicitly calculate the expectation values of the operators $(\mathcal{S}_k^i)^2$. We have

$$\begin{aligned}
(\mathcal{S}_k^0)^2 &= (n_k^1)^2 + n_k^1 n_k^2 + n_k^2 n_k^1 + (n_k^2)^2 \\
(\mathcal{S}_k^1)^2 &= (n_k^1)^2 - n_k^1 n_k^2 - n_k^2 n_k^1 + (n_k^2)^2 \\
(\mathcal{S}_k^2)^2 &= (t_k)^2 (a_k^{\dagger 1})^2 (a_k^2)^2 + t_k t_k^* \, n_k^1 a_k^2 a_k^{\dagger 2} + t_k t_k^* \, n_k^2 a_k^1 a_k^{\dagger 1} + (t_k^*)^2 (a_k^{\dagger 2})^2 (a_k^1)^2 \\
(\mathcal{S}_k^3)^2 &= -(t_k^*)^2 (a_k^{\dagger 2})^2 (a_k^1)^2 + t_k t_k^* \, n_k^1 a_k^2 a_k^{\dagger 2} + t_k t_k^* \, n_k^2 a_k^1 a_k^{\dagger 1} - (t_k)^2 (a_k^{\dagger 1})^2 (a_k^2)^2
\end{aligned} \tag{5.42}$$

Where $n_k^1 = a_k^{\dagger 1} a_k^1$ is the number operator corresponding to polarization 1 and $n_k^2 = a_k^{\dagger 2} a_k^2$ is the number operator corresponding to polarization 2. Calculating the expectation values of the operators in Eq.(5.42) on the state defined in Eq.(5.36) we get

$$\begin{aligned}
\langle (\mathcal{S}_k^0)^2 \rangle &= \frac{1}{\mathcal{A}^2} \sum_{m,n=0}^{\infty} \tanh^{2n}(r_k^1) \tanh^{2m}(r_k^2)(n^2 + 2mn + m^2) \\
&= \frac{1}{4} \left(\cosh(4r_k^1) + 2\cosh(2r_k^1)\cosh(2r_k^2) + \cosh(4r_k^2) \right) \\
\langle (\mathcal{S}_k^1)^2 \rangle &= \frac{1}{\mathcal{A}^2} \sum_{m,n=0}^{\infty} \tanh^{2n}(r_k^1) \tanh^{2m}(r_k^2)(n^2 - 2mn + m^2) \\
&= \frac{1}{4} \left(\cosh(4r_k^1) - 2\cosh(2r_k^1)\cosh(2r_k^2) + \cosh(4r_k^2) \right) \\
\langle (\mathcal{S}_k^2)^2 \rangle &= \frac{1}{\mathcal{A}^2} \sum_{m,n=0}^{\infty} \tanh^{2n}(r_k^1) \tanh^{2m}(r_k^2) m(n+1) \\
&= \cosh^2(r_k^1) \sinh^2(r_k^2) \\
\langle (\mathcal{S}_k^3)^2 \rangle &= \frac{1}{\mathcal{A}^2} \sum_{m,n=0}^{\infty} \tanh^{2n}(r_k^1) \tanh^{2m}(r_k^2) n(m+1) \\
&= \sinh^2(r_k^1) \cosh^2(r_k^2)
\end{aligned} \tag{5.43}$$

Where $\mathcal{A} = \cosh(r_k^1)\cosh(r_k^2)$ and n, m are the number operator expectation values on the state for polarization 1 and polarization 2, respectively. Calculating the fuzziness on the state from the expectation values of the operators, we get and symbolize as

$$Q_{fuzzy} = \langle(\mathcal{S}^1_k)^2 + (\mathcal{S}^2_k)^2 + (\mathcal{S}^3_k)^2 - (\mathcal{S}^0_k)^2\rangle = 4\ \sinh^2(r_k) \tag{5.44}$$

Where, for simplicity, we have taken $r^1_k = r^2_k = r_k$. We can see that the quantity is dependent on the squeezing parameter r_k. Similarly, when we consider the initial state as an excited state, the final state corresponds to the state mentioned in Eq.(5.39). Here to perform the fuzziness of the Poincaré sphere, we define the quantum Stokes operators in terms of the new creation and annihilation operators $\hat{b}_k, \hat{b}_{-k}$ and $\hat{b}^\dagger_k, \hat{b}^\dagger_{-k}$ respectively. Here, the Stokes operators are defined as

$$\begin{aligned} \mathcal{S'}^{(0)}_k &= \hat{b}^{1\dagger}_k \hat{b}^1_k + \hat{b}^{2\dagger}_k \hat{b}^2_k \ ; \ \ \mathcal{S'}^{(1)}_k = \hat{b}^{\dagger}_k \hat{b}^1_k - \hat{b}^{2\dagger}_k \hat{b}^2_k \\ \mathcal{S'}^{(2)}_k &= t_k \hat{b}^{1\dagger}_k \hat{b}^2_k + t^*_k \hat{b}^{2\dagger}_k \hat{b}^1_k \ ; \ \mathcal{S'}^{(3)}_k = i(t^*_k \hat{b}^{2\dagger}_k \hat{b}^1_k - t_k \hat{b}^{1\dagger}_k \hat{b}^2_k) \end{aligned} \tag{5.45}$$

Now, the system starts to evolve with some initial excitation. In that case, we also define the fuzziness of the Poincaré sphere exactly as defined in Eq.(5.41) with the Stokes operators defined in Eq.(5.45). For this system, the fuzziness of the Poincaré sphere, having the state defined by Eq.(5.39), we get,

$$Q'_{fuzzy} = \langle(\mathcal{S'}^1_k)^2 + (\mathcal{S'}^2_k)^2 + (\mathcal{S'}^3_k)^2 - (\mathcal{S'}^0_k)^2\rangle = 4\ \sinh^2(r'_k)$$

Where we have taken $r'^1_k = r'^2_k = r'_k$. We can see from the results in Eqs.(5.44) and (5.46) that when the squeezing parameter (r_k, r'_k) goes to zero, we can consider the state to be classical. Therefore, the higher the squeezing parameter, the higher the fuzziness of the Poincaré sphere, and thus the quantumness increases.

5.6 Measurement and Poincaré sphere

Performing the test for quantumness is not as easy as for cosmological scenarios. However, the primordial gravitational Eq.(5.23) and magnetic power spectrum Eq.(5.13) provide us a good observational measure of the squeezing parameters (r_k, ϕ_k), in terms of their strength and index. Using those measured values of (r_k, ϕ_k), we can theoretically obtain the fuzziness of the Poincaré sphere from (5.41). Therefore, for a particular value of the squeezing parameter, if that quantity is greater than zero, we can infer about the quantumness of the system. Further, Stokes parameters are also measurable quantities [169,170], which are directly related to the fuzziness. From Eq.(5.41), we can see that fuzziness is defined in terms of $\langle(\mathcal{S}_k^i)^2\rangle$. The operators $(\mathcal{S}_k^{0,1})^2$ are functions of the number operators. Thus, it can be measured from the intensity of GW and the strength of the magnetic field, respectively. However, the expectation values of the operators $(\mathcal{S}_k^{2,3})^2$ cannot be measured directly as they contain several correlation functions, such as $(a_k^{\dagger i})^2$, $n_k^i a_k^j a_k^{\dagger j}$. However, Agarwal et al. [173] in their paper have shown that these correlation functions can be measured in terms of the intensity and intensity fluctuations. The variance is defined as

$$V_{ij} = \frac{1}{2}\left(\langle\{\mathcal{S}_i, \mathcal{S}_j\}\rangle - \{\langle\mathcal{S}_i\rangle, \langle\mathcal{S}_j\rangle\}\right) \tag{5.46}$$

Where the curly brace is the anti-commutator. The diagonal elements can be calculated as

$$V_{ii} = \langle(\mathcal{S}_i)^2\rangle - (\langle\mathcal{S}_i\rangle)^2 \tag{5.47}$$

As this quantity V_{ii} can be measured [170,174] and the expectation values of the Stokes parameter $\langle\mathcal{S}_k^i\rangle$ is a measurable quantity we can write Eq.(5.41) as

$$Q_{fuzzy} = \langle(\mathcal{S}_k^1)^2 + V_{22} - (\langle\mathcal{S}_k^2\rangle)^2 + V_{33} - (\langle\mathcal{S}_k^3\rangle)^2 - (\mathcal{S}_k^0)^2\rangle \tag{5.48}$$

Therefore, experimentally measured value of the fuzziness $\langle(S_k^1)^2 + (S_k^2)^2 + (S_k^3)^2 - (S_k^0)^2\rangle$ in terms of Stokes parameters $(\mathcal{S}_k^1, \mathcal{S}_k^2, \mathcal{S}_k^3)$, can now be compared with its classical counterpart (which is zero) [167, 168]. Upon observing $\langle(\mathcal{S}_k^1)^2 + (\mathcal{S}_k^2)^2 + (\mathcal{S}_k^3)^2 - (\mathcal{S}_k^0)^2\rangle > 0$, we can infer the quantum origin of those primordial fluctuations. In principle, when we measure either a gravitational wave or a primordial magnetic field, we cannot measure a particular wave number of k. We measure a superposition of several wave numbers. Therefore, the actual measurable quantity is defined as

$$\sum_{k=k_{min}}^{k_{max}} \langle(\mathcal{S}_k^1)^2 + (\mathcal{S}_k^2)^2 + (\mathcal{S}_k^3)^2 - (\mathcal{S}_k^0)^2\rangle \tag{5.49}$$

We know that for the classical case, the quantity defined in Eq.(5.41) Q_{fuzzy} is zero, so it is never negative for any scenario. Thus, the measurement will give us

$$\sum_{k=k_{min}}^{k_{max}} \langle(\mathcal{S}_k^1)^2 + (\mathcal{S}_k^2)^2 + (\mathcal{S}_k^3)^2 - (\mathcal{S}_k^0)^2\rangle \geq 0 \tag{5.50}$$

After the measurement, if the measured quantity is greater than zero, we can conclude that the system under consideration has a quantum origin.

5.7 Pseudospin operators and Bell violation

Now we embark on a different set of operators called pseudo spin operators and their Bell violation test to further support our proposal in the last section. This set of operators can be very useful in several quantum mechanical systems. We will discuss their application in future work. When dealing with the system having continuous variables, there exists an elegant way [55, 171, 172] of constructing a set of position-dependent pseudo spin operators which satisfy the same algebra as the spin angular momentum. *To the best of our knowledge, such operators were constructed only in one dimension*. Our present study demands the generalization of those operators in two dimensions corresponding to two independent polarization modes. As a prerequisite of the spin-like operators, the following operators are defined in position (q, q') space,

$$\begin{aligned}
P_{n,m}(l) &= \int_{nl}^{(n+1)l} dq \int_{ml}^{(m+1)l} dq' \;\; |q,q'\rangle\langle q,q'|, \\
T_{n,m}(l) &= \int_{nl}^{(n+1)l} dq \int_{ml}^{(m+1)l} dq' \;\; |q,q'\rangle\langle q+l,q'+l|, \\
T^\dagger_{n,m}(l) &= \int_{(n+1)l}^{(n+2)l} dq \int_{(m+1)l}^{(m+2)l} dq' \;\; |q,q'\rangle\langle q-l,q'-l|.
\end{aligned} \tag{5.51}$$

Those are called on-site projection, forward, and backward hopping operators, respectively. When the projection and the hopping operators operate on a state, they behave as

$$
\begin{aligned}
P_{n,m}(l)\,\psi(q) &= \begin{cases} \psi(q) & ml, nl \le q < ml+l, nl+l \\ 0 & \text{otherwise} \end{cases} \\
T_{n,m}(l)\,\psi(q) &= \begin{cases} \psi(q+l) & ml, nl \le q < ml+l, nl+l \\ 0 & \text{otherwise} \end{cases} \\
T^{\dagger}_{n,m}(l)\,\psi(q) &= \begin{cases} \psi(q-l) & ml+l, nl+l \le q < ml+2l, nl+2l \\ 0 & \text{otherwise} \end{cases}
\end{aligned} \tag{5.52}
$$

The generalized pseudo spin operators are constructed from the aforementioned position space operators, and generalizing from [171], we define them as

$$
\begin{aligned}
s_z &= \sum_{\mathcal{C}=-\infty}^{\infty} (-1)^{n+m} P_{n,m} \\
s_+ &= \sum_{\mathcal{C}=-\infty}^{\infty} T_{2n,2m} \\
s_- &= \sum_{\mathcal{C}=-\infty}^{\infty} T^{\dagger}_{2n,2m}
\end{aligned} \tag{5.53}
$$

where, $\mathcal{C} \equiv (m,n)$, and l is the length of the interval. We define $s_+ = s_x + i\, s_y$ and $s_- = s_x - i\, s_y$. It can be easily shown that these three operators s_x, s_y and s_z are dichotomous, i.e, $s_x^2 = s_y^2 = s_z^2 = 1$. Moreover, they follow the usual $SU(2)$ spin algebra. Exploiting the nature of the operators, we can define the Bell-CHSH operator in terms of the pseudospin operators. For two observer 'A' having momentum **k** and observer 'B' having momentum **-k**, the maximal Bell-CHSH operator can be constructed as

$$
B^s_{CHSH} \equiv 2\sqrt{(s_z^A \otimes s_z^B)^2 + (s_x^A \otimes s_x^B)^2} \tag{5.54}
$$

On the quantum state Eq.(5.37) we now calculate the expectation value of the Bell operator B^s_{CHSH} with $r^1_k = r^2_k = r$ presented in the Fig.5.5. We know that the Bell inequality suggests that a system with a Bell-CHSH operator expectation value greater than 2 can only be described by means of quantum mechanics. Thus, it is evident from

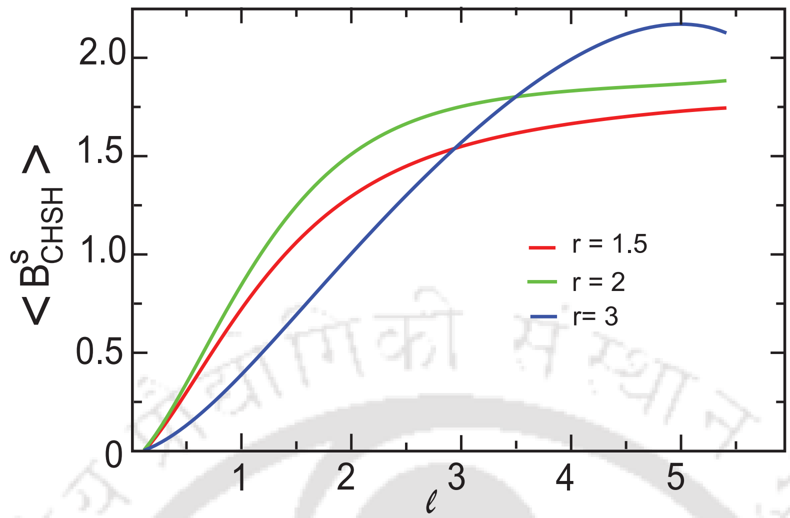

Figure 5.5: Variation of the expectation value of B^s_{CHSH} with the interval length l for different squeezing parameters r_k for $\theta_k - \frac{\phi_k}{2} = 0$

the figure that the system behaves quantum mechanically, i.e, $\langle B^s_{CHSH}\rangle > 2$, above a certain value of the squeezing parameter r_k, which is in agreement with the conclusion from our previous Poincaré sphere measurement.

5.8 Conclusion

In this work, we have proposed a Poincaré sphere fuzziness or Fuzzy sphere in terms of observable quantities to verify the quantum origin of the large-scale magnetic field and gravitational waves. For this purpose, we first constructed the squeezed quantum states for the electromagnetic and gravitational wave fluctuations during inflation and the associated power spectrum. We have seen that the evolution of the squeezing parameter is different for primordial magnetic fields and GW. In the case of the primordial magnetic field, it asymptotically gives the values $r_k = 6.9, 14.9$, and 23.4 for the coupling parameter $n = 1, 2$, and 3, respectively. In the case of GW, the squeezing parameter r_k increases asymptotically. So we can expect information about the quantum origin of the fields. Furthermore, if we consider an initial non-BD vacuum, the initial squeezing parameter naturally becomes non-zero. For example, if we assume $r_0 = 0.51$ for a mode $k = 0.8\text{MPc}^{-1}$, the final values of the squeezing parameter turn out as $r_{k=0.8} = (9.468, 9.550, 9.621)$ for $\gamma = (3, 4, 5)$ respectively in case of primordial magnetic field for the coupling parameter $n = 1$. Therefore, due to an initial excitation, there is an increase in the final value of the squeezing parameter at the end of inflation. We have then considered the Poincaré sphere fuzziness or the uncertainty of the radius in terms of quantum Stokes operators, which assume a positive value for the cosmologically evolved squeezed quantum states. Although all the terms described in Eq.(5.41) cannot be measured directly, we can measure all the terms of the variances and intensities of the Stokes parameters as defined in Eq.(5.48). Our theoretical calculation reveals that the larger the squeezing, the stronger the quantumness. Importantly, this can be confirmed by the direct measurement of Stokes parameters and primordial power spectra. Finally, we confirmed our conclusion by performing the Bell test further and considering dichotomic pseudospin operators. Other quantum diagnostics, such as quantum discord and Fano factors, could be interesting to study in the present context.

6

Conclusion and Future aspects

Contents

This chapter summarizes the work of the thesis, highlighting the important findings and generation mechanisms of large-scale magnetic fields as well as constructing appropriate observables to measure the quantum signatures of the primordial fields. Section 6.1 provides a summary of contributions and discussions. Section 6.2 concludes the chapter by providing a possible direction for future research.

6.1 Summary of contributions

The motive of this thesis has been to explore the different aspects of inflationary magnetogenesis. The generation mechanism, their evolution, and dealing with the challenges of inflationary magnetogenesis. This chapter contains the contributions from the thesis work as follows:

In Chapter 1, we introduced the outline of the thesis, discussing cosmology, motivation, and scope of the work briefly, and finally, the organization of the thesis.

In Chapter 2, we discussed the framework of inflationary magnetogenesis. The EM field without any explicit coupling is conformally invariant under a conformally flat background. Therefore, it is not possible to generate a magnetic field with sufficient strength. However, by coupling a time-dependent scalar field, generally the inflaton field, the conformal invariance can be broken, and we see that it can generate a magnetic field strength consistent with the present observation. We further discussed the challenges in inflationary magnetogenesis, namely the backreaction and the strong coupling problem. The post-inflationary evolution of the gauge field and the present-day strength of the magnetic field depend on the evolution of the Universe. In case of a prolonged reheating era after the end of inflation, the strength of the magnetic field is amplified compared to the case of instantaneous reheating due to conversion of electric field energy density to magnetic field energy density through Faraday's conversion.

In Chapter 3, we embark upon the Effective Field Theory of inflation. The spatial diffeomorphism breaks the conformal invariance of the EM field, and the EM field is produced during the inflationary era. Although the scale-invariant magnetic field does not suffer from the backreaction problem, the scale-invariant power spectra of the magnetic field cannot produce a sufficiently strong magnetic field. Therefore, by the introduction of a reheating era with a non-zero efolding number, the magnetic field strength that is consistent with the observation is achieved.

In Chapter 4, we propose a novel mechanism to produce large-scale magnetic fields. Here, we incorporate an anisotropic background to break the conformal invariance of the EM field. Due to the absence of any explicit coupling to the EM field, it is evidently free from the strong coupling problem. Furthermore, by tuning the anisotropic parameters, we can generate a sufficient strength of magnetic field consistent with the present-day observation. The proper choice of the parameters also avoids the backreaction problem of inflationary magnetogenesis. Moreover, by further introducing an elongated era of reheating after the anisotropies disappear, we can enhance the strength of the produced magnetic field. Furthermore, by the CMB observations of the magnetic field strength, we can also put constraints on the effective equation of state of the Universe.

6.2 Future aspects

The generation mechanism of large-scale magnetic fields has been widely discussed in the recent past. However, all the proposed mechanisms have their drawbacks and limits. Therefore, it is still an active area of research, and the detection of GW has shed new light on how to probe the intergalactic magnetic fields more precisely. Here, we suggest some of the possible directions to extend this work

- In our case of inflationary magnetogenesis in an anisotropic Universe, we have assumed that the anisotropies are just a perturbation over the regular FLRW metric, and we have not studied the effect of the anisotropies on the dynamics of the inflaton field. However, through a perturbative study, the observational signatures of the anisotropies on CMB can answer very fundamental questions about the origin of the Universe. In this context, we have not delved into the origin of the anisotropies.

- In this thesis, we have discussed the quantumness of primordial magnetic fields and primordial gravitational waves. However, in the case of secondary gravitational waves, the primordial magnetic fields also play an important role. Therefore, with the proper observable, we can probe the quantumness of the magnetic field embedded in the secondary gravitational wave. Probing the quantumness of magnetic fields through gravitational waves can be an exciting prospect in the direction of quantum information in the cosmological context.

A
Appendix

As we have already mentioned earlier in Chapter 3 that in this magnetogenesis scenario we can find one to one correspondence between the EFT approach and several well established models of inflationary magnetogenesis, here in this section we discussthe various magnetogenesis models can be embedded within the electromagnetic action (3.7) for suitable forms of the EFT coupling parameters $f_i(\eta)$. For example,

- The model where the EM field couples with a scalar field (generally the inflaton field), in particular the action is given by,

$$\mathcal{S}_{m1} = \int d^4x\sqrt{-g}\left[I^2(\phi)F_{\mu\nu}F^{\mu\nu}\right] \tag{A.1}$$

  where ϕ is the scalar field under consideration and $I(\phi)$ is the conformal breaking coupling function. The above magnetogenesis model without (i.e instantaneous reheating) or with reheating phase have been explored earlier in [70,92,93] where the coupling function is taken as $I(\phi(\eta)) = (a(\eta)/a_f)^n$, with $\phi = \phi(\eta)$ being determined by the background evolution of the scalar field and $a(\eta)$ is the scale factor of the FRW metric. The possible implications of an elongated reheating phase have been discussed in such magnetogenesis scenario, and moreover the parameter n is constrained for which the model predicts sufficient magnetic strength and also becomes free from various problems like the backreaction issue, the strong coupling problem etc [70,92,93].

Most importantly, the action (A.1) has a direct correspondence with the EFT action given in Eq.(3.7) when the EFT parameters get the following forms:

$$f_1(\eta) = \left(\frac{a(\eta)}{a_f}\right)^n \quad , \quad f_2(\eta) = f_3(\eta) = f_4(\eta) = 0 \tag{A.2}$$

respectively.

- On contrary to the scalar field coupled magnetogenesis model, let us consider the model where the EM field couples with the background spacetime curvature, in particular with the Ricci scalar as well as with the Gauss-Bonnet scalar curvature. The corresponding action is [95],

$$\mathcal{S}_{m2} = \int d^4x\sqrt{-g}\left[-\frac{1}{4}F_{\mu\nu}F^{\mu\nu} + f(R,\mathcal{G})F_{\mu\nu}F^{\mu\nu}\right] \tag{A.3}$$

where the coupling function $f(R,\mathcal{G})$ spoils the conformal invariance of the EM field and has the form as $f(R,\mathcal{G}) = \kappa^{2q}\left(R^q + \mathcal{G}^{q/2}\right)$, with q being the model parameter. This magnetogenesis model without (i.e instantaneous rehating) and with reheating phase have been explored in [95] where an elongated reheating phase seems to have a considerable impact on the magnetic field evolution, and in turn it predicts sufficient magnetic strength for suitable range of the reheating EoS. Moreover the above form of $f(R,\mathcal{G})$ does not lead to scale invariant magnetic or electric power spectrum for the possible values of q.

Once again, the action S_{m2} can be embedded within the EFT action (3.7), provided the EFT parameters are considered to have the following forms,

$$\begin{aligned} f_1(\eta) &= -\frac{1}{4} + \kappa^{2q}\left(R^q + \mathcal{G}^{q/2}\right) \\ f_2(\eta) &= f_3(\eta) = f_4(\eta) = 0 \end{aligned} \tag{A.4}$$

respectively, where $R(\eta) = \frac{6}{a^2}\left(\mathcal{H}' + \mathcal{H}^2\right)$ and $\mathcal{G}(\eta) = \frac{24}{a^4}\mathcal{H}^2\mathcal{H}'$, with $\mathcal{H}$ represents the conformal Hubble parameter in the FRW metric.

- In both the above magnetogenesis models, the equivalent EFT parameters like $f_3(\eta)$ and $f_4(\eta)$ become zero, mainly due to the absence of the parity violating terms in the EM field Lagrangian. However, on contrary, we can consider certain magnetogenesis models where the parity violating terms are indeed present in the EM Lagrangian and the equivalent $f_3(\eta)$ or $f_4(\eta)$ (or both) are non-zero. One of such models is explored by the authors of [?], where the EM field is considered to couple with the background Riemann tensor, particularly the action is,

$$\mathcal{S}_{m3} = \int d^4x\sqrt{-g}\left[-\frac{1}{4}F_{\mu\nu}F^{\mu\nu} - \frac{\sigma}{M^2}\tilde{R}^{\mu\nu\alpha\beta}F_{\mu\nu}F_{\alpha\beta}\right] \tag{A.5}$$

where σ is a model parameter, $R^{\alpha\beta}_{\rho\sigma}$ is the Riemann tensor and its dual is $\tilde{R}^{\mu\nu\alpha\beta} = \frac{1}{2}\epsilon^{\mu\nu\rho\sigma}R^{\alpha\beta}_{\rho\sigma}$. Due to the presence of the dual tensor in the Lagrangian, the two polarization modes of the EM field evolve differently, which in turn leads to the generation of helical magnetic field. The non-minimal coupling of the EM field to the Riemann tensor generates sufficient primordial helical magnetic fields at large scales, and the model is also free from the backreaction, strong coupling problems.

In the case of background FRW spacetime (with $a(\eta)$ being the scale factor), the non-zero components of Riemann tensor come as,

$$R^{0j}_{0i} = \left(\frac{a'^2}{a^4} - \frac{a''}{a^3}\right)\delta^j_i \quad , \quad R^{kl}_{ij} = \frac{a'^2}{a^4}\left(\delta^l_i\delta^k_j - \delta^k_i\delta^l_j\right) \ .$$

Consequently the action S_{m3}, in the FRW spacetime, turns out to be,

$$\mathcal{S}_{m3} = \int d^4x\sqrt{-g}\left[-\frac{1}{4}F_{\mu\nu}F^{\mu\nu} + \frac{\sigma}{2M^2}\left(\frac{a'^2}{a^2} + \frac{a''}{a}\right)\epsilon^{ijk}F^0_iF_{jk}\right] \ . \tag{A.6}$$

Thereby interestingly, the S_{m3} can be thought as equivalent with the EFT action given in Eq.(3.7) if the the EFT parameters have the forms like,

$$f_1(\eta) = -\frac{1}{4} \quad , \quad f_2(\eta) = 0 \ ,$$
$$f_3(\eta) = \frac{\sigma}{2M^2}\left(\frac{a'^2}{a^2} + \frac{a''}{a}\right) \quad , \quad f_4(\eta) = 0 \tag{A.7}$$

respectively. Here it may be mentioned that in [?], the authors considered an $instantaneous\ reheating$ mechanism in regard to the magnetogenesis model (A.5), however one may expect that the inclusion of a reheating phase with non-zero e-fold number will enhance the magnetic strength at present epoch compared to the instantaneous reheating case.

- As a well known one, we consider the Turner-Widrow model [30] where the action is given by,

$$\mathcal{S}_{m4} = \int d^4x\sqrt{-g}\left[-\frac{1}{4}F_{\mu\nu}F^{\mu\nu} + \frac{1}{12}RA^2\right] \tag{A.8}$$

where R is the background Ricci scalar. The presence of the effective potential term for the vector field (i.e $V(A_\mu A^\mu)$) in the above action spoils the U(1) invariance of the electromagnetic field, due to which the massive vector field gets three physical degrees of freedom: two of them are usual transverse modes and the other one is the longitudinal mode. The longitudinal mode with momentum $p^2 > R/6$ appears as a ghost field in the model, i.e a field with negative kinetic energy [179–182]. However on contrary, in the present work, it is the kinetic term of the electromagnetic field that gets coupled through the EFT parameters, and hence there is no potential term of the electromagnetic field appearing in the action. Thus the U(1) invariance is preserved in the present model, and consequently the longitudinal mode is absent. This clearly indicates that the action $\mathcal{S}_{m4}$ is not equivalent with the EFT action (3.7) considered in this work.

Bibliography

[1] B. P. Abbott *et al.* [LIGO Scientific and Virgo], "Observation of Gravitational Waves from a Binary Black Hole Merger," Phys. Rev. Lett. **116**, no.6, 061102 (2016)

[2] B. P. Abbott *et al.* [LIGO Scientific and Virgo], "GW170817: Observation of Gravitational Waves from a Binary Neutron Star Inspiral," Phys. Rev. Lett. **119**, no.16, 161101 (2017)

[3] A. A. Penzias and R. W. Wilson, "A Measurement of excess antenna temperature at 4080-Mc/s," Astrophys. J. **142**, 419-421 (1965).

[4] D. J. Fixsen, "The Temperature of the Cosmic Microwave Background," Astrophys. J. **707**, 916-920 (2009)

[5] G. Efstathiou, J. R. Bond and S. D. M. White, "COBE Background radiation anisotropies and large scale structure in the universe," Mon. Not. Roy. Astron. Soc. **258**, 1-6 (1992)

[6] G. F. Smoot *et al.* [COBE], "Structure in the COBE differential microwave radiometer first year maps," Astrophys. J. Lett. **396**, L1-L5 (1992)

[7] S. Weinberg, "Cosmology," Oxford University Press, 2008.

[8] S. Dodelson, Academic Press, 2003, ISBN 978-0-12-219141-1

[9] V. A. Rubakov and D. S. Gorbunov, "Introduction to the Theory of the Early Universe: Hot big bang theory," World Scientific, 2017, ISBN 978-981-320-987-9, 978-981-320-988-6, 978-981-322-005-8

[10] E. W. Kolb and M. S. Turner, "The Early Universe," Front. Phys. **69**, 1-547 (1990) Taylor and Francis, 2019, ISBN 978-0-429-49286-0, 978-0-201-62674-2

[11] V. Mukhanov, "Physical Foundations of Cosmology," Cambridge University Press, 2005, ISBN 978-0-521-56398-7

[12] A. R. Liddle and D. H. Lyth, "Cosmological inflation and large scale structure,"

[13] E. Hubble, "A relation between distance and radial velocity among extra-galactic nebulae," Proc. Nat. Acad. Sci. **15**, 168-173 (1929)

[14] A. G. Riess *et al.* "A 2.4% Determination of the Local Value of the Hubble Constant," Astrophys. J. **826**, no.1, 56 (2016)

[15] J. P. Huchra, "The hubble constant," 2008.
https://lweb.cfa.harvard.edu/ dfabricant/huchra/hubble/

[16] D. Baumann, "Cosmology," Cambridge University Press, 2022,

[17] D. Baumann, "Inflation," [arXiv:0907.5424 [hep-th]].

[18] A. Friedmann, "On the Possibility of a world with constant negative curvature of space," Z. Phys. **21**, 326-332 (1924)

[19] N. Aghanim *et al.* [Planck], "Planck 2018 results. I. Overview and the cosmological legacy of Planck," Astron. Astrophys. **641**, A1 (2020)

[20] A. Neronov and D. V. Semikoz, "Sensitivity of gamma-ray telescopes for detection of magnetic fields in intergalactic medium," Phys. Rev. D **80**, 123012 (2009)

[21] D. Grasso and H. R. Rubinstein, "Magnetic fields in the early universe," Phys. Rept. **348**, 163-266 (2001)

[22] A. Neronov and I. Vovk, "Evidence for strong extragalactic magnetic fields from Fermi observations of TeV blazars," Science **328**, 73-75 (2010)

[23] R. Durrer and A. Neronov, "Cosmological Magnetic Fields: Their Generation, Evolution and Observation," Astron. Astrophys. Rev. **21**, 62 (2013)

[24] E. Fenu, C. Pitrou and R. Maartens, "The seed magnetic field generated during recombination," Mon. Not. Roy. Astron. Soc. **414**, 2354-2366 (2011)

[25] N. Y. Gnedin, A. Ferrara and E. G. Zweibel, "Generation of the primordial magnetic fields during cosmological reionization," Astrophys. J. **539**, 505-516 (2000)

[26] T. Vachaspati, "Magnetic fields from cosmological phase transitions," Phys. Lett. B **265**, 258-261 (1991)

[27] G. Sigl, A. V. Olinto and K. Jedamzik, Phys. Rev. D **55**, 4582-4590 (1997) doi:10.1103/PhysRevD.55.4582 [arXiv:astro-ph/9610201 [astro-ph]].

[28] L. S. Kisslinger, "Magnetic wall from chiral phase transition and CMBR correlations," Phys. Rev. D **68**, 043516 (2003)

[29] A. G. Tevzadze, L. Kisslinger, A. Brandenburg and T. Kahniashvili, "Magnetic Fields from QCD Phase Transitions," Astrophys. J. **759**, 54 (2012)

[30] M. S. Turner and L. M. Widrow, "Inflation Produced, Large Scale Magnetic Fields," Phys. Rev. D **37**, 2743 (1988)

[31] B. Ratra, "Cosmological 'seed' magnetic field from inflation," Astrophys. J. Lett. **391**, L1-L4 (1992) doi:10.1086/186384

[32] K. Takahashi, K. Ichiki, H. Ohno and H. Hanayama, "Magnetic field generation from cosmological perturbations," Phys. Rev. Lett. **95**, 121301 (2005)

[33] J. Martin and J. Yokoyama, "Generation of Large-Scale Magnetic Fields in Single-Field Inflation," JCAP **01**, 025 (2008)

[34] R. Durrer, L. Hollenstein and R. K. Jain, "Can slow roll inflation induce relevant helical magnetic fields?," JCAP **03**, 037 (2011)

[35] R. J. Z. Ferreira, R. K. Jain and M. S. Sloth, "Inflationary magnetogenesis without the strong coupling problem," JCAP **10**, 004 (2013)

[36] R. Sharma, S. Jagannathan, T. R. Seshadri and K. Subramanian, "Challenges in Inflationary Magnetogenesis: Constraints from Strong Coupling, Backreaction and the Schwinger Effect," Phys. Rev. D **96**, no.8, 083511 (2017)

[37] T. Kobayashi, "Primordial Magnetic Fields from the Post-Inflationary Universe," JCAP **05**, 040 (2014)

[38] L. Sriramkumar, K. Atmjeet and R. K. Jain, JCAP **09**, 010 (2015) doi:10.1088/1475-7516/2015/09/010 [arXiv:1504.06853 [astro-ph.CO]].

[39] T. Fujita and R. Durrer, JCAP **09**, 008 (2019) doi:10.1088/1475-7516/2019/09/008 [arXiv:1904.11428 [astro-ph.CO]].

[40] A. Brandenburg and K. Subramanian, "Astrophysical magnetic fields and nonlinear dynamo theory," Phys. Rept. **417**, 1-209 (2005)

[41] K. Subramanian, "The origin, evolution and signatures of primordial magnetic fields," Rept. Prog. Phys. **79**, no.7, 076901 (2016)

[42] L. Biermann. Über den Ursprung der Magnetfelder auf Sternen und im interstellaren Raum (miteinem Anhang von A. Schlüter). Zeitschrift Naturforschung Teil A, 5:65, 1950.

[43] A. H. Guth, "The Inflationary Universe: A Possible Solution to the Horizon and Flatness Problems," Phys. Rev. D **23**, 347-356 (1981)

[44] D. Kazanas, "Dynamics of the Universe and Spontaneous Symmetry Breaking," Astrophys. J. Lett. **241**, L59-L63 (1980)

[45] A. D. Linde, "Inflationary Cosmology," Lect. Notes Phys. **738**, 1-54 (2008)

[46] G. E. Hale, "On the Probable Existence of a Magnetic Field in Sunspots," Astrophysical Journal, Vol. 28, November 1908, pp. 315-347.

[47] F. Finelli, F. Paci and D. Paoletti, "The Impact of Stochastic Primordial Magnetic Fields on the Scalar Contribution to Cosmic Microwave Background Anisotropies," Phys. Rev. D **78**, 023510 (2008)

[48] M. Giovannini and K. E. Kunze, "Magnetized CMB observables: A Dedicated numerical approach," Phys. Rev. D **77**, 063003 (2008)

[49] C. Bonvin, C. Caprini and R. Durrer, "Magnetic fields from inflation: The CMB temperature anisotropies," Phys. Rev. D **88**, 083515 (2013)

[50] D. Grasso and H. R. Rubinstein, "Magnetic fields in the early universe," Phys. Rept. **348**, 163-266 (2001)

[51] J. Martin, V. Vennin and P. Peter, "Cosmological Inflation and the Quantum Measurement Problem," Phys. Rev. D **86**, 103524 (2012)

[52] J. Martin and V. Vennin, "Quantum Discord of Cosmic Inflation: Can we Show that CMB Anisotropies are of Quantum-Mechanical Origin?," Phys. Rev. D **93**, no.2, 023505 (2016)

[53] J. Martin and V. Vennin, "Leggett-Garg Inequalities for Squeezed States," Phys. Rev. A **94**, no.5, 052135 (2016)

[54] J. Martin and V. Vennin, “Bell inequalities for continuous-variable systems in generic squeezed states,” Phys. Rev. A **93**, no.6, 062117 (2016)

[55] J. Martin and V. Vennin, “Obstructions to Bell CMB Experiments,” Phys. Rev. D **96**, no.6, 063501 (2017)

[56] W. H. Zurek, “Pointer Basis of Quantum Apparatus: Into What Mixture Does the Wave Packet Collapse?,” Phys. Rev. D **24**, 1516-1525 (1981)

[57] V. Mukhanov and S. Winitzki, Cambridge University Press, 2007,

[58] M. R. Haque, D. Maity and S. Pal, “Probing the reheating phase through primordial magnetic field and CMB,” Phys. Rev. D **103**, no.10, 103540 (2021)

[59] C. Cheung, P. Creminelli, A. L. Fitzpatrick, J. Kaplan and L. Senatore, “The Effective Field Theory of Inflation,” JHEP **03**, 014 (2008)

[60] S. Weinberg, “Effective Field Theory for Inflation,” Phys. Rev. D **77**, 123541 (2008)

[61] Y. Cai, Y. Wan, H. G. Li, T. Qiu and Y. S. Piao, “The Effective Field Theory of nonsingular cosmology,” JHEP **01**, 090 (2017)

[62] Y. Cai, H. G. Li, T. Qiu and Y. S. Piao, “The Effective Field Theory of nonsingular cosmology: II,” Eur. Phys. J. C **77**, no.6, 369 (2017)

[63] G. Gubitosi, F. Piazza and F. Vernizzi, “The Effective Field Theory of Dark Energy,” JCAP **02**, 032 (2013)

[64] J. Gleyzes, D. Langlois, F. Piazza and F. Vernizzi, “Essential Building Blocks of Dark Energy,” JCAP **08**, 025 (2013)

[65] F. Piazza and F. Vernizzi, “Effective Field Theory of Cosmological Perturbations,” Class. Quant. Grav. **30**, 214007 (2013)

[66] L. Dai, M. Kamionkowski and J. Wang, “Reheating constraints to inflationary models,” Phys. Rev. Lett. **113**, 041302 (2014)

[67] J. L. Cook, E. Dimastrogiovanni, D. A. Easson and L. M. Krauss, “Reheating predictions in single field inflation,” JCAP **04**, 047 (2015)

[68] A. Albrecht, P. J. Steinhardt, M. S. Turner and F. Wilczek, “Reheating an Inflationary Universe,” Phys. Rev. Lett. **48**, 1437 (1982)

[69] J. Ellis, M. A. G. Garcia, D. V. Nanopoulos and K. A. Olive, “Calculations of Inflaton Decays and Reheating: with Applications to No-Scale Inflation Models,” JCAP **07**, 050 (2015)

[70] M. R. Haque, D. Maity and S. Pal, “Probing the reheating phase through primordial magnetic field and CMB,” Phys. Rev. D **103**, no.10, 103540 (2021)

[71] B. Li, J. D. Barrow and D. F. Mota, “The Cosmology of Modified Gauss-Bonnet Gravity,” Phys. Rev. D **76** (2007), 044027

[72] S. D. Odintsov, V. K. Oikonomou and S. Banerjee, “Dynamics of inflation and dark energy from $F(R,G)$ gravity,” Nucl. Phys. B **938** (2019) 935

[73] B. M. Carter and I. P. Neupane, "Towards inflation and dark energy cosmologies from modified Gauss-Bonnet theory," JCAP **06** (2006), 004

[74] S. Nojiri, S. Odintsov, V. Oikonomou, N. Chatzarakis and T. Paul, "Viable inflationary models in a ghost-free GaussBonnet dark energy," Int. J. Geom. Meth. Mod. Phys. **13** (2016) no.05, 1630006

[75] A. de la Cruz-Dombriz and D. Saez-Gomez, "On the stability of the cosmological solutions in $f(R, G)$ gravity," Class. Quant. Grav. **29** (2012), 245014

[76] K. Bamba, Z. K. Guo and N. Ohta, "Accelerating Cosmologies in the Einstein-Gauss-Bonnet Theory with Dilaton," Prog. Theor. Phys. **118** (2007), 879-892

[77] S. Chakraborty, T. Paul and S. SenGupta, "Inflation driven by Einstein-Gauss-Bonnet gravity," Phys. Rev. D **98** (2018) no.8, 083539

[78] P. Kanti, R. Gannouji and N. Dadhich, "Gauss-Bonnet Inflation," Phys. Rev. D **92** (2015) no.4, 041302

[79] P. Kanti, R. Gannouji and N. Dadhich, "Early-time cosmological solutions in Einstein-scalar-Gauss-Bonnet theory," Phys. Rev. D **92** (2015) no.8, 083524

[80] S. D. Odintsov and V. K. Oikonomou, "Viable Inflation in Scalar-Gauss-Bonnet Gravity and Reconstruction from Observational Indices," Phys. Rev. D **98** (2018) no.4, 044039

[81] E. N. Saridakis, "Ricci-Gauss-Bonnet holographic dark energy," Phys. Rev. D **97** (2018) no.6, 064035

[82] G. Cognola, E. Elizalde, S. Nojiri, S. D. Odintsov and S. Zerbini, "Dark energy in modified Gauss-Bonnet gravity: Late-time acceleration and the hierarchy problem," Phys. Rev. D **73** (2006), 084007

[83] S. Nojiri and S. D. Odintsov, "Unified cosmic history in modified gravity: from F(R) theory to Lorentz non-invariant models," Phys. Rept. **505** (2011), 59-144

[84] S. Nojiri, S. D. Odintsov and V. K. Oikonomou, "Modified Gravity Theories on a Nutshell: Inflation, Bounce and Late-time Evolution," Phys. Rept. **692** (2017), 1-104

[85] S. Capozziello and M. De Laurentis, "Extended Theories of Gravity," Phys. Rept. **509** (2011), 167-321

[86] S. Nojiri, S. D. Odintsov and E. N. Saridakis, "Holographic inflation," Phys. Lett. B **797** (2019), 134829

[87] S. Nojiri, S. D. Odintsov, V. K. Oikonomou and T. Paul, "Unifying Holographic Inflation with Holographic Dark Energy: a Covariant Approach," Phys. Rev. D **102**, no.2, 023540 (2020)

[88] Y. Akrami *et al.* [Planck], "Planck 2018 results. X. Constraints on inflation," Astron. Astrophys. **641**, A10 (2020)

[89] G. Tasinato, "A scenario for inflationary magnetogenesis without strong coupling problem," JCAP **03**, 040 (2015)

[90] L. M. Widrow, "Origin of galactic and extragalactic magnetic fields," Rev. Mod. Phys. **74**, 775-823 (2002)

[91] A. Kandus, K. E. Kunze and C. G. Tsagas, "Primordial magnetogenesis," Phys. Rept. **505**, 1-58 (2011)

[92] T. Kobayashi and M. S. Sloth, "Early Cosmological Evolution of Primordial Electromagnetic Fields," Phys. Rev. D **100**, no.2, 023524 (2019)

[93] V. Demozzi, V. Mukhanov and H. Rubinstein, "Magnetic fields from inflation?," JCAP **08**, 025 (2009)

[94] V. Demozzi and C. Ringeval, "Reheating constraints in inflationary magnetogenesis," JCAP **05**, 009 (2012)

[95] K. Bamba, E. Elizalde, S. D. Odintsov and T. Paul, "Inflationary magnetogenesis with reheating phase from higher curvature coupling," JCAP **04**, 009 (2021)

[96] R. Beck, "Galactic and extragalactic magnetic fields," Space Sci. Rev. **99**, 243-260 (2001)

[97] K. Subramanian, "The origin, evolution and signatures of primordial magnetic fields," Rept. Prog. Phys. **79**, no.7, 076901 (2016)

[98] R. M. Kulsrud and E. G. Zweibel, "The Origin of Astrophysical Magnetic Fields," Rept. Prog. Phys. **71**, 0046091 (2008)

[99] R. Sharma, K. Subramanian and T. R. Seshadri, "Generation of helical magnetic field in a viable scenario of inflationary magnetogenesis," Phys. Rev. D **97**, no.8, 083503 (2018)

[100] R. K. Jain and M. S. Sloth, "Consistency relation for cosmic magnetic fields," Phys. Rev. D **86**, 123528 (2012)

[101] S. Kanno, J. Soda and M. a. Watanabe, "Cosmological Magnetic Fields from Inflation and Backreaction," JCAP **12**, 009 (2009)

[102] L. Campanelli, "Helical Magnetic Fields from Inflation," Int. J. Mod. Phys. D **18**, 1395-1411 (2009)

[103] K. Bamba and M. Sasaki, "Large-scale magnetic fields in the inflationary universe," JCAP **02**, 030 (2007)

[104] K. Bamba and J. Yokoyama, "Large scale magnetic fields from inflation in dilaton electromagnetism," Phys. Rev. D **69**, 043507 (2004)

[105] K. Bamba and J. Yokoyama, "Large-scale magnetic fields from dilaton inflation in noncommutative spacetime," Phys. Rev. D **70**, 083508 (2004)

[106] K. Subramanian, "Magnetic fields in the early universe," Astron. Nachr. **331**, 110-120 (2010)

[107] A. Brandenburg and K. Subramanian, "Astrophysical magnetic fields and nonlinear dynamo theory," Phys. Rept. **417**, 1-209 (2005)

[108] K. Bamba, C. Q. Geng and L. W. Luo, "Generation of large-scale magnetic fields from inflation in teleparallelism," JCAP **10**, 058 (2012)

[109] A. Dolgov, “Breaking of conformal invariance and electromagnetic field generation in the universe,” Phys. Rev. D **48**, 2499-2501 (1993)

[110] M. a. Watanabe, S. Kanno and J. Soda, “Inflationary Universe with Anisotropic Hair,” Phys. Rev. Lett. **102**, 191302 (2009)

[111] S. Kanno, J. Soda and M. a. Watanabe, “Anisotropic Power-law Inflation,” JCAP **12**, 024 (2010)

[112] T. Q. Do and W. F. Kao, “Anisotropic power-law inflation for the Dirac-Born-Infeld theory,” Phys. Rev. D **84**, 123009 (2011)

[113] G. F. R. Ellis and M. A. H. MacCallum, A Class of homogeneous cosmological models, Commun. Math. Phys. **12**, 108 (1969).

[114] G. F. R. Ellis, The Bianchi models: Then and now, Gen. Rel. Grav. **38**, 1003 (2006).

[115] V. A. Belinsky, I. M. Khalatnikov and E. M. Lifshitz, “Oscillatory approach to a singular point in the relativistic cosmology,” Adv. Phys. **19**, 525-573 (1970)

[116] C. B. Collins and S. W. Hawking, “Why is the Universe isotropic?,” Astrophys. J. **180**, 317-334 (1973)

[117] V. a. Belinsky, I. m. Khalatnikov and E. m. Lifshitz, “A General Solution of the Einstein Equations with a Time Singularity,” Adv. Phys. **31**, 639-667 (1982)

[118] A. A. Starobinsky, “Isotropization of arbitrary cosmological expansion given an effective cosmological constant,” JETP Lett. **37**, 66-69 (1983)

[119] R. M. Wald, Asymptotic behavior of homogeneous cosmological models in the presence of a positive cosmological constant, Phys. Rev. D **28**, 2118 (1983).

[120] G. W. Gibbons and S. W. Hawking, Cosmological event horizons, thermodynamics, and particle creation, Phys. Rev. D **15**, 2738 (1977).

[121] S. W. Hawking and I. G. Moss, Supercooled phase transitions in the very early Universe, Phys. Lett. B **110**, 35 (1982).

[122] D. J. Schwarz, C. J. Copi, D. Huterer, and G. D. Starkman, CMB anomalies after Planck, Class. Quant. Grav. **33**, 184001 (2016)

[123] P. K. Aluri, P. Cea, P. Chingangbam, M. C. Chu, R. G. Clowes, D. Hutsemékers, J. P. Kochappan, A. M. Lopez, L. Liu, and N. C. M. Martens, *et al.* Is the observable Universe consistent with the cosmological principle?, Class. Quant. Grav. **40**, 094001 (2023)

[124] J. D. Barrow and S. Hervik, “Anisotropically inflating universes,” Phys. Rev. D **73**, 023007 (2006)

[125] A. E. Gumrukcuoglu, C. R. Contaldi and M. Peloso, “Inflationary perturbations in anisotropic backgrounds and their imprint on the CMB,” JCAP **11**, 005 (2007)

[126] C. Pitrou, T. S. Pereira and J. P. Uzan, “Predictions from an anisotropic inflationary era,” JCAP **04**, 004 (2008)

[127] A. A. Starobinsky, S. V. Sushkov and M. S. Volkov, "Anisotropy screening in Horndeski cosmologies," Phys. Rev. D **101**, no.6, 064039 (2020)

[128] R. Galeev, R. Muharlyamov, A. A. Starobinsky, S. V. Sushkov and M. S. Volkov, "Anisotropic cosmological models in Horndeski gravity," Phys. Rev. D **103**, no.10, 104015 (2021)

[129] S. Nojiri, S. D. Odintsov, V. K. Oikonomou and A. Constantini, "Formalizing anisotropic inflation in modified gravity," Nucl. Phys. B **985**, 116011 (2022)

[130] A. A. Starobinsky, "A New Type of Isotropic Cosmological Models Without Singularity," Phys. Lett. B **91**, 99-102 (1980)

[131] A. A. Starobinsky, "Dynamics of Phase Transition in the New Inflationary Universe Scenario and Generation of Perturbations," Phys. Lett. B **117**, 175-178 (1982)

[132] A. D. Linde, "A New Inflationary Universe Scenario: A Possible Solution of the Horizon, Flatness, Homogeneity, Isotropy and Primordial Monopole Problems," Phys. Lett. B **108**, 389-393 (1982)

[133] A. Albrecht and P. J. Steinhardt, "Cosmology for Grand Unified Theories with Radiatively Induced Symmetry Breaking," Phys. Rev. Lett. **48**, 1220-1223 (1982)

[134] A. D. Linde, "Chaotic Inflation," Phys. Lett. B **129**, 177-181 (1983)

[135] S. Kanno, "Nonclassical primordial gravitational waves from the initial entangled state," Phys. Rev. D **100**, no.12, 123536 (2019)

[136] A. Ashoorioon and R. B. Mann, "Generation of cosmological seed magnetic fields from inflation with cutoff," Phys. Rev. D **71**, 103509 (2005)

[137] B. P. Abbott *et al.* [LIGO Scientific and Virgo], Phys. Rev. Lett. **116**, no.6, 061102 (2016) [arXiv:1602.03837 [gr-qc]];

[138] C. Caprini and D. G. Figueroa, Class. Quant. Grav. **35**, 163001 (2018), arXiv:1801.04268 [astro-ph.CO];

[139] B. Abbott et al. (LIGO Scientific, Virgo), Phys. Rev. Lett. **116**, 131103 (2016), arXiv:1602.03838 [gr-qc];

[140] B. Abbott et al. (LIGO Scientific, Virgo), Phys. Rev. D **93**, 122003 (2016), arXiv:1602.03839 [gr-qc];

[141] B. Abbott et al. (LIGO Scientific, Virgo), Phys. Rev. Lett. **116**, 241102 (2016), arXiv:1602.03840 [gr-qc];

[142] B. P. Abbott et al. (LIGO Scientific, Virgo), Phys. Rev. Lett. **116**, 061102 (2016), arXiv:1602.03837 [gr-qc];

[143] B. P. Abbott et al. (LIGO Scientific, Virgo), Phys. Rev. Lett. **116**, 241103 (2016), arXiv:1606.04855 [gr-qc];

[144] B. P. Abbott et al. (LIGO Scientific, VIRGO), Phys. Rev. Lett. **118**, 221101 (2017), [Erratum: Phys. Rev. Lett. **121**,no.12,129901(2018)], arXiv:1706.01812 [gr-qc];

[145] B. P. Abbott et al. (LIGO Scientific, Virgo), Astrophys. J. Lett. **851**, L35 (2017), arXiv:1711.05578 [astro-ph.HE];

[146] B. P. Abbott et al. (LIGO Scientific, Virgo), Phys. Rev. Lett. **119**, 141101 (2017), arXiv:1709.09660 [gr-qc];

[147] B. P. Abbott et al. (LIGO Scientific, Virgo), Phys. Rev. Lett. **119**, 161101 (2017), arXiv:1710.05832 [gr-qc];

[148] R. Abbott et al. (LIGO Scientific, Virgo), Phys. Rev. D **102**, 043015 (2020), arXiv:2004.08342 [astro-ph.HE];

[149] B. P. Abbott et al. (LIGO Scientific, Virgo), Astrophys. J. Lett. **892**, L3 (2020), arXiv:2001.01761 [astro-ph.HE];

[150] R. Abbott et al. (LIGO Scientific, Virgo), Astrophys. J. **896**, L44 (2020), arXiv:2006.12611 [astro-ph.HE].

[151] P. P. Kronberg, "Extragalactic magnetic fields," Rept. Prog. Phys. **57**, 325-382 (1994)

[152] A.Z. Dolginov, Phys. Rep. 162 (1988) 337.

[153] E. Asseo and H. Sol, Phys. Rep. 148 (1987) 307.

[154] T. Vachaspati, "Fundamental Implications of Intergalactic Magnetic Field Observations," Phys. Rev. D **95**, no.6, 063505 (2017)

[155] S. Kanno and J. Soda, "Polarized initial states of primordial gravitational waves," Symmetry **12**, no.4, 672 (2020)

[156] S. Koh, S. P. Kim and D. J. Song, "Gravitational wave spectrum in inflation with nonclassical states," JHEP **12**, 060 (2004)

[157] R. Holman and A. J. Tolley, "Enhanced Non-Gaussianity from Excited Initial States," JCAP **05**, 001 (2008)

[158] A. Ashoorioon, K. Dimopoulos, M. M. Sheikh-Jabbari and G. Shiu, "Reconciliation of High Energy Scale Models of Inflation with Planck," JCAP **02**, 025 (2014)

[159] A. Ashoorioon and G. Shiu, "A Note on Calm Excited States of Inflation," JCAP **03**, 025 (2011)

[160] P. D. Meerburg, J. P. van der Schaar and P. S. Corasaniti, "Signatures of Initial State Modifications on Bispectrum Statistics," JCAP **05**, 018 (2009)

[161] P. D. Meerburg, J. P. van der Schaar and M. G. Jackson, "Bispectrum signatures of a modified vacuum in single field inflation with a small speed of sound," JCAP **02**, 001 (2010)

[162] A. Ashoorioon, P. S. Bhupal Dev and A. Mazumdar, "Implications of purely classical gravity for inflationary tensor modes," Mod. Phys. Lett. A **29**, no.30, 1450163 (2014)

[163] H. V. Ragavendra, L. Sriramkumar and J. Silk, "Could PBHs and secondary GWs have originated from squeezed initial states?," JCAP **05**, 010 (2021)

[164] G. G. Stokes, Trans. Camb. Phil. Soc. 9, 399 (1852).

[165] Padgett, Miles J., and Johannes Courtial. ”Poincaré-sphere equivalent for light beams containing orbital angular momentum.” Optics letters 24.7 (1999): 430-432.

[166] Milione, Giovanni, et al. ”Higher-order Poincaré sphere, Stokes parameters, and the angular momentum of light.” Physical review letters 107.5 (2011): 053601.

[167] Malykin, G. B. ”Use of the poincare sphere in polarization optics and classical and quantum mechanics. review.” Radiophysics and quantum electronics 40.3 (1997): 175-195.

[168] Laatikainen, Jyrki, et al. ”Poincaré sphere of electromagnetic spatial coherence.” Optics Letters 46.9 (2021): 2143-2146.

[169] Berry, H. Gordon, G. Gabrielse, and A. E. Livingston. ”Measurement of the Stokes parameters of light.” Applied optics 16.12 (1977): 3200-3205.

[170] Korolkova, Natalia, et al. ”Polarization squeezing and continuous-variable polarization entanglement.” Physical Review A 65.5 (2002): 052306.

[171] Jan-Åke Larsson, Physical Review A **70**,022102 (2004)

[172] G. Gour, F.C. Khanna, A. Mann, and M. Rezven Physics Letters A **324**, 415 (2004)

[173] G. S. Agarwal, S. Chaturvedi (2003) Scheme to measure quantum stokes parameters and their fluctuations and correlations, Journal of Modern Optics, 50:5, 711-716, DOI 10.1080/09500340308235179

[174] N. Mukunda and T. F. Jordan, J. Math. Phys. 7, 849 (1966).

[175] K. Subramanian, “Can the turbulent galactic dynamo generate large scale magnetic fields?,” Mon. Not. Roy. Astron. Soc. **294**, 718 (1998)

[176] K. Subramanian, D. Narasimha, and S. M. Chitre. Thermal generation of cosmological seed magnetic fields in ionization fronts. Mon. Not. Roy. Astron. Soc., 271, November 1994.

[177] N. Aghanim *et al.* [Planck], “Planck 2018 results. VI. Cosmological parameters,” Astron. Astrophys. **641**, A6 (2020)

[178] A. G. Riess, W. Yuan, L. M. Macri, D. Scolnic, D. Brout, S. Casertano, D. O. Jones, Y. Murakami, L. Breuval and T. G. Brink, *et al.* Astrophys. J. Lett. **934**, no.1, L7 (2022)

[179] B. Himmetoglu, C. R. Contaldi and M. Peloso, “Ghost instabilities of cosmological models with vector fields nonminimally coupled to the curvature,” Phys. Rev. D **80** (2009), 123530

[180] B. Himmetoglu, C. R. Contaldi and M. Peloso, “Instability of anisotropic cosmological solutions supported by vector fields,” Phys. Rev. Lett. **102** (2009), 111301

[181] B. Himmetoglu, C. R. Contaldi and M. Peloso, “Instability of the ACW model, and problems with massive vectors during inflation,” Phys. Rev. D **79** (2009), 063517

[182] M. Karciauskas and D. H. Lyth, “On the health of a vector field with (R Aˆ2)/6 coupling to gravity,” JCAP **11** (2010), 023

[183] D. Maity and P. Saha, “Connecting CMB anisotropy and cold dark matter phenomenology via reheating,” Phys. Rev. D **98** (2018) no.10, 103525

[184] D. Maity, S. Pal, and T. Paul, Effective Theory of Inflationary Magnetogenesis and Constraints on Reheating, JCAP **05**, 045 (2021)